

**CO₂ ABSORPTION/DESORPTION IN METHYLDIETHANOLAMINE
SOLUTIONS PROMOTED WITH MONOETHANOLAMINE AND
DIETHANOLAMINE: MASS TRANSFER AND REACTION KINETICS**

BY

James Edward Critchfield, B.S.

DISSERTATION

**Presented to the Faculty of the Graduate School of
The University of Texas at Austin
in Partial Fulfillment
of the Requirements
for the Degree of**

DOCTOR OF PHILOSOPHY

THE UNIVERSITY OF TEXAS AT AUSTIN

May 1988

CO₂ ABSORPTION/DESORPTION IN METHYLDIETHANOLAMINE
SOLUTIONS PROMOTED WITH MONOETHANOLAMINE AND
DIETHANOLAMINE: MASS TRANSFER AND REACTION KINETICS

APPROVED BY SUPERVISORY COMMITTEE:

Gary Rockell
Almes R. Zier
Howard F. Rase
R. H. Bluf
W. H. Ward

Copyright
by
James Edward Critchfield
1988

To my parents

ACKNOWLEDGEMENTS

Many people contributed to the success of this project. I wish to thank Dr. Gary T. Rochelle for his patient and insightful supervision. Thanks are also due to (in no particular order): Cini Gage, Cindy Gleason, Dave Austgen, Dave Glasscock, Dave Trempel, Will White, Judy Searcy and Joe Peterson for many interesting comments and for contributing to an pleasant work environment. It was fun working with all of you. A special thanks goes to Siddik for his careful assistance in the laboratory.

Thanks also go to the Separations Research Program for funding this work.

CO₂ ABSORPTION/DESORPTION IN METHYLDIETHANOLAMINE
SOLUTIONS PROMOTED WITH MONOETHANOLAMINE AND
DIETHANOLAMINE: MASS TRANSFER AND REACTION KINETICS

Publication No. _____

James Edward Critchfield, Ph.D.
The University of Texas at Austin, 1988

Supervising Professor: Gary T. Rochelle

CO₂ absorption and desorption across an unbroken interface was studied in MethylDiEthanolAmine (MDEA) solutions with and without the presence of the promoters MonoEthanolAmine (MEA) and DiEthanolAmine (DEA). The transport rate was studied as a function of CO₂ content and driving force.

The reaction kinetics for CO₂ with MDEA were determined from high driving force experiments in order to minimize the possible effects of reactive impurities. The second order rate constant for the reaction was found to be 2.5 liter mole⁻¹ second⁻¹ at 25°C.

Extrapolation of the measured desorption rates provided estimates of the equilibrium vapor pressure in 2 molar amine solutions at 25° C with 0.1 to 1 molar CO₂. The technique was validated by comparing the estimated CO₂ vapor pressure over DEA and MDEA solutions with literature values. CO₂ vapor pressures were then measured over mixtures of DEA-MDEA and MEA-MDEA. An approximate equilibrium model correlated the mixture data fairly well, although some bias in the correlation was demonstrated at low promoter content and low CO₂ pressure.

CO₂ absorption rates were also studied as a function of driving force. At sufficiently high driving force a shuttle mechanism was shown to limit the absorption rate. At very low driving force, diffusion effects were eliminated and

the absorption rates were kinetically controlled. Good agreement was found between rate constants measured in absorption and desorption.

Speciation from the approximate equilibrium model was used to interpret the data in terms of kinetic models. MDEA was found to enhance the kinetics of the CO₂-DEA reaction in a manner consistent with complex kinetic mechanisms published in the literature. The interaction rate constant was found to be 2326 liter² mole⁻² second⁻¹ at 25°C, which is almost twice the value for DEA (1200 liter² mole⁻² second⁻¹). MDEA did not interact with the kinetics of the CO₂-MEA reaction. These facts make DEA a much more attractive promoter than would be considered on the basis of the reaction rates of CO₂ with solutions of DEA and MEA only.

CONTENTS

Acknowledgments	v
Abstract	vi
Table of Contents	viii
List of Figures	xi
List of Tables	xiv
Section 1: Introduction	1
1.1 General Introduction	1
1.1.1 The importance of kinetic data in CO ₂ - alkanolamine systems	1
1.1.2 Process types	2
1.1.3 Promotion of CO ₂ absorption/desorption	4
1.2 Equilibria	5
1.3 Reaction Rates	8
Section 2: Theory	14
2.1 Physical Mass Transfer Models	14
2.1.1 Film theory	14
2.1.2 Penetration theory	15
2.1.3 Surface renewal theory	15
2.2 Mass Transfer with Chemical Reaction	17
2.2.1 For a single bimolecular reaction: $A + \nu B \rightleftharpoons C + D$	17
2.2.2 Analytically solvable asymptotes	17
2.2.3 Transition regions	21
2.2.4 Macroscopic effects	23
2.3 Solubility and Diffusion Coefficient of CO ₂	25
2.4 Development of Reaction Rates for Reversible Reactions	28
2.5 Quantitative Treatment for a Single Reversible Reaction	30
2.6 Enhancement Factors in Mixed Solvents	35
2.6.1 Equilibrium and non-equilibrium interactions	35

	2.6.2 The shuttle mechanism	41
	2.6.3 The parallel reaction mechanism	45
	2.6.4 Quantitative technique for the parallel reactions	47
	2.6.5 Quantitative treatment of the shuttle mechanism	47
	2.7 Treatment of Desorption	47
	2.7.1 For a single reaction	47
	2.7.2 For mixed solvents	49
	2.7.3 Specifying the driving force in desorption	50
Section 3:	Experimental	51
	3.1 Apparatus and Procedures	51
	3.1.1 The high and low driving force configurations	51
	3.1.2 The absorption mode	54
	3.1.3 The desorption mode	56
Section 4:	Mass Transfer Studies	57
	4.1 Calibration of Mass Transfer Coefficients	57
	4.1.1 Mass transfer coefficients for the liquid phase	57
	4.1.2 Mass transfer coefficients for the gas phase	59
Section 5:	MDEA-Absorption and Desorption	68
	5.1 CO ₂ Absorption into MDEA Solution at High Driving Forces	68
	5.2 CO ₂ Desorption from MDEA Solution	76
Section 6:	Vapor Liquid Equilibrium	81
	6.1 DEA	81
	6.2 MDEA	85
	6.3 Mixed Systems: DEA-MDEA and MEA-MDEA	88
Section 7:	MEA-MDEA-Absorption	93
	7.1 High Driving Force	93
	7.2 Low Driving Force	93
Section 8:	DEA-Absorption and Desorption	98
	8.1 Absorption as a Function of Driving Force	98
	8.2 Desorption	101

Section 9:	DEA-MDEA-Absorption and Desorption and MEA-MDEA	
	Desorption	104
	9.1 DEA-MDEA in Absorption as a Function of Driving Force	104
	9.2 DEA-MDEA in Desorption	106
	9.3 MEA-MDEA in Desorption	109
	9.4 Comparison between DEA and MEA as Promoters	111
	9.5 Effect of Impurities on the Pseudo-First Order Rate	
	Constant for MDEA	114
Section 10:	Conclusions	116
	Notation	118
	References	121
	Appendices	131

Figures

Figure no.	Title	Page
1	The behavior of the enhancement factor as a function of the Hatta number	19
2	Effect of driving force on diffusion limitations in the measurement of the enhancement factor.....	24
3	Approximate solution technique for the enhancement factor.....	36
4	Agreement of the approximate solution technique with the full numerical solution of surface renewal theory.....	37
5	The fate of chemically reacted CO ₂ in an MEA/MDEA mixture.....	39
6	The effect of the rates of carbamate formation and conversion into bicarbonate on the limiting model which is applicable.....	40
7	Contrast of the shuttle and parallel reaction models for an instantaneous carbamate formation reaction.....	42
8	The experimental contactor is a stirred-tank reactor with an unbroken gas-liquid interface.....	52
9	Correlation of liquid phase mass transfer coefficients for both reactor configurations.....	60
10	CO ₂ absorption into fast reacting solutions.....	61
11	Lower limiting values of the gas phase mass transfer coefficient...	62
12	Apparent rate constants for CO ₂ reaction measured in 2 M MEA...	64
13	Modelled values of k_{ga} in which the contribution of liquid phase resistance has been eliminated.....	66
14	Concentration increase in the reactor during CO ₂ absorption into 2 m MDEA at 52.5°C, 0.9 atm CO ₂	69
15	CO ₂ absorption rates into 2 m MDEA	70
16	Comparison of MDEA rate constants measured under high driving force conditions with values reported in the literature.....	71

17	Effect of assumptions made in interpreting 2 m MDEA, high driving force absorption data on the resulting activation energy.....	75
18	Comparison of measured CO ₂ vapor pressures in 2 m MDEA with those predicted from the extrapolation of Jou et al's data.....	78
19	Comparison of MDEA rate constants measured in high driving force absorption and in desorption.....	80
20	Desorption rates and CO ₂ content in 2 M DEA at 25°C.....	82
21	Comparison of measured equilibria with predictions from the Kent and Eisenberg equilibrium model and literature values.....	83
22	Comparison of measured equilibria with the results of Jou et al....	86
23	Comparison of normalized equilibria with the results of Jou et al...	87
24	Attempt at fitting the system MDEA/DEA/H ₂ O/CO ₂ with three adjusted equilibria.....	89
25	Fit of the MDEA/DEA(or MEA)/H ₂ O/CO ₂ system with three adjusted equilibria.....	90
26	Attempt at fitting the system MDEA/MEA/H ₂ O/CO ₂ with three adjusted equilibria.....	92
27	The shuttle model better predicts high driving force absorption.....	94
28	Absorption of CO ₂ into 2 molal MEA/MDEA solution.....	95
29	Pseudo-first order rate constants are independent of driving force (in 2 M total amine, 30% MEA at 25°C).....	97
30	Apparent rate constants for CO ₂ absorption in 2 M DEA measured at 25°C.....	99
31	Comparison of rate constants measured in absorption with values from the literature at 25°C.....	100
32	Rate constants for CO ₂ measured under low driving forces in 2 M DEA at 25°C and a 1 atm total pressure.....	102
33	Apparent rate constants for CO ₂ reaction measured from absorption in 2 M amine (30 % DEA, 70% MDEA).....	105
34	Rate constants for CO ₂ reaction measured in 2 M DEA/MDEA at various DEA contents and at 25°C.....	107

35	Test of a kinetically non-interactive model for rate constants in DEA/MDEA mixtures.....	108
36	Test of a kinetically interactive model for rate constants in DEA/MDEA mixtures.....	110
37	A kinetically non-interactive model predicts the MEA/MDEA mixture rate constant.....	112
38	The effectiveness of MEA or DEA as a promoter depends strongly on the equilibrium amount of free amine.....	113
39	The pseudo-first order rate constant is a strong function of the impurity content.....	115
40	Results of pH titration for total carbon dioxide in 2 M MDEA.....	134

Tables

Table no.	Title	Page
1	Liquid mass transfer coefficients in the CO ₂ -H ₂ O system measured in the low and high driving force configurations.....	58
2	Experiment summary for CO ₂ absorption into fast reacting amines for the purpose of gas phase mass transfer resistance measurement.....	67
3	Parameters used in the interpretation of the experimental data for CO ₂ absorption into 2 molal MDEA in the high driving force configuration.....	73
4	Calibration of the liquid phase analytical technique.....	131
5	Calibration of the Horiba PIR-2000 analyzer.....	137
6	Values of $\sqrt{D/H}$ used in the interpretation of rate data at 25°C in 2 M solutions.....	140
7	Steady-state experiment summary (absorption).....	141
8	Steady-state experiment summary (desorption).....	143
9	Experiment summary for unsteady-state, high driving force CO ₂ absorption into 2 m MDEA.....	145
10	Tabular smoothed data for CO ₂ absorption into MDEA at high driving force.....	146
11	Experiment summary for unsteady-state, high driving force CO ₂ absorption into a 2 m MEA/MDEA mixture.....	148
12	Experiment summary for unsteady-state, moderate driving force CO ₂ absorption into a 2 m MEA/MDEA mixture.....	150
13	Calibration of the 100 Canon-Fenske viscometer.....	151
14	Viscosity data for 3.53 m and 2 m MEA/MDEA mixtures.....	152
15	Viscosity data for DEA, DEA/MDEA and MEA/MDEA mixtures, all in 2 M solutions.....	154
16	Density data for the 2 m MEA/MDEA mixtures.....	155

Section 1

INTRODUCTION

1.1 General Introduction

1.1.1 The importance of kinetic data in CO₂-alkanolamine systems

CO₂ removal from process gases is an industrially important unit operation with applications in natural gas production, refinery operation, and ammonia and hydrogen manufacture. Chemically reactive solvents, such as alkanolamines are frequently employed in this operation because they provide low circulation rates due to the existence of a chemical sink for the acid gas (Kohl and Riesenfeld, 1985). In addition, the rate of reaction of the acid gas with the solvent may be fast enough to enhance the rate of absorption, thereby reducing the contactor height required.

Though the reaction rate enhancement of mass transfer in chemically reactive solvents is an advantage in practice, it can cause a great deal of difficulty in creating an accurate design or simulation. In addition to mass transfer enhancement, the occurrence of chemical reaction in CO₂ absorption/stripping processes creates nonlinear equilibria and can result in significant heat effects due to the exothermic heat of absorption (Sardar, 1985). Because of the rate, heat and equilibrium effects, simple and approximate design procedures for absorption/stripping cannot be expected to provide an accurate design.

With the recent advent of mass transfer rate-based computer models for the design and simulation of acid gas treating systems (Hermes, 1987; Sardar, 1985; Katti and Wolcott, 1987; Yu and Astarita, 1987b; Holmes et al 1984), a need has been created for reliable experimental data on mass transfer and reaction rates. Although these models are sophisticated enough to treat gas-liquid contacting from a fundamental rate basis and therefore have the potential of more accurately predicting the performance of chemical absorbers and strippers, the models can only be as accurate as the experimental data upon which they are based. Therefore the models require accurate knowledge of reaction rates and their effect on mass

transfer. To the extent that mass transfer is liquid-phase controlled in acid gas contactors, the stage efficiency will be dependent upon the rate of chemical reaction. Therefore one's ability to predict the mass transfer rate depends on his application of valid reaction rates of the gas with the solvent.

The reaction rates of H_2S and CO_2 differ greatly in alkanolamine solutions because of the difference in their chemical natures. As a Bronsted acid, H_2S reacts directly with the amine function in an acid-base neutralization step. This neutralization is much faster than the time it takes for H_2S to diffuse into the bulk liquid. Consequently, H_2S can be considered to be in chemical equilibrium in the liquid at all points in the contactor and actual kinetic data are not necessary to model H_2S transport.

The reaction of CO_2 with a basic solvent is much slower than that of H_2S . The slower reaction rate of CO_2 is due to its nature as a Lewis acid which must hydrate before it can react by acid-base neutralization. It may also react directly with the amine to form a carbamate. The rates of hydration and carbamation are both slow enough that they may be on the order of the rate of diffusion of CO_2 and so the reaction rate may limit the overall mass transfer efficiency with respect to CO_2 . It is this fact which creates the need for reliable reaction rate data in order to model effectively acid gas contactors.

1.1.2 Process types

Chemical solvent processes may be divided into three conceptual categories distinguished by the rate at which the solvent reacts with CO_2 . The first group of processes can be termed "bulk" CO_2 treating processes, and are distinguished by their ability to remove CO_2 to very low levels. Bulk removal stresses the faster-reacting solvents available: primary and secondary alkanolamines and promoted hot carbonate salts. Promoted hot carbonate processes are widely used for bulk CO_2 removal where clean gas specifications are not stringent and the partial pressure of CO_2 is moderately high (Astarita et al, 1983).

Aqueous primary or secondary alkanolamines are generally employed for bulk CO_2 removal when the partial pressure of CO_2 in the feed is relatively low

and/or the product purity is high. Though the reaction of CO_2 with these amines is fast, it is accompanied by a highly exothermic heat of reaction (Kohl and Riesenfeld, 1985) which must be supplied in the regeneration step. Consequently, these processes can be energy intensive (Astarita et al, 1983).

The second group of processes employ tertiary or hindered alkanolamines to avoid the faster carbamate formation reaction constitute the second group- "selective" treating processes. These selective processes are capable of passing as much as 90% of the CO_2 in the feed gas while removing H_2S to very low levels (1/4 grain) (Kohl and Reisenfeld, 1985). In selective gas treating applications (such as Claus tail gas clean-up) CO_2 removal is undesirable and results in higher-than-necessary circulation rates and reboiler steam requirements. In order to save energy in these applications, the tertiary alkanolamine MethylDiEthanolAmine (MDEA) was proposed for use as a selective treating agent (Frazier and Kohl, 1957). Since that time, MDEA has become known as a solvent providing good selectivity for H_2S in the presence of CO_2 (Kohl and Riesenfeld, 1985; Vidaurri and Kahre, 1977; Blanc and Elgue, 1981).

A third, hybrid, category of processes has recently grown out of the selective treating category. These hybrid processes seek to remove most of the CO_2 present in the rich gas stream, and also seek to retain the beneficial energy characteristics of selective solvents. The increased CO_2 removals available in the hybrid processes are achieved by controlling the reaction rate of CO_2 with the solvent. The CO_2 reaction rate increase has been demonstrated industrially by "promoting" a tertiary alkanolamine solvent with a small amount of faster-reacting primary or secondary amine (Kohl and Riesenfeld, 1985).

Because these hybrid processes are among the most recent innovations in the field of acid gas treating, the solvents employed are generally considered proprietary and little public information is available on CO_2 reaction rates. In order to use the full potential of mass transfer-based contactor models to simulate and design these processes a fundamental knowledge of reaction with mass transfer is required.

1.1.3 Promotion of CO₂ absorption/desorption

It is potentially advantageous to use MDEA as a solvent for CO₂ removal because of its low heat of reaction. Unfortunately, the low rate of reaction of CO₂ with MDEA limits the feasibility of MDEA as a chemical solvent for this purpose. Promoting the reaction rate of CO₂ in MDEA solutions has received attention recently (Chakravarty et al, 1985). The use of promoted MDEA as a solvent for CO₂ removal is the basis of a process patented by BASF Aktiengesellschaft (Meissner and Wagner, 1983), in which a small amount of either monomethylmonoethanolamine or piperazine is added to enhance the absorption rate of CO₂. Kohl and Riesenfeld (1985) speculate that the mechanism of rate promotion in this process is the same as that in promoted hot carbonate processes. The promoting effect of the addition of primary or secondary alkanolamines to tertiary alkanolamine is known industrially, but experimental confirmation of the supposed promotion mechanism is sparse.

The rate enhancing effect of the presence of primary and secondary amines in MDEA was also noted as an experimental difficulty by Blauwhoff et al (1984), who measured the reaction rate of CO₂ with MDEA. Versteeg and van Swaaij (1988a) went a step further and measured the actual primary and secondary alkanolamine contaminants in MDEA. The authors modelled the effect of these contaminants and found that they significantly affected the observed enhancement factor at very low CO₂ loadings. At higher loadings, the contaminants were effectively neutralized by the presence of CO₂, and the reaction of CO₂ and MDEA was found to dominate the observed enhancement factor. Versteeg and van Swaaij (1988b) are currently investigating CO₂ absorption in mixtures of alkanolamines.

Chakravarty et al (1985) published the results of a computer model for absorption/stripping which demonstrated the potential advantage offered by promoted MDEA as a solvent for CO₂. Significant rate promotion was indicated under both absorption and desorption conditions. At the time of publication, the model was based solely on individual amine data: no mixture data were available on either rate or equilibrium. Subsequently, Toman and Weiland (1987) have

investigated the absorption of CO₂ in DEA (DiEthanolAmine)-promoted MDEA in a string-of-spheres contactor. However, no interpretation in terms of kinetic models for the CO₂-DEA reaction was presented.

Adequate prediction of transport rates in promoted solvent systems requires the ability to represent reaction rates over a wide range of conditions. Therefore, it is necessary to know the effect of CO₂ loading on the rate of reaction in promoted MDEA. Additionally, a knowledge of the reverse rates and CO₂ equilibria is required in order to model absorption and desorption in loaded solvents (conditions which are encountered in the bottom of the absorber and throughout the stripper). There are no published experimental data on CO₂ reaction with promoted alkanolamine solvents under reversible conditions.

1.2 Equilibria

The chemical reactions involving CO₂ in aqueous alkanolamines are largely dominated by acid-base buffer reactions. A set of equilibrium reactions which describes the system CO₂-MDEA-promoter-H₂O is given below.

In any representation of pH equilibria in an aqueous solvent the water dissociation constant must be specified:

$$K_w = [H^+][OH^-] \quad (1.1)$$

CO₂ must first dissolve into aqueous solution if it is to be hydrated and subsequently act as an acid. The solubility as well as the first and second dissociation constants of carbon dioxide are respectively defined as follows:

$$H_{CO_2} = \frac{P_{CO_2}}{[CO_2]} \quad (1.2)$$

$$K_1 = \frac{[H^+][HCO_3^-]}{[CO_2]} \quad (1.3)$$

$$K_2 = \frac{[H^+][CO_3^{2-}]}{[HCO_3^-]} \quad (1.4)$$

The relative magnitudes of the first and second dissociation constants are such that in MDEA solutions the HCO_3^-/CO_3^{2-} ratio is always very large except at extremely small CO_2 loadings. In this discussion, the " CO_2 loading" is defined as a mole ratio of CO_2 to total amine:

$$\text{Loading} = \frac{\text{total moles dissolved } CO_2}{\text{total moles alkanolamine}} \quad (1.5)$$

The acid dissociation constant of MDEA and promoter are considered:

$$K_a = \frac{[H^+][MDEA]}{[MDEAH^+]} \quad (1.6)$$

$$K_{a1} = \frac{[H^+][AM]}{[AMH^+]} \quad (1.7)$$

Base strength in alkanolamines follows the trend primary > secondary > tertiary (Schwabe et al, 1959; Hall and Sprinkle, 1932). The relative base strength is especially important in mixtures of primary or secondary alkanolamine and tertiary alkanolamine because the concentrations of free alkanolamines are coupled through the pH equilibria of reactions 1.6 and 1.7. If the pK_a of the primary alkanolamine far exceeds that of the tertiary alkanolamine the primary one will be preferentially protonated and will therefore exist only in very small amounts at high CO_2 loadings. If the alkanolamines have similar K_a 's then the ratio of free promoter-to-tertiary alkanolamine will be independent of the CO_2 loading. This is important because the base must be in the unprotonated form in order to enhance the mass transfer rate of CO_2 . The relative K_a values therefore play an important role in the effectiveness of a primary or secondary promoter.

The direct reaction of CO₂ with the promoter to form carbamate also affects the promoter concentration:

$$K_f = \frac{[AMCO_2^-][AMH^+]}{[CO_2][AM]^2} \quad (1.8)$$

It is convenient to combine the equilibrium relation with reactions 1.3 and 1.7 to define a "carbamate instability constant:"

$$K_c = \frac{[HCO_3^-][AM]}{[AMCO_2^-]} \quad (1.9)$$

The instability constant quantifies the tendency of the carbamate to revert into bicarbonate and free promoter in aqueous solution. Because the reaction in equation 1.9 contains the free alkanolamine, for a given value of K_c the ratio of carbamate to bicarbonate will be a function of the solution CO₂ loading. As the solution is loaded with CO₂, the pH of the solution decreases and the concentration of free alkanolamine is lowered. LeChatelier's principle requires that reaction 1.9 shift to the right under this condition. At lower CO₂ loadings the existence of free alkanolamine is favored and the reaction shifts towards the existence of carbamate. When the value of K_c is sufficiently small that the carbamate is stable, at low loadings two moles of alkanolamine react with 1 mole of CO₂: one mole of alkanolamine forms the carbamate and the other accepts the proton. If K_c is large, the carbamate is unfavored even at low loadings and a little more than one mole of alkanolamine is required per mole of CO₂.

For the purpose of equilibrium modelling of CO₂ vapor pressure over tertiary alkanolamine solutions, it is convenient to define an "overall" equilibrium constant which is the combination of equations 1.2, 1.3 and 1.6 (Hermes, 1987):

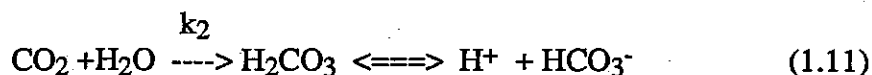
$$HK = \frac{K_a H_{CO_2}}{K_1} = \frac{[MDEA]P_{CO_2}}{[HCO_3^-][MDEAH^+]} \quad (1.10)$$

The equilibrium behavior is more complex in a mixture of primary or secondary alkanolamine and tertiary alkanolamine. The concentrations of the alkanolamines will be linked through coupling of the pH equilibria and the equilibrium of the carbamate-to-bicarbonate conversion reaction (reaction 1.9). Because of the equilibrium interactions, it can be concluded that from a thermodynamic viewpoint a good promoter is one which has both a small carbamate stability and a relatively low pK_a . Both these conditions allow for the existence of significant concentrations of free promoter at higher CO_2 loadings.

Thermodynamic effects must be coupled with reaction rate phenomena in order to truly evaluate the advantages of primary or secondary amine promoters.

1.3 Reaction rates

CO_2 reaction with aqueous alkanolamine solvents can occur through several distinct kinetic steps. In any aqueous solvent CO_2 can react directly with water to form carbonic acid, which can then be assumed to be in equilibrium with the basic solution:



Pinsent et al (1956) studied the rate of this reaction and found that at $25^\circ C$ the first order rate constant was 0.028 s^{-1} . Although the uncatalyzed hydration reaction is slow, it is subject to catalysis by anions of weak acids such as arsenite (Sharma and Danckwerts, 1963). The catalysis of reaction 1.11 by weak acids is a kinetic effect which occurs in addition to the potential buffering of the pH in the mass transfer boundary layer (Meldon et al, 1977).

Bicarbonate can also be formed from the direct reaction of CO_2 with free hydroxide:



Bicarbonate formation in this step is so much faster than hydrolysis that at pH values above 8 the contribution of hydrolysis may be neglected in the representation of the total CO₂ reaction rate. Direct bicarbonate formation has been studied extensively and the rate constants are known as a function of temperature and of the ionic strength of the solution. The second order rate constants used in this work are those of Pinsent et al (1951) and are adjusted for ionic strength dependence (Astarita et al, 1983):

$$\log_{10}k_{OH^-} = 13.635 - 2895/T + 0.08 I \quad (1.13)$$

The fate of CO₂ in aqueous alkanolamine solutions depends on the alkanolamine properties. The reaction of CO₂ with solutions of tertiary alkanolamines is different than with primary or secondary alkanolamines. Tertiary alkanolamines cannot form carbamates because of their completely substituted structure. However, there is ample experimental evidence that tertiary alkanolamines act as base catalysts for the hydrolysis of CO₂ (Barth et al, 1981; Danckwerts, 1979).

Base catalysis of hydrolysis by tertiary alkanolamines to form bicarbonate is much slower than the carbamate formation rate for unhindered primary and secondary alkanolamines. The rate law for the forward step developed from this mechanism is:

$$\text{rate}_f = k_{MDEA}[\text{CO}_2][\text{MDEA}] \quad (1.14)$$

In a recent study, Versteeg (1987) found that the rate constant for this reaction can be correlated as an increasing function of the pK_a of the tertiary alkanolamine. The author also found that in nonaqueous solvents no reaction between CO₂ and tertiary alkanolamine occurred. Both of these facts support the hypothesis that tertiary alkanolamines enhance CO₂ absorption through base catalysis of the hydrolysis reaction.

Relatively poor agreement exists among the reported rate data for the tertiary alkanolamine MDEA, although all investigators agree the reaction appears to be

second order overall (Barth et al, 1981; Blauwhoff et al, 1984; Versteeg, 1987; Tomjec et al, 1986; Yu and Astarita, 1985; Haimour et al, 1985). The range of rate constants is about 2.2 to 7.6 $\text{M}^{-1}\text{s}^{-1}$ at 25° C. At the time of this writing the discrepancy among reported rate constants for MDEA has not been rectified.

Base catalysis of the hydrolysis reaction is probably not limited to tertiary alkanolamines. Because of their greater basicity, it is probable that primary and secondary alkanolamines are better catalysts for the hydrolysis reaction than tertiary alkanolamines. However, the contribution of base catalysis to the overall reaction rate in primary and secondary alkanolamines is difficult to detect experimentally because these amines also react quickly with CO_2 to form carbamates.

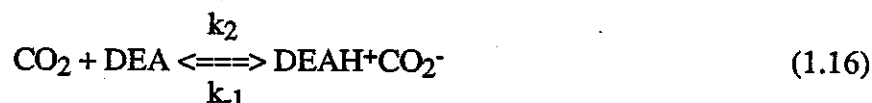
Primary or secondary alkanolamines form carbamates to a greater or lesser degree depending on K_c , the carbamate instability constant. The available literature on the reaction rate of CO_2 with primary and secondary alkanolamines has been reviewed by Blauwhoff et al (1984). For the primary alkanolamine MonoEthanolAmine (MEA), the reaction mechanism appears to be first order in both CO_2 and MEA (second order overall), and Blauwhoff concludes that fairly good agreement exists among the rate constants determined by all investigators. The data of Hikita et al (1977) represent the majority of the literature well:

$$\log_{10} k_{\text{MEA}} = 10.99 - 2152 / T \quad (1.15)$$

The units of the second order rate constant are $\text{M}^{-1}\text{s}^{-1}$ and the units of temperature are ° K. Some scatter exists in the values reported at 25° C. The reported range is 5720 to 8400 $\text{M}^{-1}\text{s}^{-1}$ (Blauwhoff et al, 1984) with an average value of 6700 $\text{M}^{-1}\text{s}^{-1}$. Insufficient information is available in the literature to interpret the rate constant as a function of ionic strength, although Laddha and Danckwerts (1982) results indicate that the presence of carbonate anion increases the rate constant.

DEA exhibits a complex reaction with CO_2 . Blauwhoff et al's (1984) review of the literature on the rate of CO_2 reaction with DEA shows that significant scatter exists in the reported values of both the reaction order and the rate constants.

Blauwhoff et al (1984) and Danckwerts (1979) found that the complex kinetics proposed by Caplow (1968) must be employed in order to explain the fractional order (between first to second order in DEA concentration) found within their data. The reaction has been postulated to proceed through an activated zwitterion intermediate. The mechanism for CO₂ reaction with DEA as presented by Blauwhoff et al is as follows:



If such an intermediate actually exists in the kinetic mechanism, terms corresponding to its deprotonation must appear in the derived rate law:

$$\text{rate}_f = \frac{k_2[\text{CO}_2][\text{DEA}]}{1 + \frac{k_{-1}}{\sum k_b[\text{base}]}} \quad (1.18)$$

Blauwhoff and coworkers studied the reaction over a wide range of concentrations and validated the rate law by demonstrating that *all* bases present in solution, not just DEA, must be considered in the proton abstraction step. This conclusion indicates that the decomposition of the intermediate (equation 1.17) may be the limiting step in the formation of the DEA-carbamate. Additionally, Blauwhoff et al found that the rate constant for proton abstraction increases in the series H₂O - DEA - OH⁻; stronger bases are apparently more effective in abstracting the proton.

Blauwhoff et al also suggested that there is no qualitative distinction between the mechanisms for CO₂ reaction with primary and secondary alkanolamines. The apparent second order overall kinetics found with MEA are

simply a limiting case of the complex mechanism in which the zwitterion formation rate is the slow step and the proton abstraction is fast:

$$\text{rate}_f \approx k_2[\text{CO}_2][\text{MEA}] \text{ if } \frac{k_1}{\sum k_b[\text{base}]} \ll 1 \quad (1.19)$$

The intermediate reaction order for DEA found by Laddha and Danckwerts (1981) and by Blauwhoff et al (1984) may be explained as resulting from similar rates for both reaction steps. The rate law allows the overall reaction order to vary with base concentration as is indicated in the results of these two studies. The rate law predicts that at high DEA concentrations the proton abstraction step becomes fast due to the presence of excess base (DEA) in solution, and therefore condition 1.19 is fulfilled and overall second order kinetics are observed. At very low concentrations of DEA the proton abstraction step can become more important and higher order kinetics would be observed.

Laddha and Danckwerts (1982) also showed that the rate of CO_2 reaction with DEA was enhanced by addition of the carbonate anion. The authors indicate that the rate of the proton abstraction step was enhanced to the point that the zwitterion formation step became limiting (as in the condition of equation 1.19). However, the presence of carbonate and sulfate anions in solution also appeared to increase the rate of zwitterion formation to some extent. The work of Laddha and Danckwerts demonstrates that the effect of ionic strength on the complex mechanism is not well understood and cannot be correlated as simply as the effect in equation 1.13.

Experimental confirmation of the rate law and mechanism postulated above has been limited to absorption conditions at which the equilibrium CO_2 vapor pressure was negligible. The need to formulate a reversible model in terms of the zwitterion mechanism is obvious in order to represent conditions in the top of the absorber or in a stripper. The extension of the model to these conditions requires the definition of a reverse reaction rate constant and an overall equilibrium constant relating reactants and the products.

If an overall equilibrium constant is applied to the postulated kinetic mechanism, then other possible reactions involving the reactants and products must be considered to be in equilibrium. For instance, if significant amounts of CO_2 are present as HCO_3^- , then carbamate must be in equilibrium with HCO_3^- in order to specify the reversibility effects through use of an overall equilibrium constant. If HCO_3^- and carbamate are not in equilibrium, then an equilibrium model cannot correctly predict the concentration of carbamate for use in specifying the driving force of the CO_2 reaction.

The rate of this conversion is not well known. Jensen et al (1954) studied the rate of carbamate conversion to bicarbonate and carbonate at 18°C in MEA and DEA. Their results indicate that the carbamate reverted first back to CO_2 and alkanolamine; the observed rate constants for carbamate reversion could be predicted by assuming the controlling step was the conversion of CO_2 to bicarbonate and carbonate through the rate in equation 1.12. This result agrees with the reversion mechanism postulated by Caplow (1968) for basic amines.

Alper and Danckwerts (1976) measured the rate of CO_2 absorption into MEA solutions and found that the absorption rate was enhanced by the presence of arsenite. The authors concluded that the conversion of carbamate to bicarbonate, which would normally be slow enough to occur in the bulk liquid, was enhanced by the presence of arsenite. Because arsenite is known to catalyze the conversion of CO_2 into carbonic acid, the fact that the absorption rate was enhanced indicates that even in the MEA solution the carbamate to bicarbonate conversion rate is limited by the slow CO_2 conversion step.

The results of Sada et al (1976) for CO_2 absorption into MEA solutions at very long contact times also indicate that the conversion reaction is slow. The conversion reaction was found to be five orders of magnitude slower than carbamate formation, a fact which indicates that the conversion reaction is slow enough to be limited by CO_2 conversion into bicarbonate.

Few mass transfer experiments have been conducted under conditions where the reversibility of the reaction is important, possibly because of the difficulty inherent in analyzing the results of such experiments.

Section 2

THEORY

2.1 Physical Mass Transfer Models

2.1.1 Film theory

The film model for mass transfer resistance across a phase boundary was first proposed by Nernst (1904). The model assumes that all resistance to mass transfer is located in a "stagnant film" at the phase boundary. A steady-state profile of the diffusing species exists between fixed boundary values at both sides of the film. Consequently, the gradient of the diffusing species will exhibit a discontinuity at the boundary between the film and the bulk of the phase. This model, though a gross simplification of reality, has found extremely wide application because of its simplicity. It has also been noted (Sherwood et al, 1975) that this simple theory provides very accurate results. The film theory equation for mass transfer of a diffusing species in a binary system is easily integrated to yield the mass transfer rate (R_a) as a function of driving force ($\Delta[A]$). For a sparingly soluble gas (A) diffusing through a liquid, the rate equation becomes:

$$R_a = \frac{D a \Delta[A]}{L} = k_l^0 a \Delta[A] \quad (2.1)$$

The important observation that can be drawn from equation 2.1 is that the "mass transfer coefficient", or the constant of proportionality in the equation (k_l^0), is itself proportional to the first power of the diffusion coefficient. Experimental investigations of gas-liquid mass transfer in stirred tanks have found the actual power on the diffusion coefficient to be closer to 0.5. This inconsistency is a major limitation of the film theory as applied to gas absorption.

2.1.2 Penetration theory

Higbie (1935) proposed a more realistic theory based on an unsteady-state model of gas-liquid surfaces. Underlying Higbie's penetration theory is the fact that during gas-liquid contacting, the liquid surface is often not exposed long enough to reach a steady-state. Conceptually, surface is created and destroyed before saturation occurs. In this case, a penetration model describing unsteady-state transport into the liquid surface is a more realistic model than the steady-state film theory. The transient diffusion of gas into the stagnant liquid occurs for some contact time t before the surface is destroyed. The average mass transfer rate is then:

$$R_a = 2 a \Delta[A] \sqrt{\frac{D}{\pi t}} = k_l^0 a \Delta[A] \quad (2.2)$$

The proportionality constant between flux and driving force can be interpreted as an average mass transfer coefficient:

$$k_l^0 = 2 \sqrt{\frac{D}{\pi t}} \quad (2.3)$$

Higbie's theory provides a proportionality between k_l^0 and the 0.5 power of the diffusion coefficient. This proportionality is closer to the value of 2/3 predicted from the Chilton-Colburn analogy. It also represents the bulk of experimental data on mass transfer in contactors of relatively low values of t , such as short wetted-wall columns, packed columns and liquids surrounding gas bubbles (Bird et al, 1960).

2.1.3 Surface renewal theory

Danckwerts (1970) extended Higbie's theory to allow for a distribution of contact times. In contacting equipment such as stirred vessels, it is physically realistic to expect a distribution of surface agitation; therefore Danckwerts'

extension increases the physical validity of Higbie's model. Danckwerts' surface renewal theory provides for fresh fluid elements to reach the surface and remain for some contact time, the value of which is anywhere between zero and infinity. A mean steady-state flux is calculated by integrating over the full range of contact times which are weighted by the distribution of surface ages. The following equation for the average absorption rate is the result of integration:

$$R_a = \sqrt{D} s \Delta[A] \quad (2.4)$$

The proportionality constant between flux and driving force is dependent on s , the fractional surface renewal rate. The surface renewal model agrees with penetration theory in predicting the dependence of the mass transfer coefficient on the 0.5 power of the diffusion coefficient:

$$k_1^0 = \sqrt{D} s \quad (2.5)$$

As will be discussed later, the gas-liquid transport data in this project were generated in a stirred tank reactor, which exhibits contact times much larger than those found in industrial contactors such as packed or tray towers. Because of the different dependence of the mass transfer coefficient on the diffusion coefficient predicted between the film model and the penetration/surface renewal models, there is an uncertainty about the correct model choice for this type of gas-liquid contactor. In a review article on gas absorption in stirred tanks, Bin (1984) found that the reported experimental dependencies of k_1^0 on the diffusion coefficient varied over the range 0.4 to 0.8. In this work the surface renewal model, with its realistic diffusion coefficient dependence, was chosen to represent mass transfer.

The mass transfer model must be integrated with kinetic information in order to predict the combined effects of reaction and mass transfer. The transport problem is complicated by the necessity of including chemical equilibria in the analysis; however, in the next section some simple limiting cases are identified.

2.2 Mass Transfer with Chemical Reaction

2.2.1 For a single bimolecular reaction: $A + \nu B \rightleftharpoons C + D$

In the presence of chemical reaction, a reaction rate term must be added to the diffusion equation in order to account for the depletion or production of the gas within the liquid:

$$D_a \frac{\partial^2 [A]}{\partial x^2} = \frac{\partial [A]}{\partial t} + \text{Rate}_f \quad (2.6)$$

$$\text{Rate}_f = k_{n+1}[A][B]^n$$

where n is the reaction order of the species B (not necessarily the same as the stoichiometric coefficient) expressed here in an irreversible manner.

The introduction of the chemical reaction and the associated chemical equilibria into the above equation can introduce nonlinearities which make the explicit, analytical solution of the equation impossible. However, depending on the speed of the reaction in comparison with the speed of mass transfer, certain asymptotically limiting expressions can be developed. These limits are presented here for comparison purposes; the approximate solution technique adopted for representing the full range of reaction rates will be described in detail later.

2.2.2 Analytically solvable asymptotes

The transport of a reactive, sparingly soluble gas to and from a solvent is a classic problem in mass transfer with chemical reaction. For a single bimolecular reaction, a dimensionless reaction rate parameter (commonly called the Hatta number) can be defined:

$$Ha = \frac{k_{n+1}[B]_b^n D}{(k_l^0)^2} \quad (2.7)$$

The Hatta number gives an indication of the relative speeds of chemical reaction and mass transfer. Under certain conditions, the Hatta number is directly related to the enhancement factor, E , which represents transport rate enhancement due to the effects of chemical reaction. The enhancement factor is defined simply as:

$$E = \frac{R_a \text{ with reaction}}{R_a \text{ in the absence of reaction}} \quad (2.8)$$

The true relationship of Ha and E is shown qualitatively in figure 1. When Ha is small, the rate of reaction is sufficiently slow that it does not seriously affect the transport rate, and E is essentially equal to 1. In this regime, called the "slow" regime, the reaction kinetics are obviously not needed to represent the total mass transfer rate.

As the rate of reaction increases with respect to the rate of diffusion, the transport rate increases until it is dominated by the reaction rate. In this regime, called the fast, or pseudo-first order regime, the enhancement factor is proportional to the square root of the rate constant. The regime is termed "pseudo-first order" because no gradient in the liquid reactant occurs and therefore the interface conditions can be represented by the bulk conditions: no change in the liquid reactant concentration occurs. When no liquid reactant gradient exists the reaction order of the liquid phase reactant can be lumped into a "pseudo-concentration" and the pseudo-first order rate constant can be defined:

$$\text{rate}(A) = k_0 [A] = k_{n+1} [B]_b^n [A] \quad (2.9)$$

$$k_0 = k_{n+1} [B]_b^n \quad (2.10)$$

where n is the known reaction order of reactant B ($n=1$ for a bimolecular reaction)

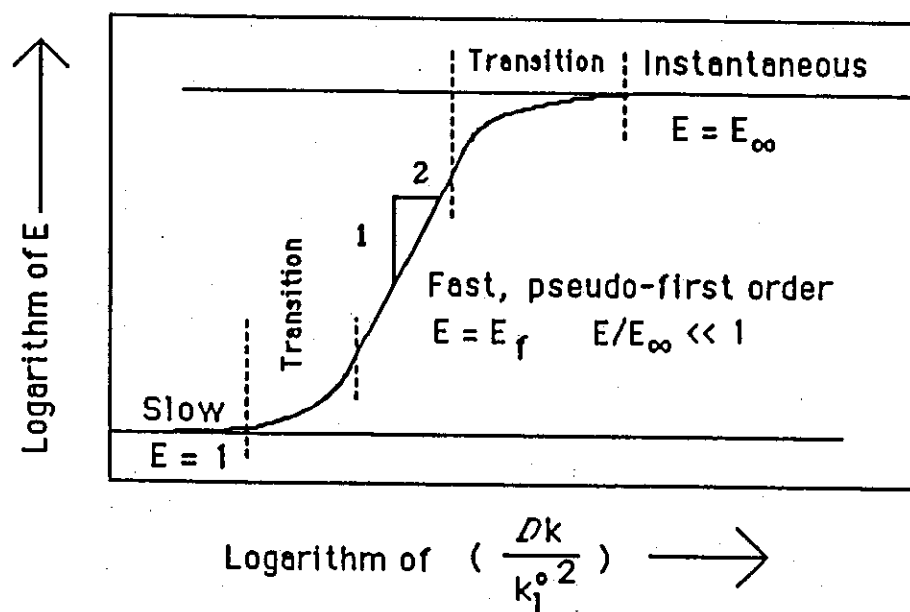


Figure 1: The behavior of the enhancement factor as a function of the Hatta number. At large values of the rate constant (or small mass transfer coefficients) the instantaneous limit is approached.

The proportionality described for the fast, pseudo-first order regime can be demonstrated by the development of the enhancement factor. Equation 2.6 can be easily solved for conditions where the interface concentration of reactant B is approximately the same as that in the bulk liquid. Integrating equation 2.6 for film theory ($\partial[A]/\partial t \approx 0$) leads to the equation for the flux of A. A change of variable is defined in which the driving force ($A_i - A_b$) is replaced by the variable \dot{A} :

$$D \frac{d[A]}{dx} = \sqrt{2D} \int \text{rate}(\dot{A}) d\dot{A} = \sqrt{2D} k_o \int (\dot{A}) d\dot{A} \quad (2.11)$$

$$= \sqrt{D k_o \dot{A}^2} \quad (2.12)$$

$$= \dot{A} \sqrt{D k_o} \quad (2.13)$$

Equation 2.14 is developed from the definition of the enhancement factor:

$$E_F = \frac{\dot{A} \sqrt{D k_o}}{k_l \dot{A}} = \frac{\sqrt{D k_o}}{k_l} \quad (2.14)$$

The advantage of conducting experiments in the fast regime is that the measured mass transfer rate is independent of the mass transfer coefficient because the mass transfer rate is completely controlled by the reaction rate and is therefore independent of the liquid hydrodynamics. Operation in this regime is the goal of experiments designed to measure reaction rate constants and reaction order of the liquid phase reactant because the order may be determined by varying the liquid phase concentration without concern about the effects of liquid agitation rate.

The apparent rate constant can be defined as a rate of absorption or desorption normalized with the driving force (ΔP):

$$k_{app} = \left(\frac{R}{a \Delta P \frac{\sqrt{D}}{H}} \right)^2 \quad (2.15)$$

In the absence of diffusion effects, the apparent rate constant will equal the pseudo-first order rate constant defined by equation 2.10.

Equation 2.11 for the flux neglects the contribution of the physical diffusion of the gas to the overall mass transfer rate. Neglecting this effect is a good assumption in the fast reaction regime since by definition the net reaction rate is large in comparison with the rate of physical diffusion.

The next asymptotic limit can be defined when the rate of reaction is *much* faster than the rate of diffusion. The reaction is so fast that chemical equilibrium is attained at the gas-liquid interface and the transport rate becomes independent of the reaction rate. Instead of being limited by the reaction rate, the transport rate is limited by the rate of diffusion of liquid reactants to the interface. Under these conditions, mass transfer occurs in the instantaneous regime. The enhancement factor corresponding to the instantaneous regime represents an upper bound on the potential enhancement of mass transfer.

In the instantaneous regime the interface concentration of liquid reactants is determined by chemical equilibrium and can be calculated by application of an equilibrium model with the gas concentration at the interface (Chang and Rochelle, 1980; Olander, 1960). A simple explicit equation is presented by Astarita et al (1983) for the limiting case of absorption with a single irreversible instantaneous reaction for the film theory (for equal diffusivities):

$$E_{\infty-\text{irrev}} = 1 + \frac{[B]_b}{[A]_i} \quad (2.16)$$

2.2.3 Transition regions

The definition of asymptotic regimes is important in the evaluation of experimental data. Most investigations of reaction rates in gas absorption are conducted with the intent of operation within the fast reaction regime. However, the range of applicability of the regime is somewhat poorly defined. Astarita et al

(1983) proposed the following approximate equation for representing the transition between the slow and the fast regimes:

$$E_{s-F} = \sqrt{1 + \frac{k_o D}{k_l^2}} \quad (2.17)$$

The rate of transport in the transition region is:

$$R = \sqrt{k_l^2 + k_o D} \quad a \Delta[A] \quad (2.18)$$

Astarita et al (1983) concluded that the approximate equation is accurate to within 10% of the results of both film and surface renewal theories for the transition region.

Ulrich (1983) concluded that the transition between the slow to the fast regime was largely complete for values of the enhancement factor greater than 4. He noted that at enhancement factors greater than 4 the effects of mass transfer on the measured value of the rate constant could be neglected without introducing more than 7% error in the enhancement factor:

$$\text{if } E > 4 \text{ then } k_o D \gg k_l^2$$

$$\text{and so } E_{s-F} \approx E_F = \frac{\sqrt{k_o D}}{k_l} \quad (2.19)$$

If the mass transfer coefficient is known with some degree of confidence, inclusion of the "1+" term in the enhancement factor can give more accurate results. The "1+" term is included in the function form for the slow-to-fast transition and the fast reaction regime enhancement factors as an approximation in this work.

The transition from the fast to the instantaneous regime is more difficult to handle. As the reaction rate begins to exceed the rate of diffusion in the liquid, significant gradients of liquid reactants are created. When the reaction becomes this fast, it will occur largely near the interface and the rate can be calculated if interface

concentrations are known. In the transition region the assumption of pseudo-first order conditions begins to break down. Significant gradients of liquid reactants occur and so the interface composition can no longer be represented by the bulk composition.

In order to calculate the reaction rate at the interface, the diffusivities of the liquid reactants must enter into the solution technique since the interface conditions must be calculated from diffusion and reaction rate considerations. Consequently, approximate techniques which have been developed to represent this transition region are generally numerical (iterative) in format. The sharpness of the transition depicted in figure 1 is a characteristic of the individual reaction and approximate treatment of this transition region can require system-specific adjustable constants (Astarita et al, 1983).

Sharma and Danckwerts (1963) proposed the following criterion for determining the importance of this transition. The criterion was developed from consideration of the solution capacity for both mass transfer and reaction rate:

$$Q = \frac{E_F}{E_\infty} \quad \text{and} \quad E \approx E_F \quad \text{if} \quad Q \ll 1 \quad (2.20)$$

Unfortunately, the criterion is somewhat qualitative. Therefore the difficulty associated with the use of this criterion is the question of exactly how small Q must be in order to completely neglect diffusion effects.

2.2.4 Macroscopic effects

The applicable enhancement factor regime will vary as a function of driving force in a given contactor and solution composition. Figure 2 shows the qualitative behavior of the enhancement factor as a function of driving force for a bimolecular reaction. At very low values of the driving force only small liquid phase gradients occur and the fast reaction regime applies. As the driving force increases so does the importance of liquid phase gradients until eventually liquid diffusion controls

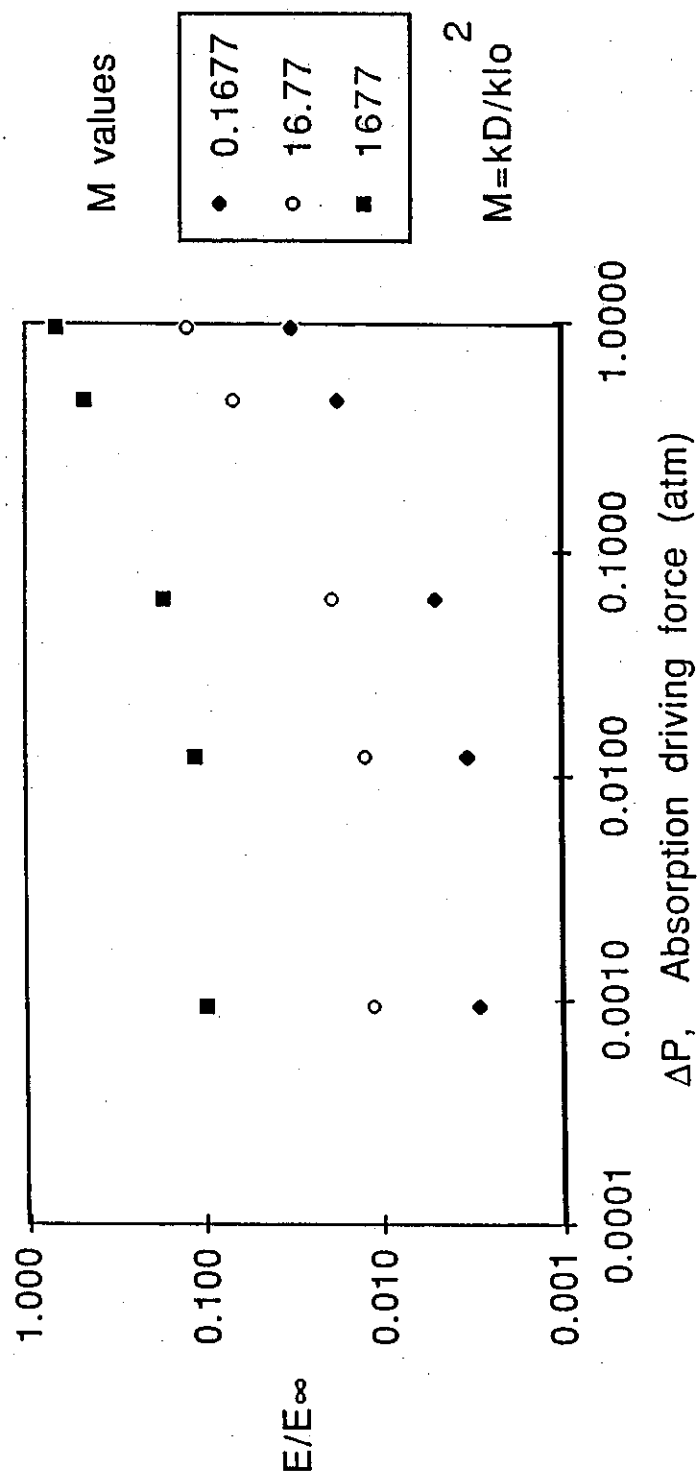


Figure 2: Effect of driving force on diffusion limitations in the measurement of the enhancement factor. At lower driving force diffusion limitations are minimized.

the transport rate. In the limit of very large driving forces the instantaneous enhancement factor is approached.

The effect of variation of the mass transfer coefficient is also shown on figure 2. When diffusion effects are important, variation of the mass transfer coefficient will change the resulting value of the enhancement factor. Under conditions where the enhancement factor is in the fast reaction regime, it is independent of the driving force and inversely proportional to the mass transfer coefficient.

Figure 2 shows that it is possible to verify experimentally the relative importance of diffusion and reaction effects on mass transfer. It also indicates that for a given value of the mass transfer coefficient a finite range of rate constants can be determined at a given driving force. This range of rate constants can be expanded by lowering the driving force. However, an experimental limit obviously exists on the minimum measurable size of the driving force. Therefore a limited range of enhancement factors can be determined at pseudo-first order conditions in a given contactor, even with control of the driving force.

A more quantitative treatment of mass transfer with chemical reaction is required to handle the transition between regimes. The ultimate goal of this work is to represent reaction and mass transfer in mixed solvents in which the components may react at widely different rates. The transition regions cannot therefore be ignored: a set of conditions which gives the pseudo-first order regime for one component may well give a transition region for the other. Because of this complexity a technique must be adopted for representing the entire range of enhancement factors.

2.3 Solubility and Diffusion Coefficient of CO₂

If a measured rate of absorption can be shown to lie in the fast, pseudo-first order reaction regime then it can yield a value of the rate constant for the reaction without consideration of mass transfer contributions. However, from equation 2.13 it is evident that the interface free dissolved gas concentration and an estimate of the diffusion coefficient of the gas must be known in order to calculate a rate

constant. The interface partial pressure is usually known and therefore the interface free dissolved gas concentration can be estimated from a Henry's law relationship. Unfortunately, this also requires a knowledge of the Henry's law constant for the gas in the solution of interest. It is unfortunate because it is very difficult to measure the physical solubility and diffusion coefficient of a reactive gas in the solution of interest.

In practice it is only necessary to know the product of the solubility and the square root of the diffusion coefficient and not the individual values provided that the conditions of the fast, pseudo-first order regime apply:

$$R_a = \sqrt{k_o} a P_i \frac{\sqrt{D}}{H} \quad (2.21)$$

The combined parameter \sqrt{D}/H must still be estimated since it cannot be measured directly under conditions where the reaction rate would contribute to the mass transfer rate. One technique which has been used to estimate this value directly in the solution of interest is to measure the absorption rate in a contactor which exhibits very fast physical mass transfer--mass transfer fast enough that the reaction rate is slow by comparison. The absorption rate would then be governed by equation 2.3 (if penetration theory represents the contacting) and not by equation 2.21; therefore the physical mass transfer coefficient must be known with confidence in order to obtain \sqrt{D}/H . The parameter measured this way could then be used to interpret data from a contactor in which mass transfer is slow enough that the reaction rate controls the absorption rate.

One limitation is immediately obvious. The technique is limited to somewhat slow reactions since purely physical absorption must be achieved in the fast contactor. In practice, the reaction rates of 1' and 2' alkanolamines are too fast to apply this technique. Haimour and Sandall (1984) were successful in measuring the combined parameter for CO₂ absorption into aqueous MDEA solutions at low temperatures and short contact times in a laminar jet.

A more approximate yet more generally applicable technique has become widely accepted for estimating the combined parameter for CO₂ in aqueous

alkanolamine solutions. Although the solubility and diffusion coefficient of the chemically reactive CO_2 cannot be directly measured, both can be directly measured for N_2O , which is a very similar gas (Sada et al, 1978). The assumption is then made that the effects of solution composition on N_2O are the same as the effects on CO_2 . The " N_2O analogy" is then applied:

$$\frac{D_{\text{CO}_2\text{-AMINE}}}{D_{\text{CO}_2\text{-H}_2\text{O}}} = \frac{D_{\text{N}_2\text{O-AMINE}}}{D_{\text{N}_2\text{O-H}_2\text{O}}} \quad (2.22)$$

$$\frac{H_{\text{CO}_2\text{-AMINE}}}{H_{\text{CO}_2\text{-H}_2\text{O}}} = \frac{H_{\text{N}_2\text{O-AMINE}}}{H_{\text{N}_2\text{O-H}_2\text{O}}} \quad (2.23)$$

Haimour et al's (1985) direct measurements of the combined parameter confirm the analogy for MDEA solutions. Versteeg (1987) has recently published an extensive study of the diffusion coefficient of N_2O in a variety of amines and over a range of temperatures and proposed the following modified Stokes-Einstein relationship:

$$(D_{\text{N}_2\text{O}} \mu_k)^{0.8}_{\text{AMINE}} = (D_{\text{N}_2\text{O}} \mu_k)^{0.8}_{\text{H}_2\text{O}} \quad (2.24)$$

where μ_k is the kinematic viscosity of the solution.

The correlation is very useful because it allows the estimation of CO_2 diffusion coefficient with only a knowledge of the solution's viscosity, a quantity which is easily determined experimentally. The N_2O solubility must still be known in order to estimate the combined parameter.

Blauwhoff et al (1984) present empirically correlated values of the combined parameter for several amines over a wide concentration range. However, only values at 25°C were correlated. The values of the solubility and diffusion coefficient parameter used in data interpretation are shown in tabular form in appendix B.

2.4 Development of Reaction Rates for Reversible Reactions

When the reaction becomes fast enough with respect to mass transfer to consider diffusion effects, the reversibility of the reaction may also be an issue. Consider a single bimolecular reaction representing the reaction of a volatile component, A, with a liquid phase reactant, B:



The forward and reverse reaction rates are then:

$$\text{rate}_f = k_1[A][B] \quad (2.26)$$

$$\text{rate}_r = k_2[C][D] \quad (2.27)$$

At equilibrium these two rates are by definition equal and the equilibrium constant can be defined as:

$$K = \frac{k_1}{k_2} = \frac{[C][D]}{[A][B]} \quad (2.28)$$

When non-equilibrium conditions prevail the rate of change of reactant and product concentrations can be described by unsteady-state mole balances. In a volume of reacting liquid, the rate of change of reactant A is expressed as follows:

$$\frac{\partial[A]}{\partial t} = k_1[A][B] - k_2[C][D] \quad (2.29)$$

If the equilibrium relationship defined by equation 2.28 is substituted into the mole balance, then an expression is formed in terms of only the forward rate

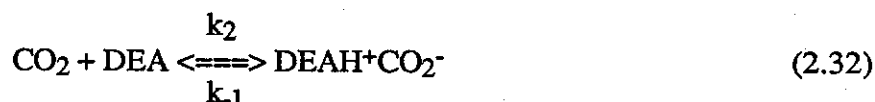
constant and the reaction driving force. The reaction driving force represents the displacement from thermodynamic equilibrium, so the representation of the driving force must contain estimates of the equilibrium concentrations of reactants. This estimate is calculated from the known solution concentration of reactant B and the equilibrium constant K:

$$\frac{\partial[A]}{\partial t} = k_2([A][B] - K[C][D]) = k_2([A][B] - [A]_e[B]) \quad (2.30)$$

Since the value of the concentration of reactant B is specified in the calculation, it can be separated from the driving force:

$$\frac{\partial[A]}{\partial t} = \text{rate} = k_2[B]([A] - [A]_e) \quad (2.31)$$

If the reaction occurs in more than one step, a more complex equilibrium must be defined. Consider the case of reaction of DEA with CO₂. For a reversible reaction, an additional rate constant must be considered for the reverse of step 2 (Caplow, 1968):



From an unsteady-state balance on the CO₂ concentration, and assuming a pseudo-steady-state concentration of the zwitterion, the following rate law can be derived:

$$\text{rate} = \frac{k_2[\text{CO}_2][\text{DEA}]\sum k_b[\text{base}] - k_1[\text{DEACO}_2^-]\sum k_b[\text{baseH}^+]}{k_1 + \sum k_b[\text{base}]} \quad (2.34)$$

Equation 2.34 can only be reduced to a simple form analogous to that of equation 2.31 if an overall equilibrium constant is defined between the reactants of the two steps and the products of the second step for each base (including DEA):

$$K_b = \frac{[\text{DEACO}_2^-][\text{baseH}^+]}{[\text{CO}_2][\text{DEA}][\text{base}]} = \frac{k_2 k_b}{k_{-1} k_{-b}} \quad (2.35)$$

With these definitions, the complex rate equation can be reduced to:

$$\text{rate} = \frac{k_2 [\text{DEA}] \sum k_b [\text{base}]}{k_{-1} + \sum k_b [\text{base}]} ([\text{CO}_2] - [\text{CO}_2]_e) \quad (2.36)$$

This equation can be put into the form of the rate law used by Laddha and Danckwerts (1981) by dividing both the numerator and the denominator by the quantity $k_2 \sum k_b [\text{base}]$ (and by performing suitable algebra):

$$\text{rate} = \frac{[\text{DEA}]([\text{CO}_2] - [\text{CO}_2]_e)}{\frac{1}{K_2} + \frac{1}{\sum k_{b\text{-eff}} [\text{base}]}} \quad (2.37)$$

$$\text{where for each base in solution } k_{b\text{-eff}} = \frac{k_b k_2}{k_{-1}}$$

Equation 2.37 is important because it demonstrates that it is possible to obtain the same reaction rate constants from reaction rate measurements regardless of the direction of the driving force. This conclusion is limited to conditions at which equations 2.32 and 2.33 represent the dominant mechanism for CO_2 reaction.

2.5 Quantitative Treatment for a Single Reversible Reaction

In order to predict exactly mass transfer enhanced by a reversible reaction, the diffusion equation must be integrated in combination with an equilibrium model which can provide reaction driving forces at each point in the liquid film. This

diffusion/reaction equation is coupled with a similar equation for each species involved in the reacting system. Several researchers have solved this equation numerically for various types of reaction kinetics (Ulanowicz and Frazier, 1968; Brian and Beaverstock, 1965; Cornelisse et al, 1980; Blauwhoff and Van Swaaij, 1982; Katti and Wolcott, 1987). Because the existence of chemical reaction makes the system of equations nonlinear, numerical solution of the equations is required for exact answers, and the full solution of the equations can be expensive in terms of computational time. Considering that the solution of the diffusion/reaction equations is the fundamental routine in a typical absorber/stripper model and as such is called literally thousands of times (Hermes, 1987), full solution of the equations is impractical.

Consequently, a number of researchers have published approximate solution techniques which require less solution time (DeCoursey, 1982; Hikita and Asai, 1964; Hikita et al, 1979; Jhaveri, 1969; Onda et al, 1970(a-c); Ouwerkerk, 1978; Roper et al 1962). In general, these techniques apply an approximation to the profile of liquid reactants in solution in order to force the equation into a form which can be integrated. The techniques usually assume that the reaction occurs near the interface and so must predict the interface conditions in order to establish the appropriate reaction rate. The resulting solutions are algebraic in form rather than differential.

In this work the approximate solution technique derived by DeCoursey (1982) is applied to the diffusion/reaction problem. The function form requires the application of a model for the instantaneous enhancement factor to provide an upper limit on the reaction enhancement. Approximate surface renewal theory (Chang and Rochelle, 1980) is adopted for this purpose.

DeCoursey's technique allows for the evaluation of the reaction rate at the gas-liquid interface. The interface composition must be known in order to calculate the reaction rate; this composition is determined in an iterative manner. In addition, the profile of CO_2 near the interface is corrected for the effects of reversibility of the reaction.

A condition of zero flux of charge is superimposed on the equations by requiring that all charged species have the same diffusion coefficients.

The equations used are as follows:

DeCoursey's Equation 28 is:

$$E = \left\{ 1 - \frac{M_R \beta \emptyset}{(C_9 - 1)(C_9^2 - 1 - M_R \beta)} - \frac{C_9 \emptyset}{C_9 - 1} \right\} \sqrt{1 + M_R \beta} + \frac{C_9 M_R \beta \emptyset}{(C_9 - 1)(C_9^2 - 1 - M_R \beta)} + \frac{C_9 \emptyset}{C_9 - 1} \quad (2.38)$$

Where:

M_R is the dimensionless rate constant, and is expressed in terms of mass transfer coefficients instead of fractional surface renewal:

$$M_R = \frac{k_2 [\text{Base}]_b D_{\text{CO}_2}}{k_1 \sigma^2} \quad (2.39)$$

β is the normalized interface concentration of the primary liquid reactant:

$$\beta = \frac{[\text{Base}]_i}{[\text{Base}]_b} \quad (2.40)$$

\emptyset is an adjusted driving force for the reaction:

$$\emptyset = \frac{[\text{CO}_2]_{ei} - [\text{CO}_2]_b}{[\text{CO}_2]_i - [\text{CO}_2]_b} \quad (2.41)$$

The value of \emptyset is bounded between unity, which represents the maximum possible rate enhancement (instantaneous reaction regime) and zero, which indicates that liquid diffusion is unimportant (bulk conditions \approx interface conditions).

$[\text{CO}_2]_{ei}$ is the concentration of free CO_2 which is at chemical equilibrium with the predicted interface composition.

$[\text{CO}_2]_i$ is the actual free CO_2 concentration at the gas-liquid interface. It is determined from the Henry's Law relationship.

C_9 is a constant in the equation the value of which was set at 1.1.

The combination of $M_R\beta$ yields an evaluation of the reaction rate parameter at interfacial, rather than bulk liquid, conditions. To find the value of β , which represents the free reactant concentration at the interface, a diffusional correction is applied to predict the total interface concentration of CO_2 . The total CO_2 concentration is approximated as: $\text{CO}_{2,\text{total}} \approx \text{HCO}_3^- + \text{CO}_3^{2-} + \text{AMCO}_2^-$. The diffusional correction applied considers the difference between the diffusion coefficients of CO_2 and of the ionic products:

$$[\text{CO}_{2,\text{total}}]_i = \frac{R_a}{k_{10} a \left(\frac{D_{\text{IONS}}}{D_{\text{CO}_2}} \right)^{0.5}} + [\text{CO}_{2,\text{total}}]_b \quad (2.42)$$

In real solutions it is likely that the reactants are sufficiently dissimilar in size, shape and chemical nature that their diffusion coefficients will be unequal. In this real case, the effect of unequal diffusivities must be considered in the treatment of mass transfer rate enhancement. In the fast reaction regime, diffusion effects are by definition unimportant and therefore the diffusion coefficient difference is inconsequential. However, in the instantaneous regime the diffusion of reactants is rate controlling and so the diffusion coefficient ratio must enter the enhancement factor equation.

Chang and Rochelle (1980) showed that in the case of instantaneous reactions the full numerical solution for surface renewal theory with unequal diffusivities could be approximated by substituting the square-root dependency of the diffusion coefficient ratio into the film theory equation:

$$E_{\infty\text{-irrev}} \approx 1. + \left(\frac{D_B}{D_A} \right)^{0.5} \frac{[B]_b}{[A]_i} \quad (2.43)$$

This engineering approximation can also be applied to reversible cases and reactions of other stoichiometries. However, in the real solutions of interest consideration must be given to the fact that the reaction products of CO₂ with amine solvents are ionic in nature. Since the ionic species are likely to have unequal diffusion coefficients, the treatment of the mass transfer enhancement factors must contain the constraint that no net flux of electrical charge is possible within the liquid. This physically real condition results in the creation of "effective" diffusion coefficients calculated from this constraint. The practical effects of this phenomenon have been treated by Astarita et al (1983) and the result for a binary system is that the effective diffusion coefficients of the ions must be equal. In the treatment of this work, the diffusion coefficients of all liquid phase components (except CO₂) are set equal to the MDEA diffusion coefficient:

$$D_{\text{MDEA}} = D_{\text{MDEAH}^+} = D_{\text{IONS}} \quad (2.44)$$

where D_{IONS} denotes the diffusion coefficients of all ion products and reactants.

A value of 0.41 was used for the ratio of the diffusion coefficients of MDEA and CO₂, which was assumed to be independent of temperature and viscosity.

The constraint of equation 2.44 eliminates the possibility of unrealistic potential gradients being formed in the calculation of enhancement factors. Therefore in the diffusional correction (equation 2.42), the mass transfer coefficient for CO₂ has been corrected for the difference in the diffusion coefficients with the square-root dependency of approximate surface renewal theory.

With the total interface concentration of CO₂ specified from the application of equation 2.42, an equilibrium speciation model can be applied to the known solution composition at the interface. The speciation model yields the value of

$[\text{Base}]_i$ at the specified CO_2 loading, and also yields the value of $[\text{CO}_2]_{ei}$ for use in calculation of the adjusted driving force. Implicit in the solution procedure is the assumption that the concentration of free CO_2 is small enough to neglect in comparison to the total CO_2 concentration. This assumption is true for pH values much greater than the pK value for the first dissociation constant of carbonic acid (≈ 6.3).

Figure 3 shows the flowcharted logic for this solution procedure. The approximate technique has been verified by comparison with a full numeric solution for absorption with a binary reversible reaction (Glasscock, 1987). Figure 4 shows the deviation of the approximate technique from the numerical results for a range of enhancement factors. The parameters used in creating figure 4 are typical of an MDEA solution. The agreement is quite good and validates the approximate technique for a second order reversible reaction.

The solution technique should also apply for the case of more complex kinetics (such as for DEA) since the development of DeCoursey's technique is in terms of the pseudo-first order rate constant, which is adjusted for deviations from pseudo-first order behavior. It is assumed that the technique is applicable to complex kinetics; however, this assumption has not been checked with numerical results. A comparison with a full numerical solution must be made before a conclusion can be drawn on the applicability of the technique. Therefore the DeCoursey technique has not been used to interpret experiments on complex reaction kinetics.

2.6 Enhancement Factors in Mixed Solvents

2.6.1 Equilibrium and non-equilibrium interactions

When more than one liquid reactant is present, the solution to equation 2.6 becomes further complicated by the possible existence of equilibrium and non-equilibrium interactions between the liquid reactants. Equilibrium interactions certainly exist in mixed alkanolamine solvents, where the amine concentrations are linked through pH equilibria.

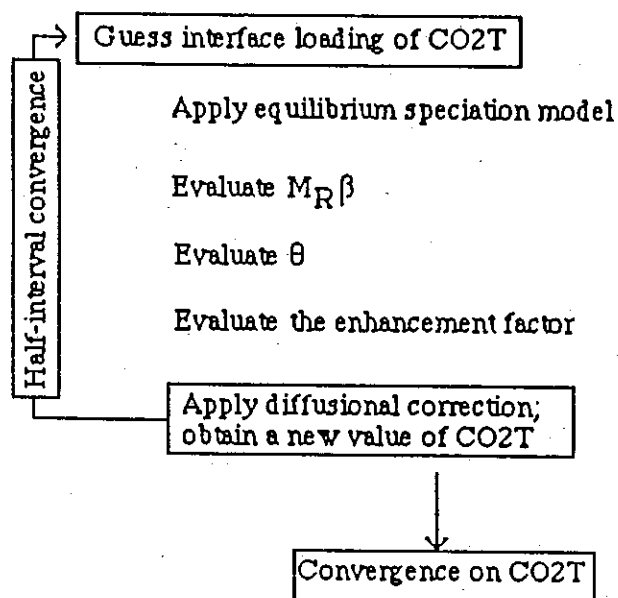


Figure 3: Approximate solution technique for the enhancement factor. Calculation is an iterative process in which the interface total CO₂ content is estimated.

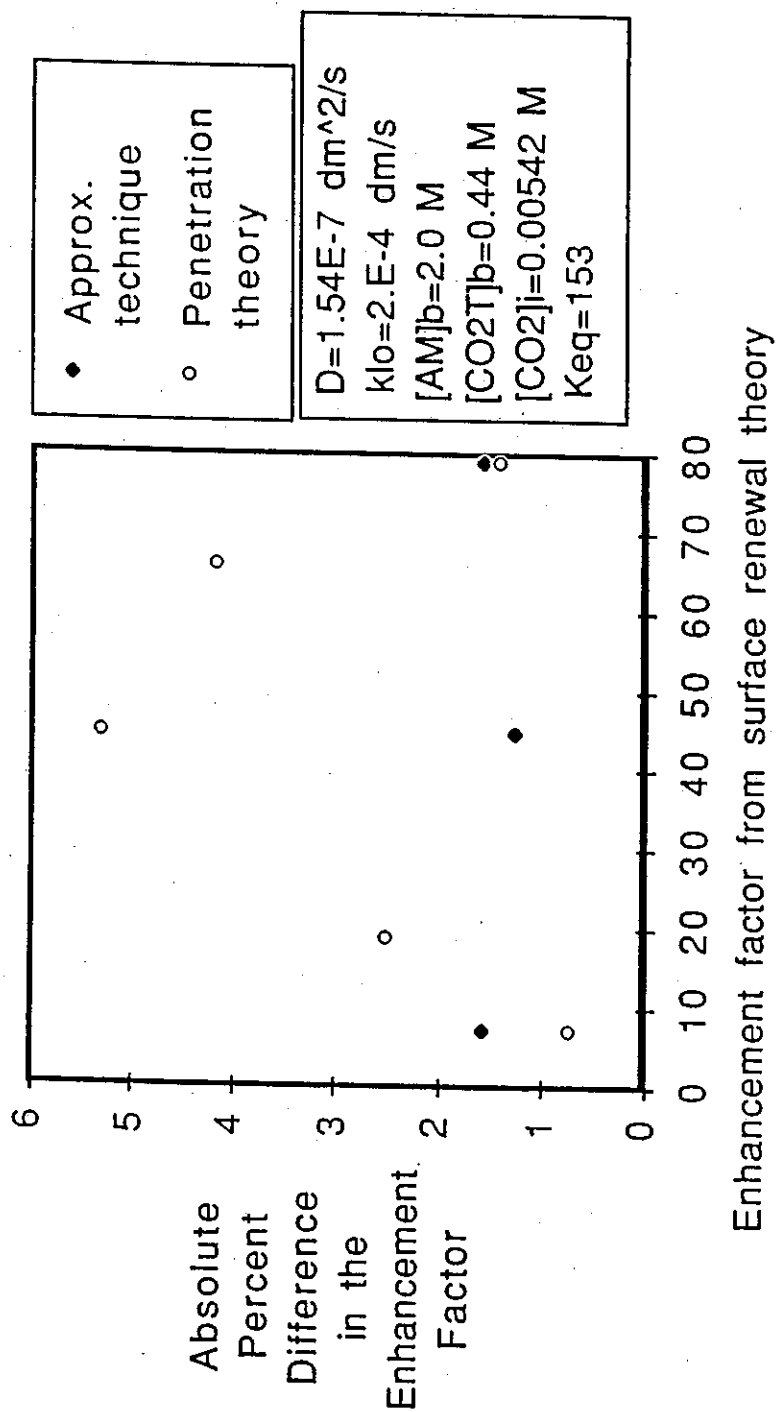


Figure 4: Agreement of the approximate solution technique with the full numerical solution of surface renewal theory. The results shown were generated with a diffusion coefficient ratio (amine/ CO_2) of 0.6 and for the bimolecular reaction: $CO_2 + AM \rightleftharpoons HCO_3^- + AMH^+$

Two types of non-equilibrium interactions between the solvents can exist. First, if the reaction of CO_2 with one of the liquid reactants is complex and behaves according to the complex kinetics of equation 2.37, the other liquid reactant can enter into the kinetics of carbamate formation. This interaction is purely kinetic and will exist regardless of diffusion effects in the liquid. Consequently, the existence of this interaction can be established by determination of rate constants under pseudo-first order conditions.

The second type of interaction is a mass transfer effect which arises mainly from the stability of the carbamate produced from reaction of CO_2 with the promoter.

CO_2 which absorbs into a mixture of 1' or 2' alkanolamine and 3' alkanolamine can react to form carbamate and/or bicarbonate. In the presence of a large amount of tertiary alkanolamine, carbamate formation is less favored thermodynamically as the chemical sink for CO_2 . This fact can be proven by considering the equilibrium behavior of a mixture of 1' or 2' alkanolamine and a 3' alkanolamine. When no 1' or 2' alkanolamine is present, the favored chemical sink for CO_2 is of course bicarbonate: no carbamate can form. It is easy to see then that as the composition of the alkanolamine mixture approaches a purely 3' alkanolamine solution, a significant amount of the CO_2 present must exist in the bicarbonate form at equilibrium. This behavior is shown in figure 5 which was generated through application of a thermodynamic model.

Although equilibrium requires the bicarbonate to be favored at small 1' or 2' amine concentrations in the mixture, from a purely kinetic viewpoint the carbamate is the favored sink for CO_2 . The rate of carbamate formation by reaction with the 1' or 2' alkanolamine is much faster than the rate of bicarbonate formation. It is possible that under some conditions more carbamate will form upon CO_2 absorption than is thermodynamically favorable at the bulk liquid conditions: the carbamate formed must then revert to the stable bicarbonate form. Consideration of the rate of this conversion leads to two simple models describing CO_2 absorption into mixture solvents.

Figure 6 qualitatively defines the two simple models in terms of the relative reaction rates of carbamate formation and conversion into bicarbonate. The

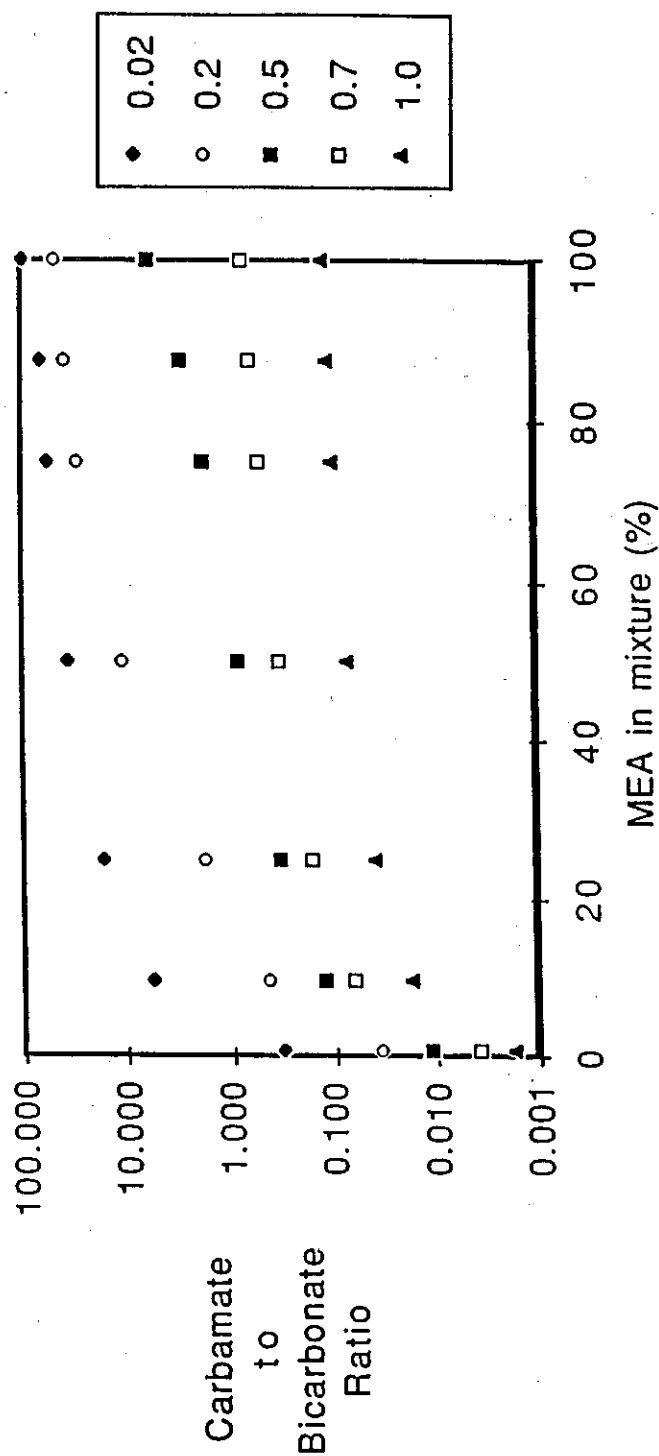


Figure 5: The fate of chemically reacted CO₂ in an MEA/MDEA mixture. The mixture behaves more like a tertiary amine as the MEA content decreases and the loading increases. Loadings (mole total CO₂/mole amine) are shown in the key.

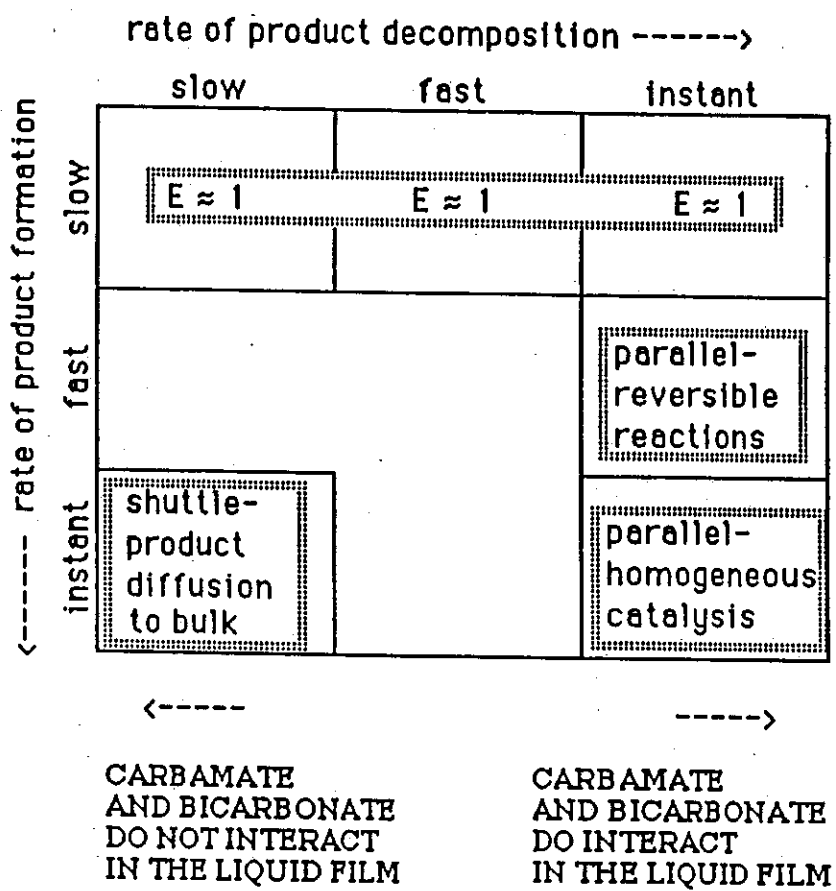


Figure 6: The effect of the rates of carbamate formation and conversion into bicarbonate on the limiting model which is applicable.

distinction between the two models is most meaningful for absorption under the condition where the carbamate formation rate is instantaneous, and the interface is highly loaded with respect to promoter. The correct application of the simple models can have a consequence on observed enhancement even for slower reaction of the promoter since it defines the correct value of the instantaneous limiting enhancement factor.

In the following discussion of the two models, the rate of the reaction of bicarbonate formation is assumed to be fast enough that the bulk liquid will be in thermodynamic equilibrium. This is the likely case provided that the rate of bicarbonate formation itself would enhance mass transfer. Therefore the effect of finite rate reactions in the bulk liquid need not be treated in this analysis.

2.6.2 The shuttle mechanism

The "shuttle" mechanism is operative when the carbamate formed from the CO_2 -promoter reaction is not in equilibrium with the HCO_3^- formed from reaction of CO_2 with the tertiary alkanolamine. The conversion of carbamate into bicarbonate occurs slowly through the conversion of free CO_2 into bicarbonate. In the conceptual model, no direct kinetic path for the conversion of carbamate into bicarbonate exists within the interface region.

In the shuttle mechanism case, the total reaction rate enhancement possible will depend mainly on the speed with which the promoter can diffuse from the bulk liquid. The promoter concentration at the interface is not buffered by equilibrium of the carbamate with the HCO_3^- , so the mass transfer enhancement capacity will be largely independent of the tertiary alkanolamine concentration at the interface. The steps in the shuttle mechanism are described below and are depicted in figure 7. The shuttle mechanism is in reality a special case of combined parallel reactions (carbamate formation and bicarbonate formation with the 3' amine) and consecutive reactions (conversion of carbamate into bicarbonate). The consecutive reaction is considered to occur in an equilibrium step in the bulk liquid:

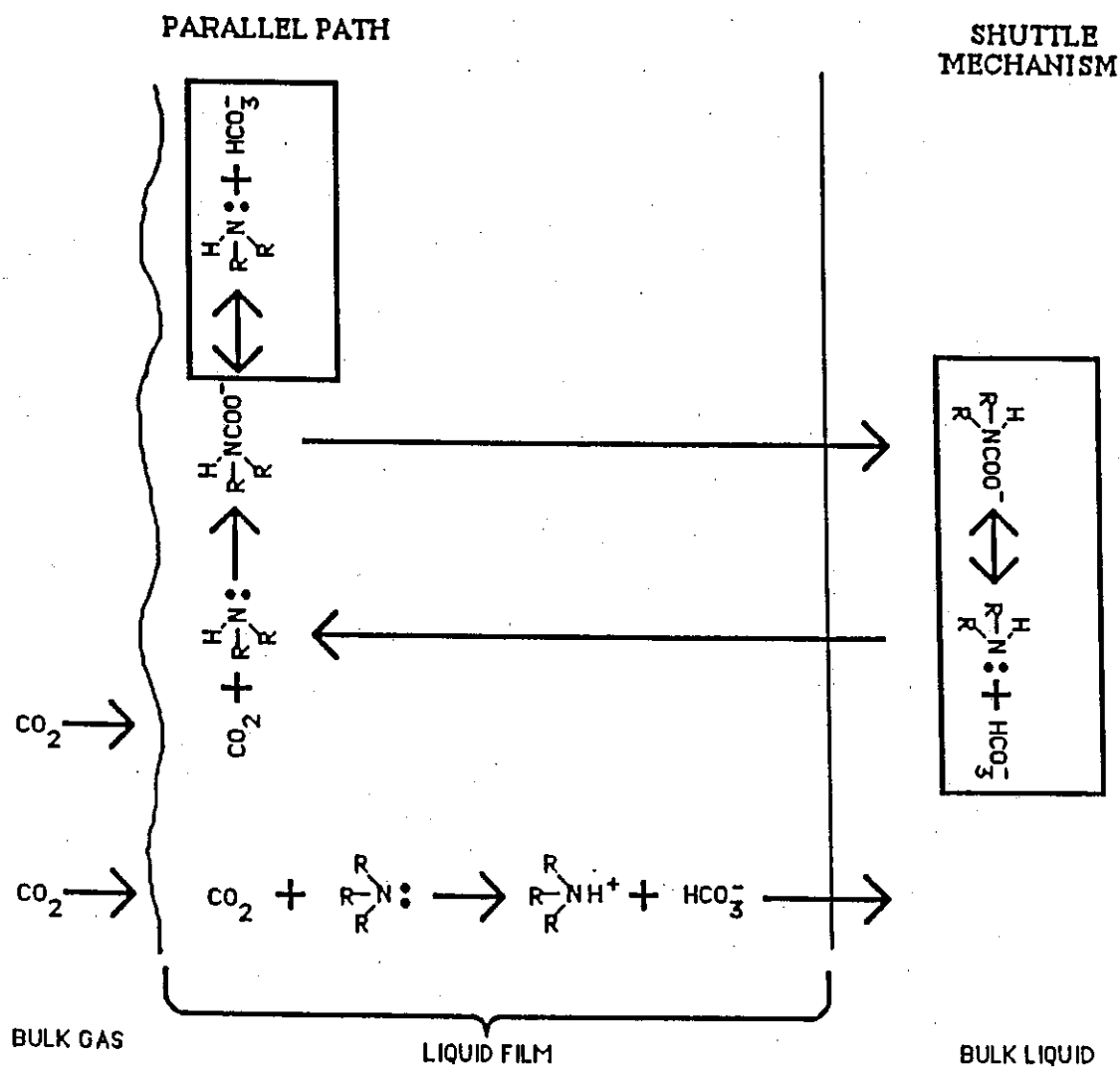


Figure 7: Contrast of the shuttle and parallel reaction models for an instantaneous carbamate formation reaction. The contrast lies in the location at which conversion of the carbamate into bicarbonate can take place.

- 1) CO₂ absorbs into the interface.
- 2) CO₂ reacts instantly with promoter, promoter is completely depleted at the interface. CO₂ reacts much more slowly with the tertiary alkanolamine to form HCO₃⁻.
- 3) The product of the CO₂ reaction is kinetically stable--it is not in equilibrium with the HCO₃⁻ at this point. CO₂ diffuses to the bulk liquid (bound up as carbamate).
- 4) The CO₂-promoter product comes to equilibrium with the bulk liquid composition; the promoter is liberated by the decomposition of carbamate. The promoter must diffuse back to interface before again becoming active.

As was discussed previously, decomposition of the carbamate may be quite slow. Carbamate must decompose by reversing completely to CO₂, which then may react with free base (OH⁻) or hydrolyze with water. Either of these two CO₂ conversion reactions are slow enough compared to the formation of carbamate that when the carbamate is thermodynamically stable, it may be considered to be the kinetically stable form of CO₂. Therefore in amine-promoted solutions with relatively stable carbamates, a shuttle mechanism is likely to apply at high driving forces in absorption.

A quantitative treatment of the shuttle mechanism follows. For instantaneous promoter reaction with CO₂, the diffusion of promoter governs the mass transfer enhancement:

$$E_{\infty\text{-prom}} = 1 + \sqrt{\frac{D_{\text{prom}}}{D_{\text{CO}_2}}} \frac{[\text{PROM}]_b}{\sqrt{[\text{CO}_2]_i}} \quad (2.45)$$

At sufficiently high values of the interface CO₂ concentration, the value of the $E_{\infty\text{-prom}}$ will be quite small. Under conditions where the CO₂ concentration is large (at high absorption driving forces) the rate of the reaction of CO₂ with the tertiary alkanolamine solvent may contribute to the observed rate. The overall enhancement factor in a shuttle step at sufficiently high driving forces is:

$$E_{\infty\text{-shuttle}} = E_{\infty\text{-prom}} + E_{F\text{-solv}} - 1 \quad (2.46)$$

In the limit of very high driving forces and low promoter contents, $E_{\infty\text{-prom}}$ approaches unity. Therefore under these conditions the shuttle mechanism predicts that the promoter effect on the overall enhancement factor will become unimportant.

In the shuttle mechanism where large transport rates are occurring in solvents containing significant amounts of promoter, the following condition will apply:

$$E_{\infty\text{-prom}} \gg E_{F\text{-solv}} \gg 1 \quad (2.47)$$

Therefore the net transport rate of CO_2 will be in this case controlled by the amount of promoter in the bulk solution and is not a function of the amount of tertiary alkanolamine present:

$$R_a \approx k_1^0 a \sqrt{\frac{D_{\text{prom}}}{D_{\text{CO}_2}}} \frac{[\text{PROM}]_b}{v} \quad (2.48)$$

Different behavior may be exhibited at very low driving forces. If the promoter- CO_2 reaction is finite in rate, then at low interface CO_2 concentrations the CO_2 -promoter reaction may not be limited by diffusion of the promoter. In this case, the rate of the CO_2 -promoter reaction must be considered in the enhancement factor. At sufficiently low driving forces it is possible that mass transfer is governed by the fast, pseudo-first order reaction regime and the overall enhancement factor will become as follows:

$$E_F = \sqrt{E_{F\text{-prom}}^2 + E_{F\text{-solv}}^2} - 1 \quad (2.49)$$

Equation 2.49 expresses the additivity of pseudo-first order rate constants as was indicated by Jhaveri (1969). If equation 2.49 applies it does not matter whether or not the reaction products (carbamate and bicarbonate) are at equilibrium

since very little product will be formed with respect to the reactant concentration. Interactions in the carbamate formation kinetics can be evaluated in this case without consideration of the kinetic stability of the carbamate.

2.6.3 The parallel reaction mechanism

A "parallel" mechanism exists in the case where the product of the promoter reaction decomposes quickly enough (with respect to the speed of diffusion) that it can be considered to be in equilibrium at every point within the solution. Essentially, this model assumes that a very fast direct conversion step for carbamate into bicarbonate. Because of the instantaneous equilibrium interaction of the reaction products neither the CO₂-promoter reaction or the CO₂-dominant solvent reaction can be forced to completion without also forcing the other to completion. The interaction of the reaction products means that the product of the promoter reaction need not diffuse to the bulk liquid in order to be regenerated. In this case, the interface concentration of the promoter may be considered to be buffered by the presence of the tertiary alkanolamine. Therefore the mass transfer limit in this case is defined by a "parallel" mechanism since an overall equilibrium at the interface expresses the maximum possible reaction enhancement. This case is conceptually the same as that developed by Astarita et al (1981) for homogeneous catalysis of CO₂ absorption in potassium carbonate solutions by arsenious anion.

Figure 7 also depicts the steps in the parallel mechanism for CO₂ absorption:

- 1) CO₂ first absorbs into the gas-liquid interface.
- 2) CO₂ immediately combines chemically with the promoter.
- 3) The reaction product dissociates instantaneously to reach its equilibrium concentration as defined by interface composition.
- 4) The dissociation of the CO₂-promoter reaction product results in the liberation of promoter at the interface. The amount of free promoter is therefore controlled by the chemical equilibrium interaction of the reaction products.

Note that in concept the difference between the shuttle and the parallel mechanism lies primarily in the fact the product of the CO₂-promoter reaction does not diffuse in the latter mechanism before it is regenerated.

Because the interface concentration of promoter is buffered by the presence of the dominant solvent, it will be less limited by diffusion phenomena; it will not be affected until the interface loading begins to also affect the dominant solvent concentration. Consequently, very large mass transfer enhancements are possible when mass transfer occurs by this mechanism as opposed to the shuttle mechanism.

The parallel mechanism is treated for instantaneous formation reactions by:

$$E_{\infty\text{-parallel}} = E_{\infty\text{-prom}} + E_{\infty\text{-solv}} - 1 \quad (2.50)$$

In the above equation, $E_{\infty\text{-prom}}$ and $E_{\infty\text{-solv}}$ are defined by the difference in the equilibrium compositions at the bulk and interface CO₂ concentrations.

The instantaneous limiting behavior of the parallel model is such that at high driving force and at large promoter content the absorption rate is a function of both the promoter content and the dominant solvent content. A condition similar to that of equation 2.47 cannot be applied in the case of the parallel model since the mass transfer capacity of the solution will be affected by both the dominant solvent and the promoter. This result is an important distinction between the shuttle and the parallel models:

$$R_{\infty} \approx k_1^0 a \left\{ \sqrt{\frac{D_{\text{prom}}}{D_{\text{CO}_2}}} \frac{[\text{PROM}]_b}{v} + \sqrt{\frac{D_{\text{solv}}}{D_{\text{CO}_2}}} [\text{SOLV}]_b \right\} \quad (2.51)$$

No distinction can be seen between the shuttle and parallel models in the fast, pseudo-first order reaction case. The lack of distinction is due to the formation of reaction products at the interface in only negligible amounts; the stability of the products therefore cannot be an issue in determining the enhancement factor.

2.6.4 Quantitative technique for the parallel reactions

The preceding cases are too limiting to cover all practical conditions. A solution technique which allows for variation in the rate of reaction and therefore the applicable mass transfer regime for each reaction must be considered. The modified DeCoursey technique can be applied only in the case of parallel reactions since a common equilibrium limit is used for both solvents. The equations for the DeCoursey technique are derived in terms of the reaction factor, M_R , which is additive. An overall "pseudo"-first order reaction is defined by the common equilibrium in the reaction driving force:

$$\text{reaction rate}_i = \frac{M_{R_i} k_1^{o2}}{D_{CO_2}} ([CO_2] - [CO_2]_e) \quad (2.52)$$

and in the parallel mechanism

$$\text{reaction rate}_{\text{total}} = \text{rate of promoter(1)} + \text{rate of dominant solvent(2)}$$

$$\begin{aligned} &= \frac{M_{R_1} k_1^{o2}}{D_{CO_2}} ([CO_2] - [CO_2]_e) \\ &+ \frac{M_{R_2} k_1^{o2}}{D_{CO_2}} ([CO_2] - [CO_2]_e) \end{aligned} \quad (2.53)$$

therefore

$$M_{R_{\text{total}}} = M_{R_1} + M_{R_2} \quad (2.54)$$

2.6.5 Quantitative treatment of the shuttle mechanism

Because the shuttle mechanism is based on the assumption of product stability at the interface and product equilibrium in the bulk liquid, a somewhat empirical instantaneous limit must be assigned. The DeCoursey treatment for the

parallel reaction case cannot be extended to the shuttle case because the treatment requires the application of an equilibrium model at the interface. This concept is inconsistent with the interface carbamate stability assumed in the shuttle model. Therefore only the shuttle limit, which considers the carbamate formation to be irreversible and instantaneous at the interface (equation 2.46), is considered in this work. The approach to this limit is not treated.

2.7 Treatment of Desorption

2.7.1 For a single reaction

In order to study the reactions under desorption conditions, the effect of the direction of the driving force on the mass transfer enhancement must be known. Astarita and Savage (1980a; 1980b) and Savage et al (1980) showed that the mathematical treatment of desorption was identical to the treatment of absorption provided that the effect of the differing boundary conditions was considered.

Astarita et al (1983) showed that for reactions in which the rate equation is an odd function of the driving force ($\text{rate}(-\Delta) = -\text{rate}(\Delta)$) the enhancement factor is unaffected by the direction of the driving force in the fast, pseudo-first order regime. Because the reaction order for CO_2 appears to be unity for both the carbamate formation and bicarbonate formation reactions (Alvarez-Fuster et al, 1981), the requirement is satisfied for the fast reaction regime in alkanolamine solvents.

Since it was concluded earlier that subject to the limitations of equation 2.37 the direction of driving force has no effect on the reaction rate model for the complex reactions, it is established that the same rate constant can be measured under absorption and desorption conditions (provided that pseudo-first order assumptions apply).

In the limit of infinitely fast reactions, the application of an equilibrium model at interface and bulk conditions to predict enhancement factors is rigorous regardless of the direction of the driving force (Danckwerts, 1968; 1970). The effect on the enhancement factor in the transition between the fast and the

instantaneous regimes is less certain. However, in his paper on fast and reversible reactions, DeCoursey (1982) maintains that his approximate solution technique should apply to desorption conditions.

In the desorption experiments performed in this work low driving forces were employed in order to avoid the transition region. Therefore the approximate model was not needed for the interpretation of the rate constant. The model was used to establish the size of the parameter "Q" in order to assure that pseudo-first order conditions were achieved.

2.7.2 For mixed solvents

In mixtures of alkanolamines the direction of the driving force can affect the enhancement factor if in absorption a shuttle mechanism applies to the mixture (Astarita et al 1981). The results of Astarita et al's (1981) development of the shuttle mechanism dictate that if a promoter acts under a shuttle mechanism at large absorption driving forces then the conversion reaction is sufficiently slow that the desorption rate should not be affected.

A shuttle mechanism is not possible in desorption because there is no "sink" at the interface in which the carbamate/bicarbonate reversion reaction can be assumed to equilibrate (Astarita et al, 1981). Consequently, the desorption rate of CO₂ from a mixture of alkanolamines cannot be described by a shuttle-type mechanism under large driving forces. If the carbamate/bicarbonate conversion reaction is slow enough to indicate a shuttle limit in absorption, then under desorption conditions the lack of a chemical sink at the interface mandates that the reaction will not affect mass transfer in the region of the interface.

Therefore subject to the limitations of equation 2.37, if the desorption rate is truly reaction rate controlled then the kinetic constants measured in desorption and in absorption should be the identical. The rate constants will agree only if the diffusion limitation of the shuttle mechanism is avoided in the determination of the rate constants in absorption. Comparison of experimental results from absorption and desorption conditions can therefore prove the applicability of equation 2.37.

2.7.3 Specifying the driving force in desorption

If the enhancement factor under desorption conditions can be represented, then the rate constant can be determined from a rate measurement if the driving force is well known. In desorption the driving force is specified by the difference between the equilibrium vapor pressure and the interface partial pressure. In the simplest case, which is desorption under high driving force and in the fast reaction regime, the rate of desorption is proportional to the equilibrium vapor pressure of the solution:

$$R = a \sqrt{k_o D} \Delta \approx -a \sqrt{k_o D} A_{eb} \quad (2.55)$$

For the purpose of measuring rate constants in desorption, accurate estimation of the equilibrium vapor pressure is vital since the error in vapor pressure will be squared in the determined pseudo-first order rate constant. For very fast reactions it is often necessary to measure the rate constant under small driving forces. When the interface and bulk pressures are close enough that the interface pressure cannot be ignored in the driving force then the error in the estimate of the bulk pressure can result in dramatic errors in the determined value of the rate constant.

Desorption experiments are by necessity conducted at high solution loadings since a finite CO₂ vapor pressure is required. At the high solution loadings a significant amount of the reactive amine will be neutralized. Consequently, interpretation of the measured pseudo-first order rate constants in desorption experiments is complicated by the need to apply an equilibrium speciation model. The need for a speciation model is a primary difference between desorption and absorption experiments.

Section 3

EXPERIMENTAL

3.1 Apparatus and Procedures

3.1.1 The high and low driving force configurations

CO₂ mass transfer was studied in a batch liquid, continuous gas stirred cell reactor (figure 8). The total reactor volume was approximately 2 liters. The reactor was equipped with four evenly-spaced baffles. At the low agitation rates used, the gas-liquid interface was confirmed to remain unbroken by visual observation through the plexiglass walls of the reactor. Consequently, the geometric area was assumed to be equal to the mass transfer area. Alper et al (1980) experimentally demonstrated the validity of this assumption for a similar reactor.

Although the plexiglass wall of the reactor proved to be a good insulator, at high and low temperatures some heat transfer did occur through the sides and lid of the reactor. To correct for heat loss or gain, and for the exothermic heat of reaction at high fluxes, temperature control was affected by continually circulating hot (or cold) water through a stainless steel heating coil immersed in the liquid phase. A Lauda M-20 Heating Circulator capable of maintaining temperature from 0 to 90° C was used for this purpose. Temperature in the reactor was determined by a mercury thermometer.

Two major reactor configurations were employed. Large mass transfer coefficients were necessary in order to measure rate constants in fast reacting solutions. Good liquid mixing and high mass transfer coefficients were achieved by agitating the liquid phase with a 0.38 dm six-bladed turbine impellor.

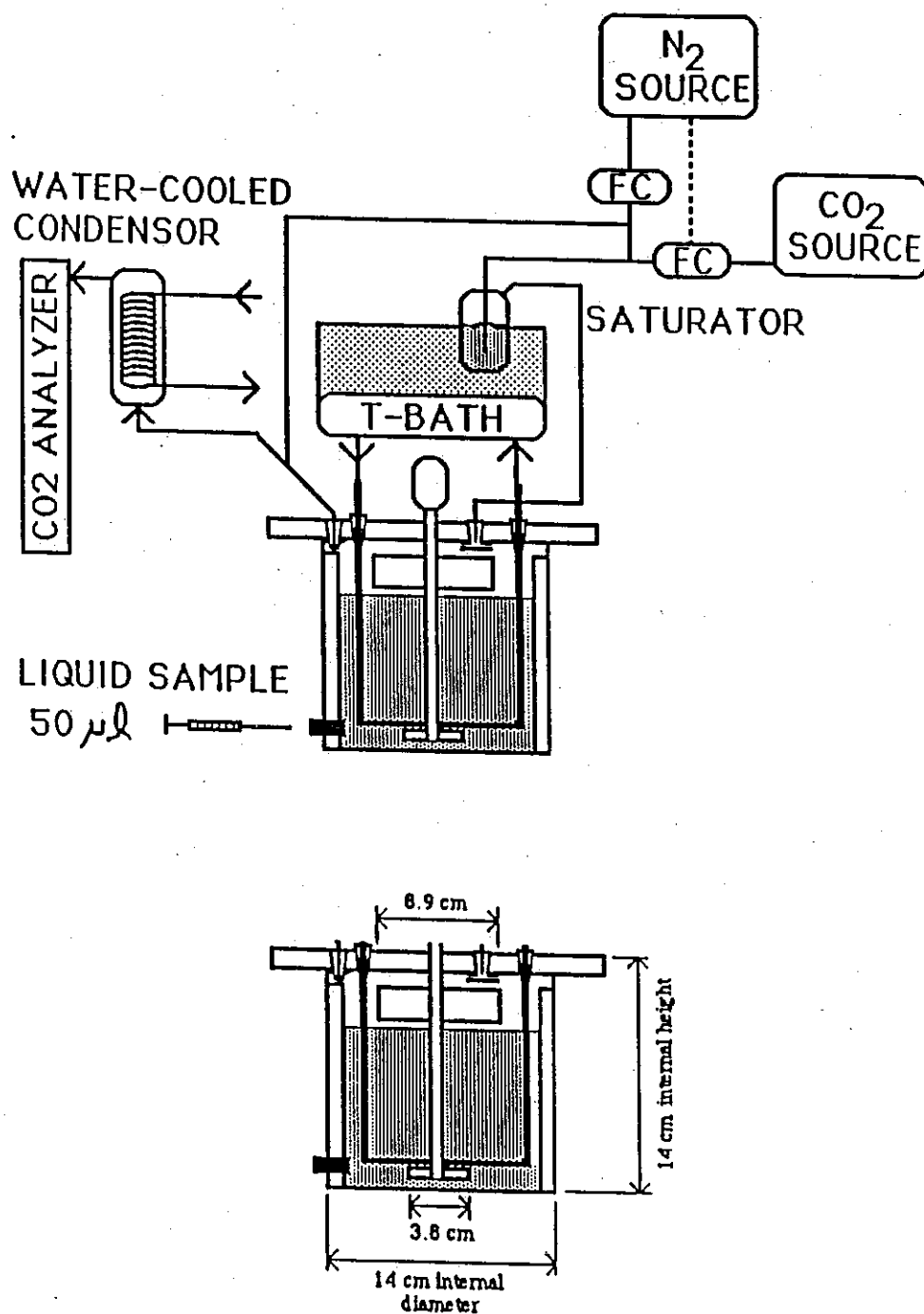


Figure 8: The experimental contactor is stirred-tank reactor with an unbroken gas-liquid interface.

It was also necessary to provide small driving forces in order to insure reaction rate control of mass transfer. Since the gas phase of the reactor was continuous, a well-mixed assumption had to be applied in order to establish the driving force for absorption or desorption. Gas mixing was aided by use of a large working liquid volume (1.8 liter) which reduced the size of the gas space. The small gas space was agitated with a 0.89 dm six-bladed turbine impellor mounted on a common shaft with the liquid agitator. The combination of low driving forces and large liquid volumes created the advantage of very small liquid phase composition changes within an experiment. In the low driving force configuration the geometric gas-liquid contacting area was calculated to be 1.46 dm^2 .

A second reactor configuration was also used to measure rate constants for slow-reacting MDEA solutions. Very low mass transfer coefficients were necessary to insure reaction rate control of mass transfer. Additionally, possible impurity effects are most important for the slow-reacting solutions. As demonstrated in equation 2.46, if a shuttle mechanism applies high-driving force conditions help to reduce the effect of primary and secondary amine impurities on the measured rate.

Therefore experiments on the CO_2 -MDEA reaction rate were conducted in high driving force absorption with a less effective agitator (a 0.25 dm magnetic stirrer bar at 380 rpm) in order to provide the smaller mass transfer coefficients. Because the gas phase was essentially pure CO_2 (and water vapor), gas phase mixing was unimportant and less liquid volume could be employed (600 ml) in these experiments. In this reactor configuration additional equipment obscured the gas-liquid interface, resulting in a smaller mass transfer area (1.26 dm^2).

The turbine bladed impeller was found to provide better control of the agitation rate, and the greater liquid volume allowed assumption of pseudo-steady state conditions with respect to the liquid phase concentration of CO_2 .

CO_2 transport rate data were measured under two distinct sets of conditions: absorption and desorption.

3.1.2 The absorption mode

In the high-driving force absorption mode the CO_2 transport rate was determined by tracking the increase of total dissolved CO_2 with time. The liquid samples were analyzed for total inorganic carbon with an Oceanography International Model 525 Total Carbon Analyzer. The technique used was comprised of liberating all the CO_2 from a known volume of sample and detecting the CO_2 with an infrared analyzer. The response of the analyzer was integrated and the area compared with area measured for Na_2CO_3 standards (appendix A). A reactor sample volume of 50 microliters was used every time. The analytical technique was accurate to within 2-4% over the range of 1-30 mM CO_2 : samples containing more than 30 mM of total dissolved carbon dioxide had to be diluted before injection. When dilution of samples was used, the reactor sample was injected into 1,2,3, or 4 ml of distilled water. The diluted sample was sealed and injected quickly to limit losses to (or gains from) the atmosphere. The diluted samples were injected 4-6 times and the results were averaged to minimize random error in the analytical technique.

The analytical procedure was cross-checked by pH titration and by a mass balance technique (Appendix A). The experimental procedure consisted of first preheating the desired amine solution in the reactor. In the absorption mode, the amine solutions used were essentially free of CO_2 initially, except in a few of the experiments, where partially loaded amine solution was charged to the reactor. After the amine solution was heated to the desired temperature, flow of CO_2 -bearing gas of known composition was initiated and agitation of the reactor commenced. The CO_2 content of the inlet gas was controlled with a set of parallel Brooks Mass Flow Controllers (model 5850C), and could be varied in a continuum from 0% to 100% CO_2 . The total gas flow rate was initially high only for the first 5 minutes in order to purge the gas phase of the reactor.

In absorption experiments in which the gas phase was comprised solely of CO_2 and water vapor, the inlet gas flow rate was lowered after purging to the point that a slight positive flow was maintained through the reactor. This was done to

minimize water balance effects in higher temperature experiments. The range of operating temperatures possible in the reactor was limited on the low end by the maximum flow rate of ice water through the reactor coil, and was approximately 5° C. The upper limit was provided by the saturation of the gas phase with water. Though the water exiting the the outlet gas was condensed and returned to the reactor, as the gas phase became more than approximately 60% water, uncertainty was introduced into the CO₂ partial pressure. The actual CO₂ partial pressure was determined by subtracting the contribution of water (assumed to be at saturation).

The water vapor pressure at the gas-liquid interface was approximated as that over pure water at the temperature of the solution. The reactor was never operated at higher than 1 inch Hg gauge pressure, so the effective upper limit in temperature was approximately 85° C.

For experiments utilizing less than pure CO₂ feeds, the flowrate after purging was determined by controlling the outlet gas composition. A constant N₂ carrier flow rate was maintained and the CO₂ content of the outlet gas was measured with a CO₂ analyzer. The Infrared Industries IR703 analog CO₂ analyzer was employed for moderate driving force experiments, and was calibrated for ranges of 0-10 and 0-30 volume % CO₂. A Horiba PIR-2000 analyzer with ranges of 0-0.05, 0-0.15, and 0-0.25 volume % CO₂ was also available for extremely low CO₂ partial pressure experiments. Experiments at less than 100% CO₂ feed were limited to conditions below 40° C in order to avoid complications with the water balance. In experiments using large feed gas rates, the feed gas temperature was controlled by first passing the feed gas through a saturator maintained at the reactor temperature. Condensed water in the outlet gas was not returned to the reactor in these experiments.

Depending on the size of the driving force the absorption rate could be determined either from mass balance on the inlet and outlet gas or from the concentration increase in the liquid phase as a function of time.

3.1.3 The desorption mode

The high mass transfer coefficient configuration was used in all desorption experiments. A known flowrate of CO₂-free N₂ was passed over the CO₂-loaded amine solutions and was then sent through the CO₂ analyzer. Therefore desorption rates could be determined by mass balance from the known carrier gas flow rate and exit gas CO₂ composition (instead of tracking CO₂ concentration). This procedure proved to be necessary in desorption experiments because the net transport rates in desorption were found to be about 2 orders of magnitude smaller than in high-driving force absorption. The difference in rates was due to the smaller driving forces possible experimentally in desorption. It was found that the net change in composition was so small that for all practical purposes the liquid concentration was constant throughout the course of a desorption experiment. This observation was checked by mass balance on the liquid phase composition at the conclusion of each experiment.

Because of the negligible change in liquid composition, the desorption experiments always allowed a steady-state interpretation of the experimental data. In addition to determining the rate of desorption, it was found that the equilibrium value of the CO₂ partial pressure could be estimated from the desorption experiments. The estimation of the equilibrium CO₂ partial pressure was achieved by successively lowering the carrier gas rate to a very low value (< 30 cc/min N₂). The determined rates were plotted as a function of exit gas CO₂ partial pressure, and the desorption rates were extrapolated to zero in order to project the equilibrium CO₂ partial pressure. At relatively high equilibrium CO₂ partial pressures, the outlet gas from the reactor was diluted with CO₂-free N₂ before being sent into the Horiba analyzer.

The liquid phase mass transfer characteristics of the stirred cell reactor were quantified by studying CO₂ absorption and desorption in distilled water at room temperature.

Section 4

MASS TRANSFER STUDIES

4.1 Calibration of Mass Transfer Coefficients

4.1.1 Mass transfer coefficients for the liquid phase

The liquid-phase mass transfer characteristics of the reactor were determined by measuring the rate of absorption and desorption of CO₂ into distilled water at room temperature and at varying agitator speeds. All experiments were conducted at 1 atm nominal CO₂ pressure; other experimental conditions are summarized in table 1. The values of the physical mass transfer coefficient were calculated assuming that the effective mass transfer area was equal to the geometric area.

In the absence of surface rippling it was found that the liquid-phase mass transfer coefficient in the reactor was well correlated by:

$$Sh = a Sc^{1/2} Re^n \quad (4.1)$$

where:

$$Sh = \frac{k_l^0 d_{imp}}{D_{CO_2}}$$
$$Sc = \frac{\mu}{\rho D_{CO_2}}$$
$$Re = \frac{d_{imp}^2 V \rho}{\mu}$$

In the low driving force (turbine impellor) configuration, surface rippling effects were not detectable at Reynolds numbers lower than 5000. Below this limit the resulting power on the Reynolds number is 0.77 for the turbine impellor, which agrees well with the values of 0.7 found by Hikita et al (1975) and 0.66 found by Haimour et al (1985). In the high driving force configuration, the magnetic stirrer

Table 1a; Liquid mass transfer coefficients in the CO₂-H₂O system measured in the low driving force configuration (turbine bladed agitator, $a=1.46 \text{ dm}^2$, liquid volume=1800 ml).

Date	Stirrer Speed RPM	Type abs or des	Total CO ₂ mM		PCO ₂ % of 1 atm		Rate $\times 10^6 \text{ gmol/s}$		$k_1^{0.5} a \times 10^4 \text{ dm}^3/\text{s}$	
			initial	final	initial	final	initial	final	Range	Average
Jun 25, 1987	205	abs	1.23	4.79	97.2	97.2	9.1	9.1	—	2.77
Jun 28, 1987	206	des	3.94	2.65	0.147	0.0916	1.28	0.798	2.97-3.15	3.05
Jun 29, 1987	145	des	6.99	5.77	0.203	0.161	1.77	1.40	2.34-2.47	2.45
Jun 30, 1987	145	des	3.44	2.77	0.8116	0.0709	0.798	0.618	2.31-2.35	2.33
Jul 1, 1987	125	abs	1.7	4.3	97.2	97.2	7.36	6.38	—	2.02
Jul 1, 1987	154	abs	0.57	3.18	97.2	97.2	9.32	7.71	—	2.39
Jul 3, 1987	114	des	8.25	7.2	0.185	0.162	1.61	1.41	1.89-1.95	1.90
Jul 3, 1987	168	des	6.87	6.44	0.207	0.189	1.81	1.66	2.55-2.63	2.58
Jul 3, 1987	185	des	6.08	5.63	0.194	0.176	1.70	1.54	2.73-2.81	2.80
Jul 4, 1987	262	des	4.14	3.76	0.182	0.162	1.60	1.42	3.84-3.93	3.90
Jul 4, 1987	339	des	3.47	3.14	0.191	0.174	1.67	1.52	4.91-4.96	4.95
Jul 4, 1987	445	des	2.85	2.51	0.212	0.191	1.86	1.67	6.70-6.84	6.80
Jul 4, 1987	506	des	2.13	1.83	0.201	0.169	1.76	1.48	8.36-8.85	8.55

Other conditions:

$T=23^\circ\text{C}$

$d_{\text{imp}}=1.5 \text{ in}$ (turbine impellor)

$Sc=503$

$\mu=0.98 \text{ cP}$

$DCO_2=1.95 \times 10^{-7} \text{ dm}^2/\text{s}$

N₂ sweep rate in desorption experiments was 1279 cc/min

Liquid volume was 1800 ml

$a=1.46 \text{ dm}^2$

Table 1b; Liquid mass transfer coefficients in the CO₂-H₂O system measured in the high driving force configuration (magnetic stirrer, $a=1.26 \text{ dm}^2$, liquid volume=600 ml).

Date	Stirrer Speed RPM	Type abs or des	Total CO ₂ mM		PCO ₂ % of 1 atm	Rate $\times 10^6 \text{ gmol/s}$ Average	$k_1^{0.5} a \times 10^4 \text{ dm}^3/\text{s}$ Average
			initial	final			
Dec 19, 1986	240	abs	1.96	4.83	97.2	4.3	1.34
Dec 19, 1986	166	abs	2.51	4.73	97.2	2.9	0.95
Dec 19, 1986	96	abs	2.99	4.70	97.2	2.37	0.77
Dec 19, 1986	386	abs	2.79	6.88	97.2	5.43	1.81
Dec 19, 1986	377	abs	1.96	5.80	97.2	4.91	1.65
Dec 19, 1986	577	abs	2.30	6.86	97.2	6.23	2.05

Other conditions:

$T=23^\circ\text{C}$

$d_{\text{imp}}=1.0 \text{ in}$ (magnetic stirrer)

$Sc=503$

$\mu=0.98 \text{ cP}$

$DCO_2=1.95 \times 10^{-7} \text{ dm}^2/\text{s}$

Liquid volume was 600 ml

$a=1.26 \text{ dm}^2$

was a less effective agitator and consequently exhibited a weaker dependence on the Reynolds number ($n=0.56$). The results are presented in figure 9.

The Schmidt number was not varied in these experiments. The one-half power on the Schmidt number was employed because the surface renewal theory was assumed to represent mass transfer in the contactor.

Bin's (1984) review article on mass transfer in stirred tanks shows that the reported dependence varies widely between researchers (0.7 to 1.5). Bin concludes that the possible presence of surface active agents and the existence of geometric differences between systems prevents comparison between systems based solely on the Reynolds number dependence. The observed powers of 0.77 and 0.56 in the current work are therefore only useful for correlation of mass transfer coefficients in each configuration. The mass transfer coefficient for each configuration was therefore adjusted for solutions of other viscosities (aqueous alkanolamines) by the use of equation 4.1. Viscosity and density data were collected for use in equation 4.1 and are presented in tabular form in Appendix B.

4.1.2 Mass transfer coefficients for the gas phase

Attempts were made to measure the gas phase mass transfer coefficient by measuring the absorption rate of CO_2 into highly reactive solutions. If the absorption rate is limited by gas phase resistance a change in the reactivity of the liquid phase should not effect the observed rate. Figure 10 shows CO_2 absorption rates as a function of absorption driving force for three solutions of various reactivities. It is evident that the reactivity of the liquid makes a strong contribution and therefore the gas phase resistance to mass transfer cannot completely control the observed rates. Figure 11 shows the values of the limiting k_{ga} calculated by normalizing the measured absorption rate with the driving force. This limiting value of k_{ga} represents the minimum possible value since no contribution of liquid phase resistance is considered in the calculation:

$$k_{ga} \approx \frac{R}{\Delta P} \quad (4.2)$$

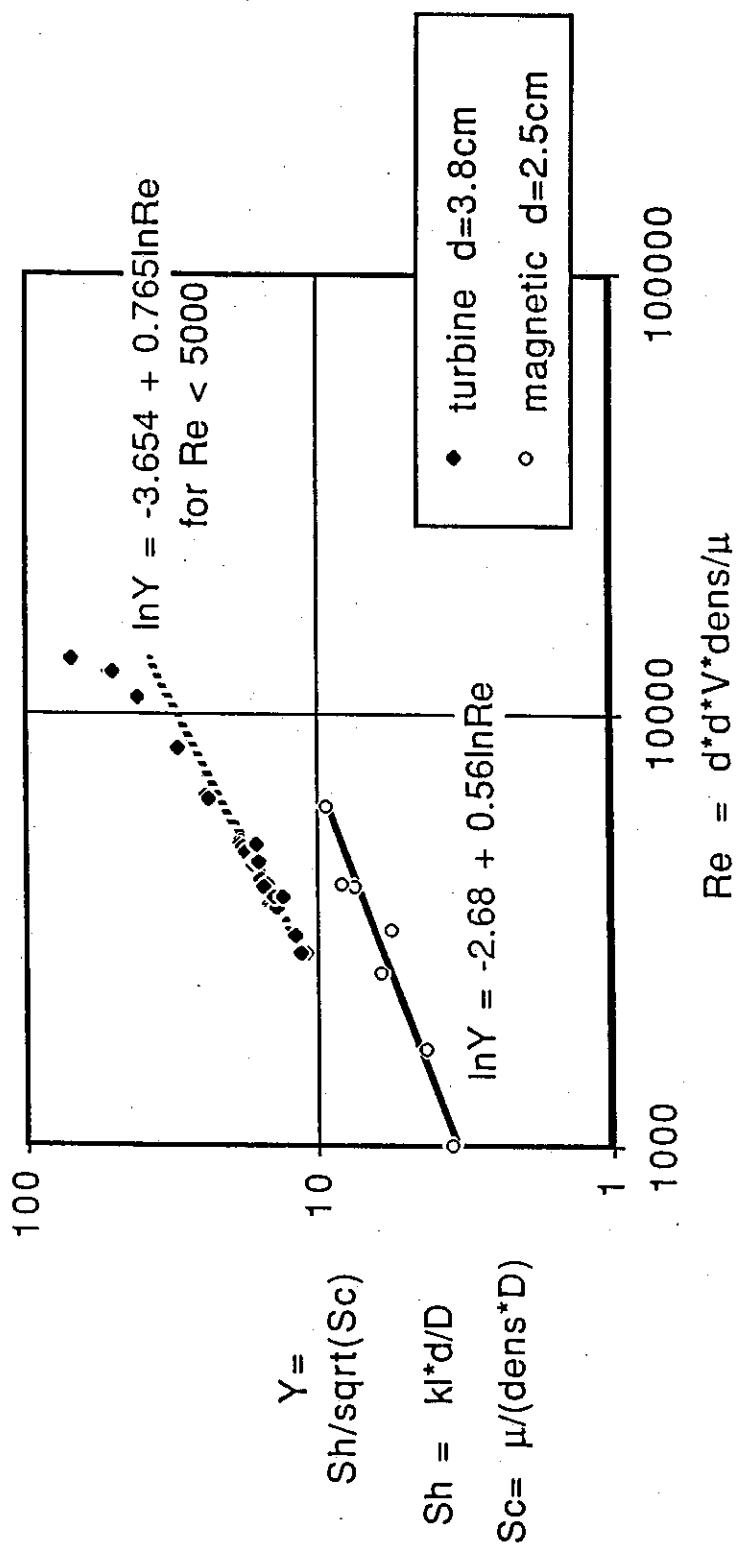


Figure 9: Correlation of liquid phase mass transfer coefficients for both reactor configurations. The system employed is $\text{CO}_2\text{-H}_2\text{O}$ in both absorption and desorption at 23°C .

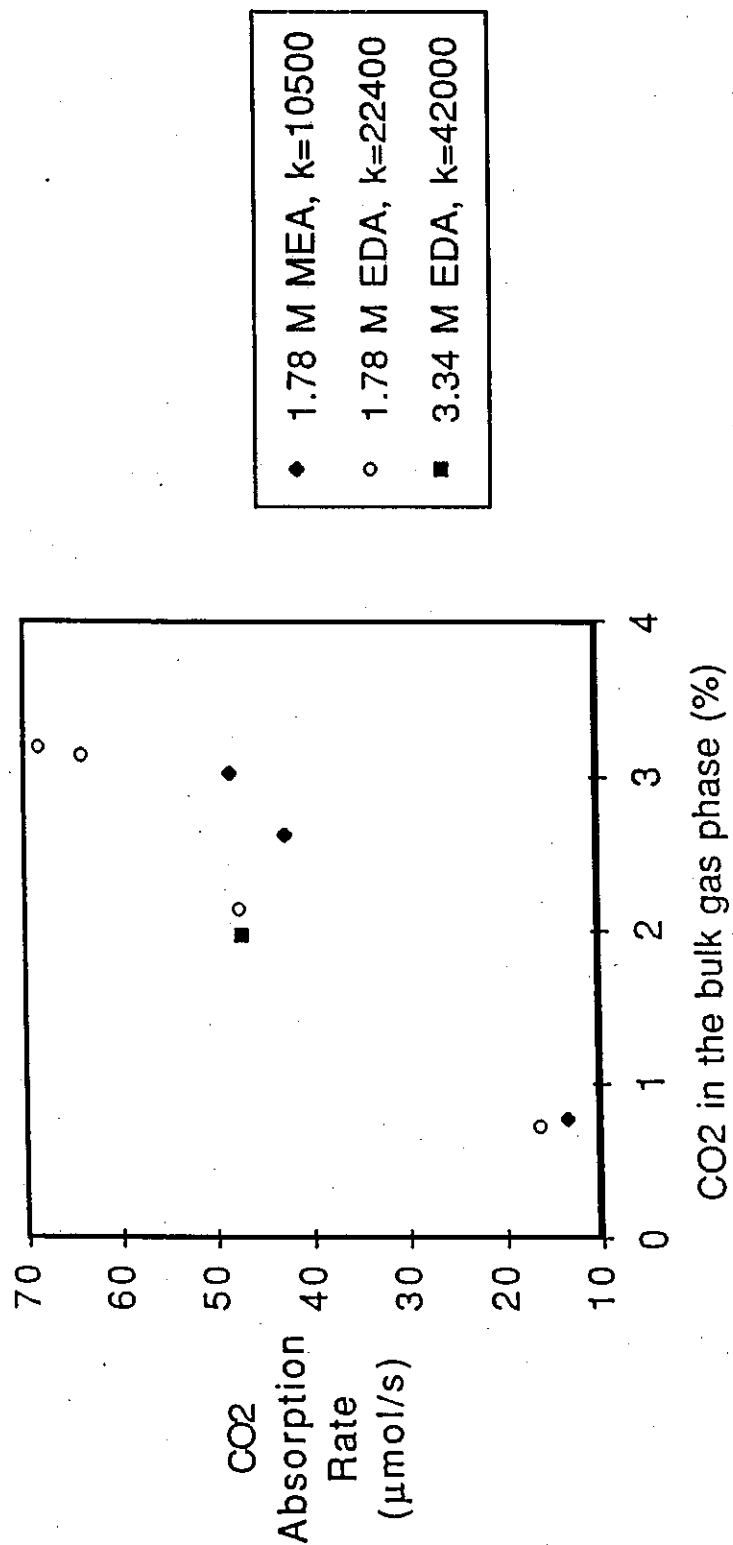


Figure 10: CO₂ absorption into fast reacting solutions. If gas phase resistance controlled the reactivity of the liquid phase would not affect the observed rate. The systems (shown in the legend) were studied at 25° C and at 207 rpm.

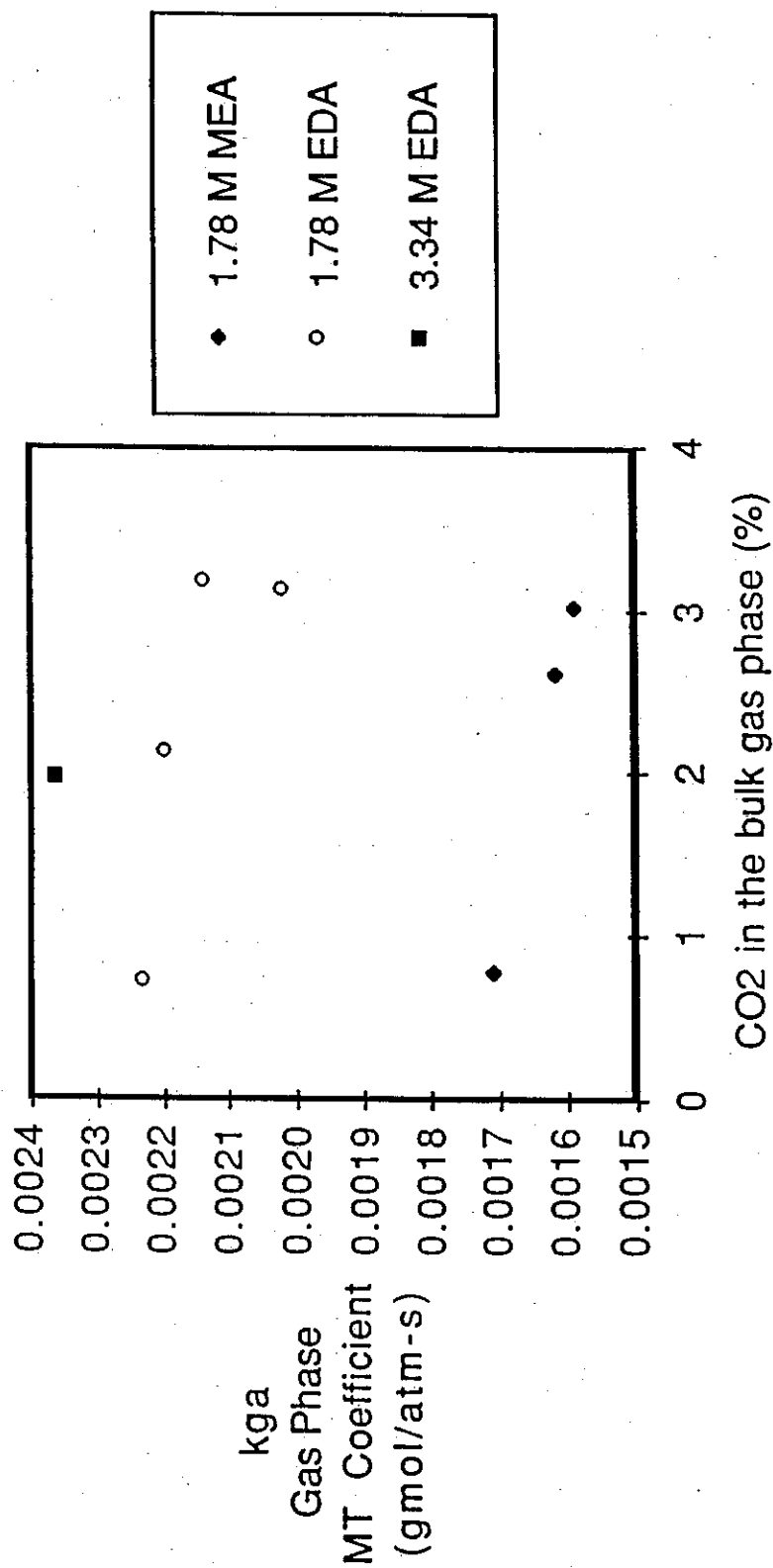


Figure 11: Lower limiting values of the gas phase mass transfer coefficient. The values are calculated assuming that the gas phase resistance is the controlling step in absorption.

Because the values of k_{ga} vary with driving force and with the liquid phase reactivity, the liquid phase resistance cannot be ignored and the values in figure 11 represent gross underestimates of the true values.

The calculation of k_{ga} is greatly simplified if the effect of liquid phase gradients can be minimized experimentally. This was attempted in the data shown in figure 12. The effect of agitator speed on the apparent rate constants was determined in 2 M MEA at very low driving forces in order to minimize the effect of liquid phase gradients. In the absence of liquid phase gradients, the determined rate constant should not vary with absorption driving force. The data at high agitation rates exhibit only a very weak driving force dependence.

In the absence of gas phase resistance, the measured apparent rate constant should equal the literature value and should also not be a function of the agitator speed. However, the measured values demonstrate a large dependence on the agitator speed. Therefore, in these data both the gas and liquid phase resistances play a role.

A more rigorous technique was adopted for estimating k_{ga} which considers the contribution of the liquid phase resistance to the overall rate. The value of the rate constant at 25° C per Hikita et al (1977) was used to calculate the liquid phase mass transfer resistance in the modelling of the experiments. The liquid phase resistance is known from the kinetic limit for fast, pseudo-first order reactions:

$$k_l^0 E \approx \sqrt{k_o D} \quad (4.3)$$

With the liquid contribution defined, the gas phase contribution to the overall mass transfer rate was estimated from (Astarita et al, 1983):

$$R = \frac{\frac{a\sqrt{k_o D}}{H + \frac{a\sqrt{k_o D}}{k_{ga}}} (P_g - P_b)}{H + \frac{a\sqrt{k_o D}}{k_{ga}}} \quad (4.4)$$

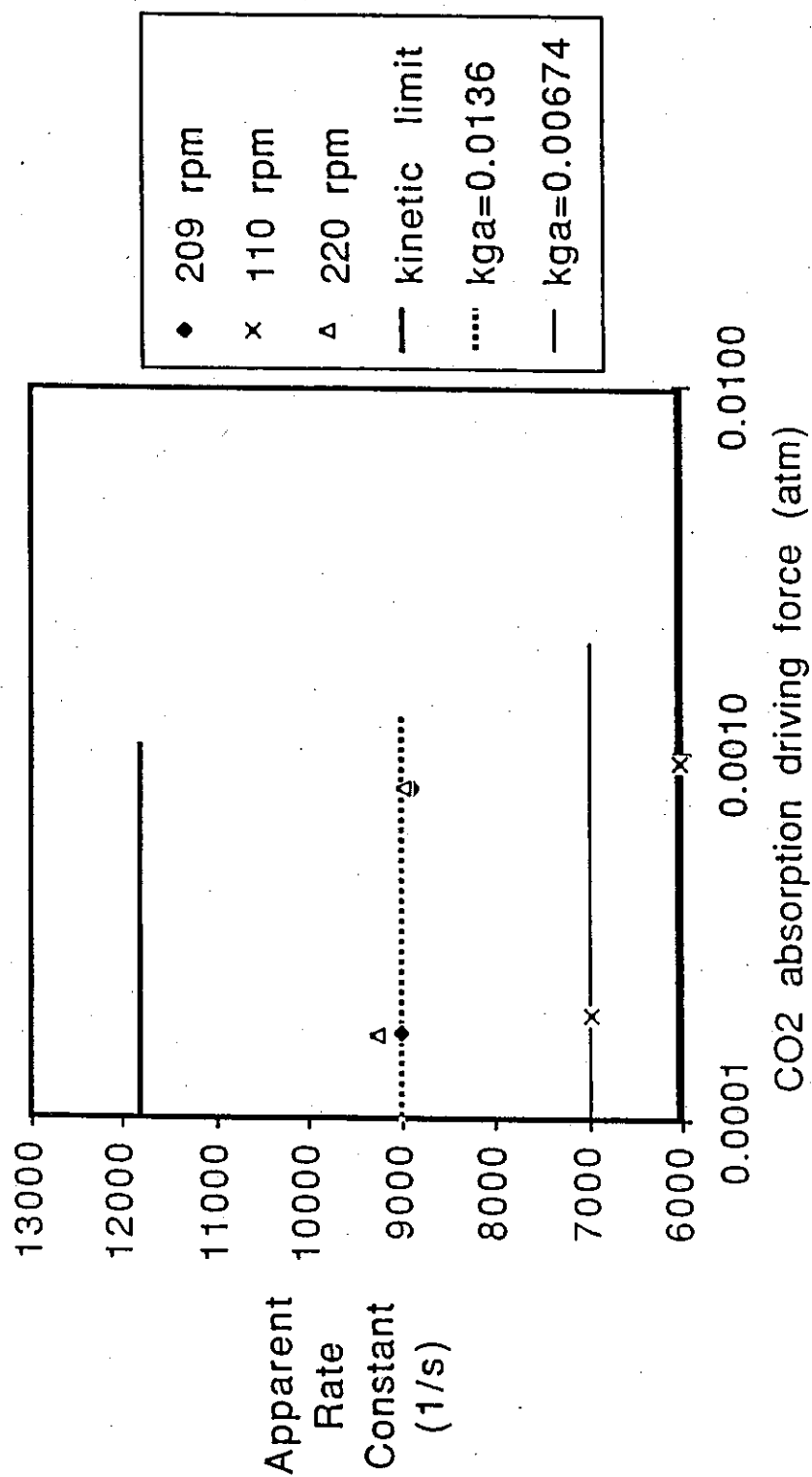


Figure 12: Apparent rate constants for CO₂ reaction measured in 2 M MEA. Some gas phase resistance is evidenced by the low values of the rate constant observed.

Figure 13 shows the values of k_{ga} determined from equation 4.4. The percentage contribution of gas phase resistance to the overall resistance is shown in table 2. The values of k_{ga} determined by this technique are much larger than the lower limiting values of figure 11 and the rigorously calculated values show less dependence on the liquid conditions. However, because the experiments were still largely controlled by liquid phase resistance, the estimates obtained from equation 4.4 be strongly effected by the parameters used to represent the liquid phase contribution. Consequently, the values of k_{ga} from equation 4.4 are still an approximation and are used only to establish order-of-magnitude effects in the interpretation of experimental data.

The existence of gas phase resistance indicates that a maximum exists on the value of the reaction rate constant which can be measured with confidence in the reactor. From the values of k_{ga} in table 2, it can be shown that for a gas phase resistance contribution less than 10% of the overall resistance the maximum pseudo-first order rate constant is approximately 5000 s^{-1} at the higher agitator speeds. At the lowest agitation rates used approximately 10% gas phase resistance would be encountered for rate constants on the order of 1000 s^{-1} . Therefore the higher agitation rate was employed in all low driving force experiments unless otherwise noted.

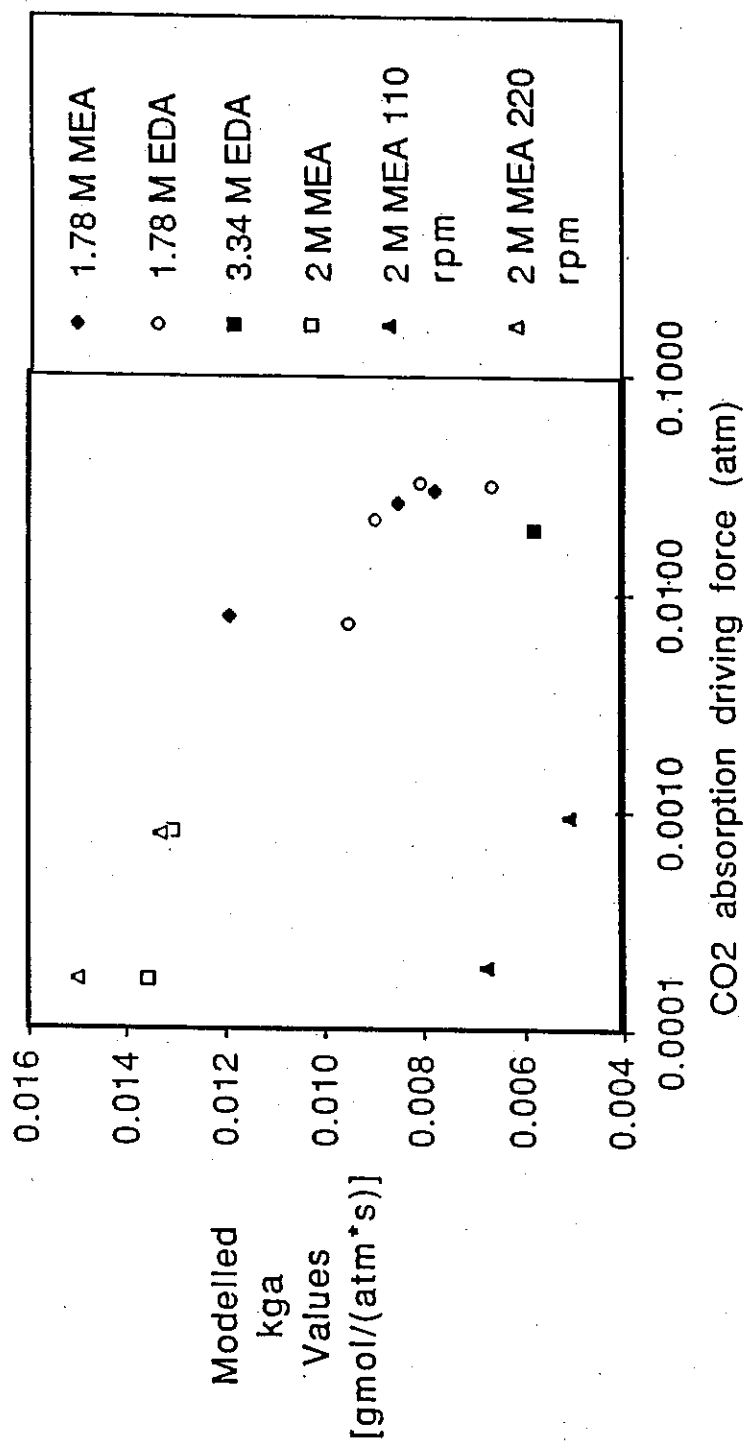


Figure 13: Modelled values of k_{ga} in which the contribution of liquid phase resistance has been eliminated. Data are at 25° C and at 207 or 209 rpm (except as indicated).

Table 2: Experiment summary for CO₂ absorption into fast reacting amines for the purpose of gas phase mass transfer resistance measurement. All experiments were conducted with the low driving force configuration (turbine bladed agitator, $a=1.46 \text{ dm}^2$, liquid volume=1800 ml).

Date	Type	Conc. M	k_{app} known s^{-1}	Total CO ₂ M		PCO ₂ % of 1 atm	Rate $\times 10^7$	k_{ga} (min) gmol/s (atm·s)	k_{ga} modelled gmol/ (atm·s)	%gas resis- tance	RPM
Apr 8, 1987	MEA abs	1.78	10500	21.36	32.49	0.79	135	0.001709	0.01192	14	207
Apr 7, 1987	MEA abs	1.78	10500	1.94	16.59	2.62	423	0.001615	0.00847	19	207
Mar 10, 1987	MEA abs	1.78	10500	1.70	52.16	3.03	481	0.001587	0.00777	20	207
Apr 7, 1987	EDA abs	1.78	22400	23.91	40.23	0.74	165	0.00223	0.0095	24	207
Apr 6, 1987	EDA abs	1.78	22400	0.986	24.92	2.15	473	0.0022	0.00899	25	207
Mar 20, 1987	EDA abs	1.78	22400	14.97	43.09	3.15	637	0.002021	0.00661	31	207
Mar 11, 1987	EDA abs	1.78	22400	6.36	49.97	3.19	682	0.002138	0.00803	27	207
Apr 7, 1987	EDA abs	3.34	42000	40.06	81.02	1.98	468	0.002364	0.0058	41	207
Nov 18, 1987	MEA abs	2.0	11800	2.36		0.0172	3.15	0.00183	0.01356	14	209
Nov 18, 1987	MEA abs	2.0	11800	2.36		0.0192	3.09	0.00161	0.00674	24	110
Nov 18, 1987	MEA abs	2.0	11800	2.36		0.0170	3.15	0.00185	0.01497	12	220
Nov 18, 1987	MEA abs	2.0	11800	21.06		0.0802	14.6	0.00182	0.01309	14	209
Nov 18, 1987	MEA abs	2.0	11800	21.06		0.0951	14.2	0.00149	0.00508	29	110
Nov 18, 1987	MEA abs	2.0	11800	21.06		0.0800	14.6	0.00183	0.01332	14	220

Other conditions and parameters used in calculation of k_{ga} values:

$T=25^\circ\text{C}$

$D_{CO_2} = 1.6 \times 10^{-7} \text{ dm}^2/\text{s}$

$H \approx 30 \text{ l-atm/gmol}$

$P_i - P_b = P_i$

$a=1.46 \text{ dm}^2$

$d_{imp}=3.5 \text{ in}$

Liquid volume=1800 ml

Section 5

MDEA-ABSORPTION AND DESORPTION

5.1 CO₂ Absorption into MDEA Solution at High Driving Forces

The rate of CO₂ absorption into 2 molal MDEA (approximately 20 wt% or 1.7 molar) was determined over the temperature range 9.5-77° C and at 1 atm nominal CO₂ pressure. Typical results are shown in figure 14. The experiments were conducted under conditions of high driving force, unsteady-state absorption with the magnetic stirrer (high driving force) configuration of the reactor. The liquid phase was treated as a batch reactor and the incremental total CO₂ concentration was monitored. The slope of the data shown in figure 14 must be determined in order to calculate the absorption rate and therefore the second order CO₂-MDEA rate constant. The modified DeCoursey model was used to smooth the data and extract the rate constants. The success of the smoothing is also shown in figure 14.

Figure 15 shows the smoothed absorption rates at various temperatures. Note that the overall absorption rate increases with temperature until the reduction in the partial pressure of CO₂ with temperature begins to affect the rate. The absorption rate at 77° C is actually less than that at 60° C, even though the rate constant must increase with temperature. The effect of loading on the CO₂ absorption rate is evident in figure 15; as the free MDEA is depleted by increased CO₂ loading, the driving force for both absorption and the reaction is diminished.

Figure 16 is an Arrhenius plot of the rate constants extracted from the smoothed rates shown in figure 15. It was hoped that with the low mass transfer coefficients obtained in the reactor that the absorption rates should be kinetically controlled and therefore be completely independent of the mass transfer coefficient. However, the data at higher temperatures were shown by the modelling to be partly controlled by diffusion of the reactants; the transition between the fast and instantaneous reaction regimes was encountered.

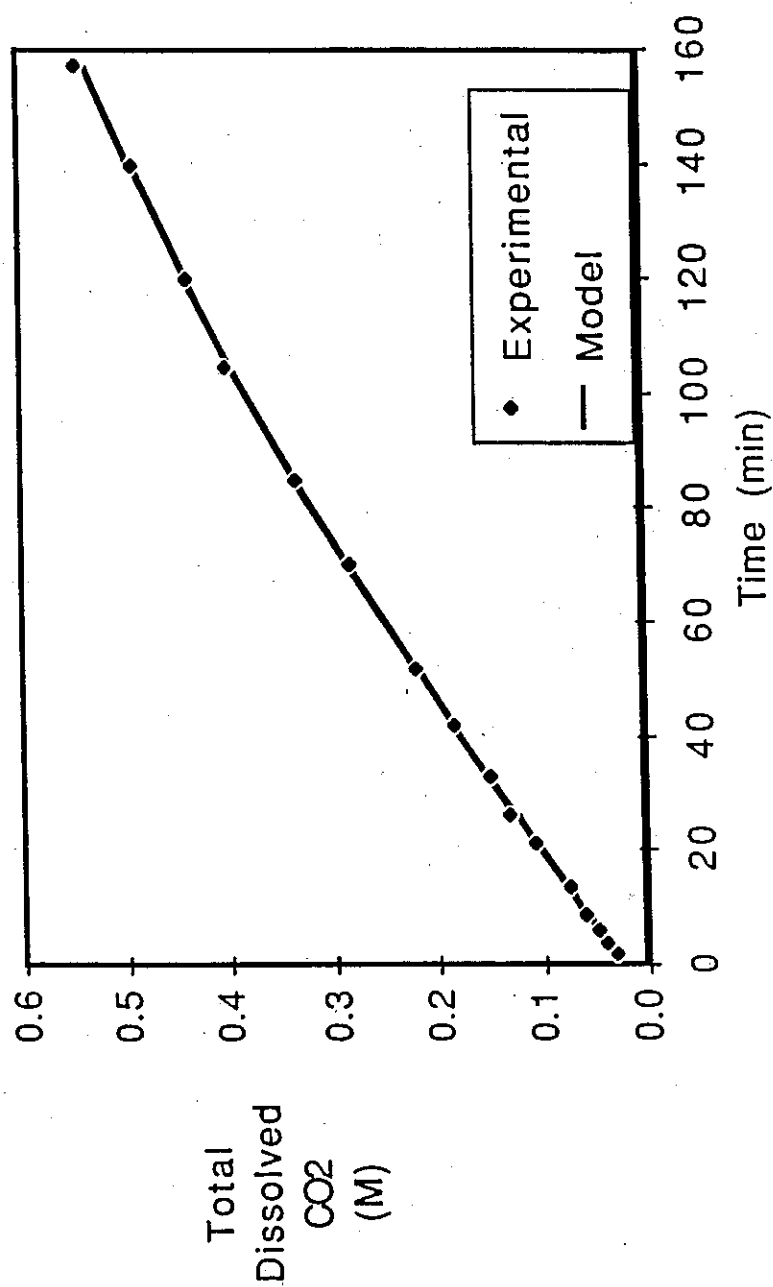


Figure 14: Concentration increase in the reactor during CO₂ absorption into 2 m MDEA at 52.5° C, 0.9 atm CO₂. The data were collected in the high driving force reactor configuration.

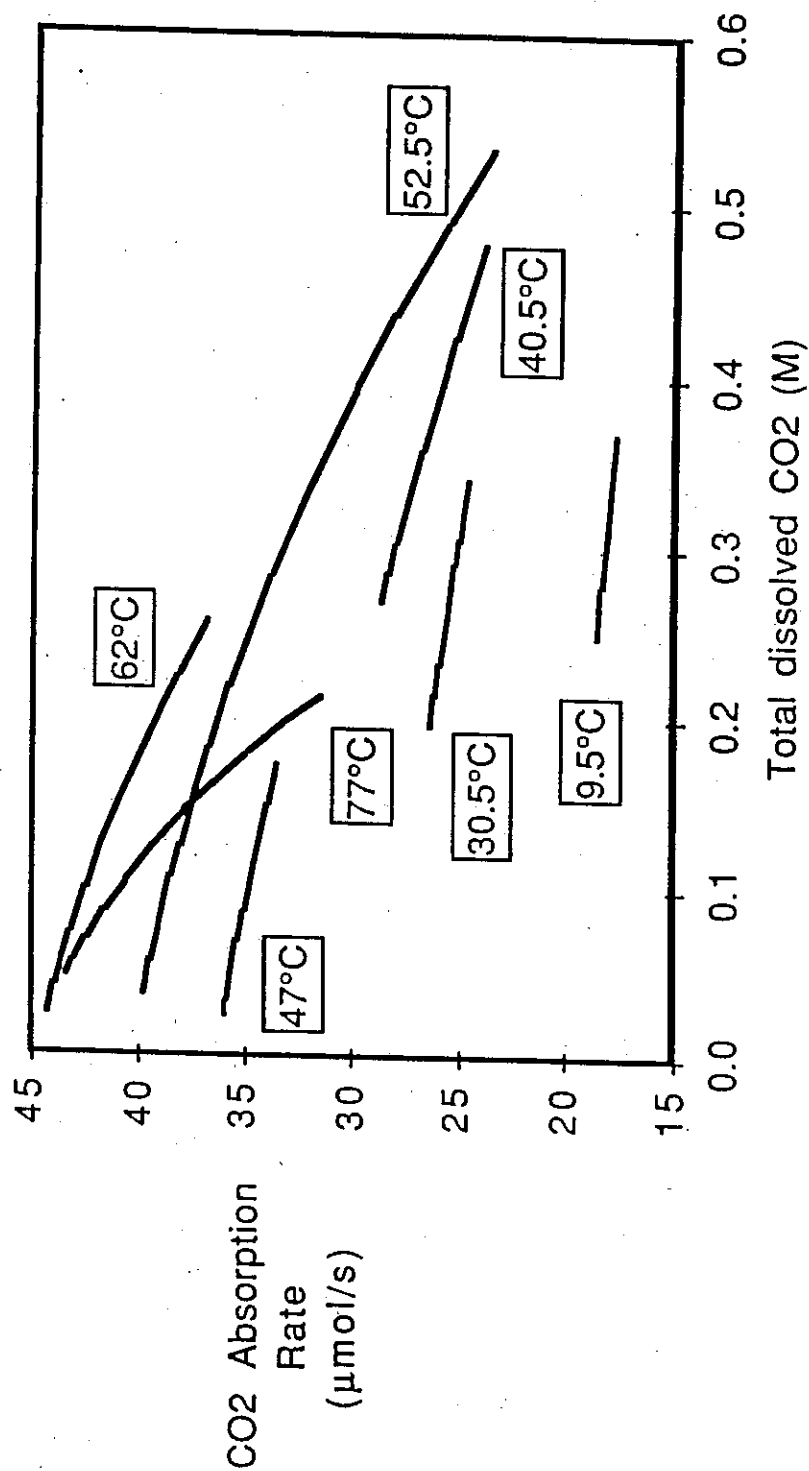


Figure 15: CO₂ absorption rates into 2 m MDEA. Data were collected at 1 atm nominal CO₂ pressure and in the high driving force reactor configuration. The curves shown were smoothed by the approximate model.

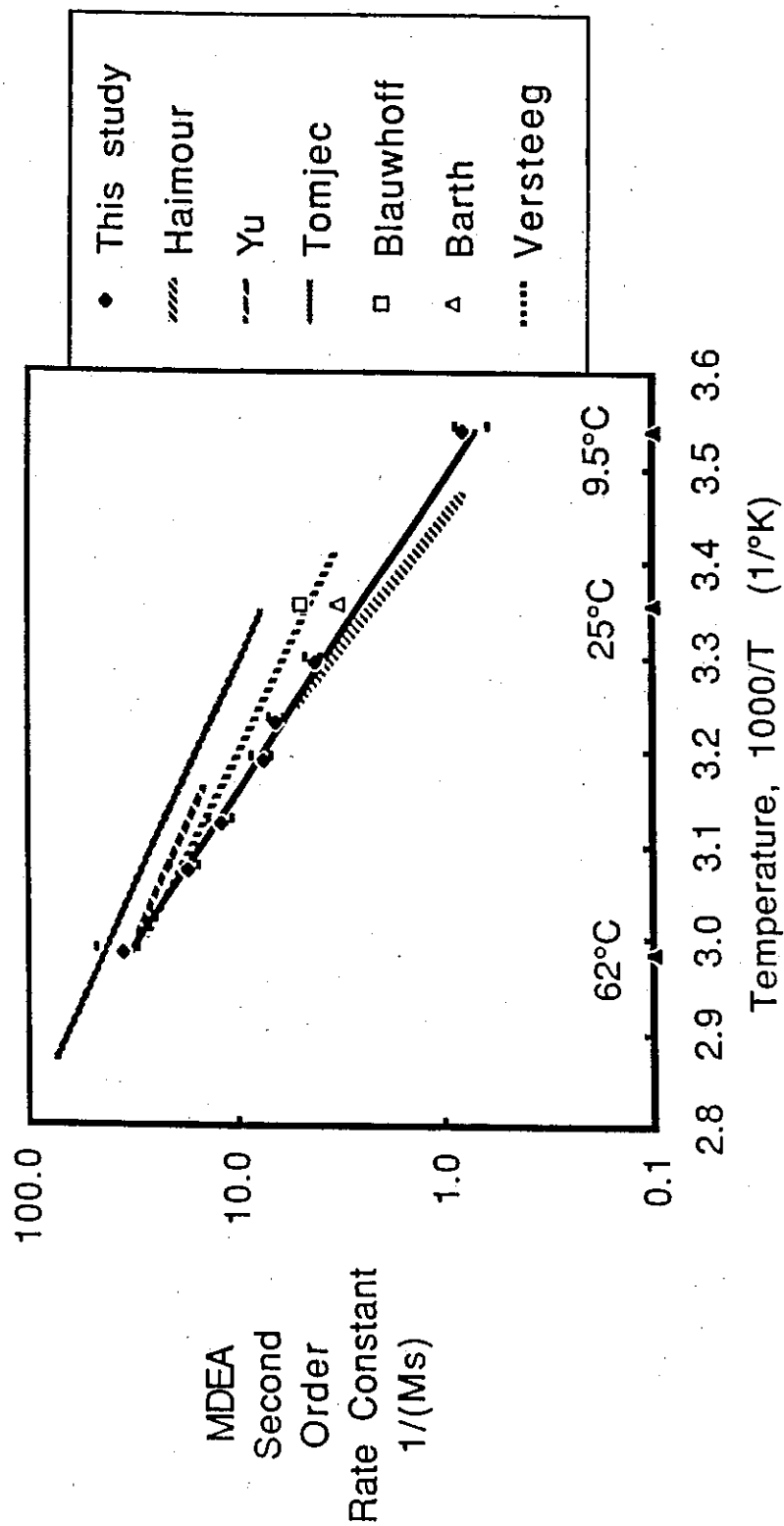


Figure 16: Comparison of MDEA rate constants measured under high driving force conditions with values reported in the literature.

A separate difficulty was encountered in the low temperature data. The rate constant became small enough at 9.5° C that physical diffusion of CO₂ contributed to the overall absorption rate. The transition from the fast reaction regime into the slow reaction regime was encountered because of the slow reaction rate.

The sensitivity of the rate constant to a 20% change in the mass transfer coefficient is shown in figure 16 as error bars around the experimental values. The rate data collected at 77° C were found to be so strongly affected by the instantaneous limit that the 77° C data were not used to generate a value of the rate constant. The approach to this limit is demonstrated in the high value of the criterion of equation 2.20 (0.6).

The values of the criterion for each temperature are shown in table 3. Note that in none of the experiments is the criterion completely satisfied, and therefore the correction to the interface composition is necessary. The importance of this diffusional correction arises from the low values of the mass transfer coefficient in the reactor system (approximately 1 E-3 cm/s), and is not necessarily indicative of mass transfer limits in industrial practice, where the liquid phase mass transfer coefficients are typically at least an order of magnitude larger.

The experimentally determined values of the second order rate constant (from 9.5 to 62° C) are very well correlated with an activation energy of 13.7 kcal/gmol and a pre-exponential factor of $2.8 \times 10^{10} \text{ M}^{-1}\text{s}^{-1}$.

$$k_2 = 2.8 \times 10^{10} \exp\left(\frac{-6895}{T}\right) \quad (4.5)$$

The data agree well with those of Haimour et al (1985), which indicate an activation energy of 16.4 kcal/gmol and a pre-exponential factor of $2.2 \times 10^{12} \text{ M}^{-1} \text{ s}^{-1}$. The value of the activation energy indicated by this work is much greater than the value of 9.2 kcal/gmol found by Yu et al (1985) and by Tomjcek et al (1986). However, these authors interpreted their rate data in terms of pseudo-first order rate constants (as in equation 2.10), not second order rate constants. Both the investigations were conducted in contacting equipment yielding mass transfer coefficients similar in size to those in the present work. Therefore the apparent

Table 3; Parameters used in the interpretation of the experimental data for CO₂ absorption into 2 molal MDEA in the high driving force configuration.

Temp. °C	Total CO ₂ content molar		HCO ₂ atm/M	DCO ₂ cm ² /s (x 10 ⁵)	PCO ₂ atm	pK _a	k ₁ ⁰ cm/s (x 10 ³)	E/E _{∞,rev}	k ₂ (Ms) ⁻¹
	init	final							
9.5	0.23	0.37	20.8	0.93	0.99	8.81	0.82	0.19	0.81
30.5	0.18	0.34	37.1	1.42	0.96	8.41	1.05	0.23	4.0
36.5	0.03	0.21	42.4	1.58	0.94	8.31	1.12	0.24	6.3
40.5	0.25	0.48	45.9	1.70	0.92	8.24	1.16	0.26	7.3
47	0.02	0.17	51.8	1.90	0.90	8.12	1.24	0.28	12
52.5	0.03	0.53	56.7	2.08	0.90	8.01	1.31	0.33	17
62	0.01	0.26	65.0	2.42	0.82	7.84	1.42	0.41	35
77	0.04	0.22	77.0	3.01	0.59	7.56	1.61	0.62	(150)

activation energy indicated by their data should contain contributions from diffusion effects and should be corrected for these effects in order to truly interpret the data in terms of the second order rate constants.

Versteeg (1987) measured the rate constant in contacting equipment with similar values of the mass transfer coefficient, but under much lower driving forces. A numerical model was used to confirm that pseudo-first order conditions applied. His results indicate an activation energy of 10.2 kcal/gmol.

The difference in reported activation energies warrants the investigation of the sensitivity of the results to assumptions made in interpreting the experimental data. Figure 17 shows the effect of assumptions made in the analysis of the data. The line on the plot which exhibits the largest activation energy (13.7 kcal/gmol) is for the fully corrected data: the reaction MDEA-CO₂ was treated as fully reversible, and the interface composition was corrected for the build-up of reaction products. Additionally, the difference in the diffusivities of the reaction products and of CO₂ was considered in the analysis. As can be seen in figure 17, the line corresponding to the assumption of pseudo-first order conditions exhibits an energy of 9.1 kcal/gmol, which agrees with the value of the apparent activation energy found by Yu et al (1985) and by Tomjec et al (1986). In later work Yu and Astarita (1987a) indicated that the activation energy resulting from their interpreted data was 14 kcal/gmol.

It is interesting to note that the values of the rate constant for the MDEA-CO₂ reaction determined at low temperature are much less sensitive to the assumptions made in treating the data. This is an important point in that at low temperature the fully corrected data agree closely with Haimour, who apparently did not make the corrections yet only measured the rate constant up to 35° C. The higher temperature investigations of Yu and of Tomjec agree closely with each other, yet exhibit the low activation energy which may indicate the effect of encroaching reversibility.

It can be concluded from this study of CO₂ absorption into MDEA that lower driving forces and higher mass transfer coefficients are necessary in order to examine reaction rates in the promoted solvents. Larger mass transfer coefficients and lower driving forces reduce the value of Q (equation 2.20) in a given

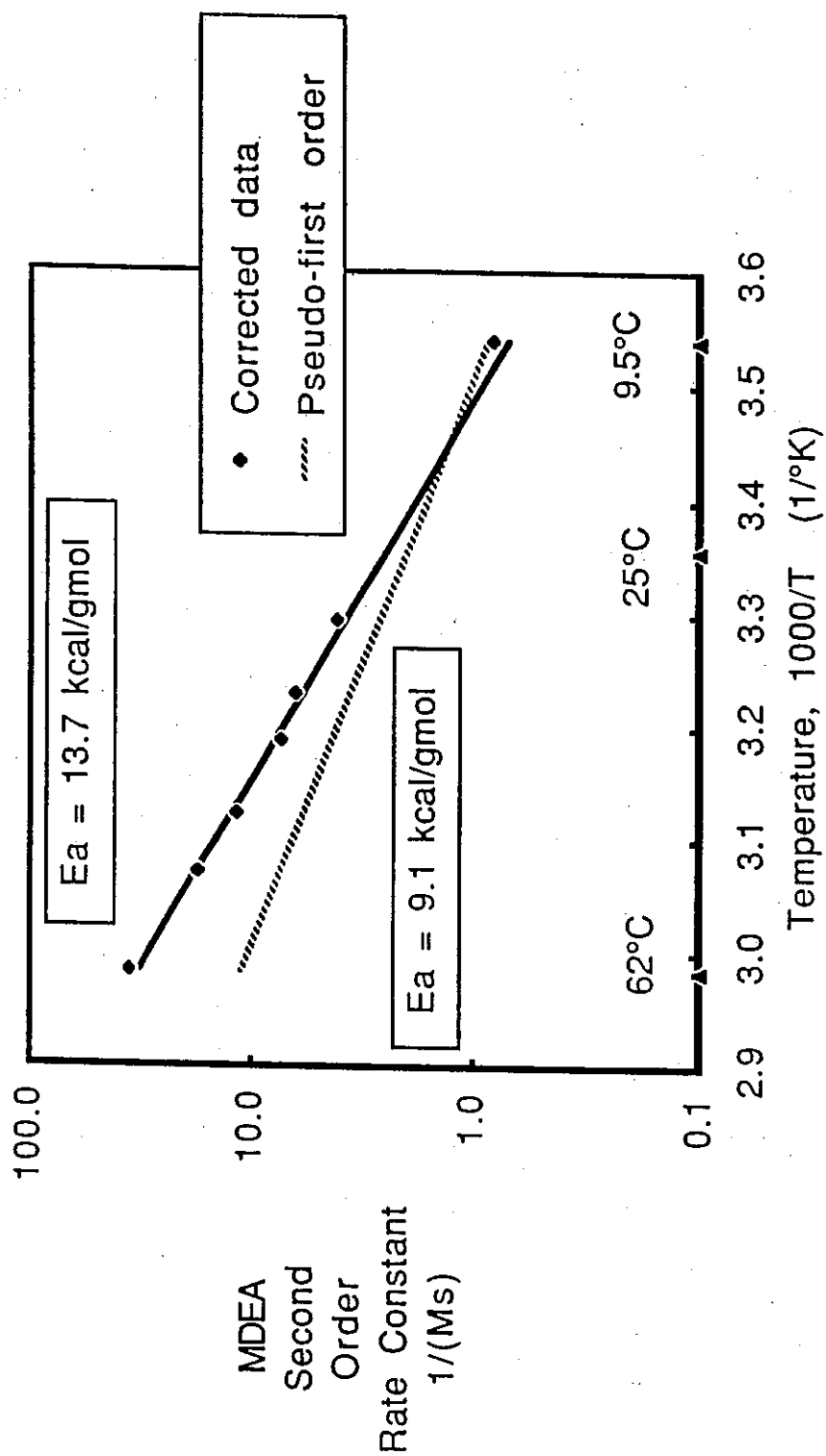


Figure 17: Effect of assumptions made in interpreting 2 m MDEA, high driving force absorption data on the resulting activation energy.

experiment and allow larger rate constants to be determined before encountering the transition into the instantaneous reaction regime.

The difference in absolute magnitude between the MDEA rate constants cannot be resolved from the results of this work. Barth et al (1984) and Blauwhoff et al (1984) both indicate the importance of potential primary and secondary amine impurities on the observed absorption rate of CO₂ in a slowly reacting amine like MDEA. Simulations by Versteeg (1987) indicate the dramatic effect of the presence of these impurities on the measured enhancement factor, and showed that the effect could be diminished by rectifying the amine. Versteeg's simulations also indicate that the higher solution loadings in this work should help eliminate the impurity effects. Impurity effects on the observed rate constant is discussed in Section 9 of this work.

This elimination of impurity effects in Versteeg's simulations is based on the assumption that the impurities are much stronger bases than MDEA and are therefore preferentially protonated at higher loadings. Because researchers commonly use MDEA in the purity provided and have not quantified the impurities, the discrepancy in the magnitude of rate constants reported cannot be resolved if it is due to impurity effects.

MDEA is commonly supplied at a purity of 99+% (Wolcott, 1987). However, the source of impurities in MDEA may not be solely from the MDEA manufacture. MDEA is known to degrade somewhat under high carbonation and high temperatures (Chakma and Meisen, 1987). The possible effect of degradation products on the observed reaction rate is unknown but a problem of importance especially in selective removal applications.

5.2 CO₂ Desorption from MDEA Solution

In order to test the reversibility of the mechanism for the CO₂-MDEA reaction, experiments were conducted to measure the rate constants in desorption. An estimate of the equilibrium vapor pressure is necessary to extract rate constants from the measured desorption rates. Estimates of CO₂ vapor pressures were obtained by analyzing both liquid and gas phases after agitating the closed reactor for at least one hour. Figure 18 shows the results of the equilibrium vapor pressure estimations compared with an extrapolation of Jou et al's (1981) equilibrium data for MDEA (Hermes, 1987). The difference shown in figure 18 is significant because in the extraction of rate constants the equilibrium vapor pressure is squared.

In the CO₂-MDEA desorption experiments, the conditions employed were 15-40° C and 2 m MDEA. Loadings ranged from 0.87 to 0.97 M total CO₂. A CO₂-free N₂ stream was passed over the agitated solution and the desorption rate was calculated from the known gas outlet flowrate and CO₂ composition. Since the gas phase was obviously less than 100% CO₂, the low driving force (turbine impellor) configuration was used in these experiments to insure good gas phase mixing. However, the larger mass transfer coefficients encountered in this configuration constrained the minimum temperature that could be employed: below 15° C the rate constant could not be estimated with confidence.

Because the rate and equilibrium experiments were conducted separately, the loadings at each condition were not identical. In order to approximate the equilibrium value at slightly different loadings than that measured in the equilibrium work, the following equation was used:

$$\frac{P_{\text{CO}_2}(\text{at } Y_{\text{exp}})}{P_{\text{CO}_2\text{-meas}}} = \frac{Y_{\text{exp}}^2 (1 - Y_{\text{meas}})}{Y_{\text{meas}}^2 (1 - Y_{\text{exp}})} \quad (5.1)$$

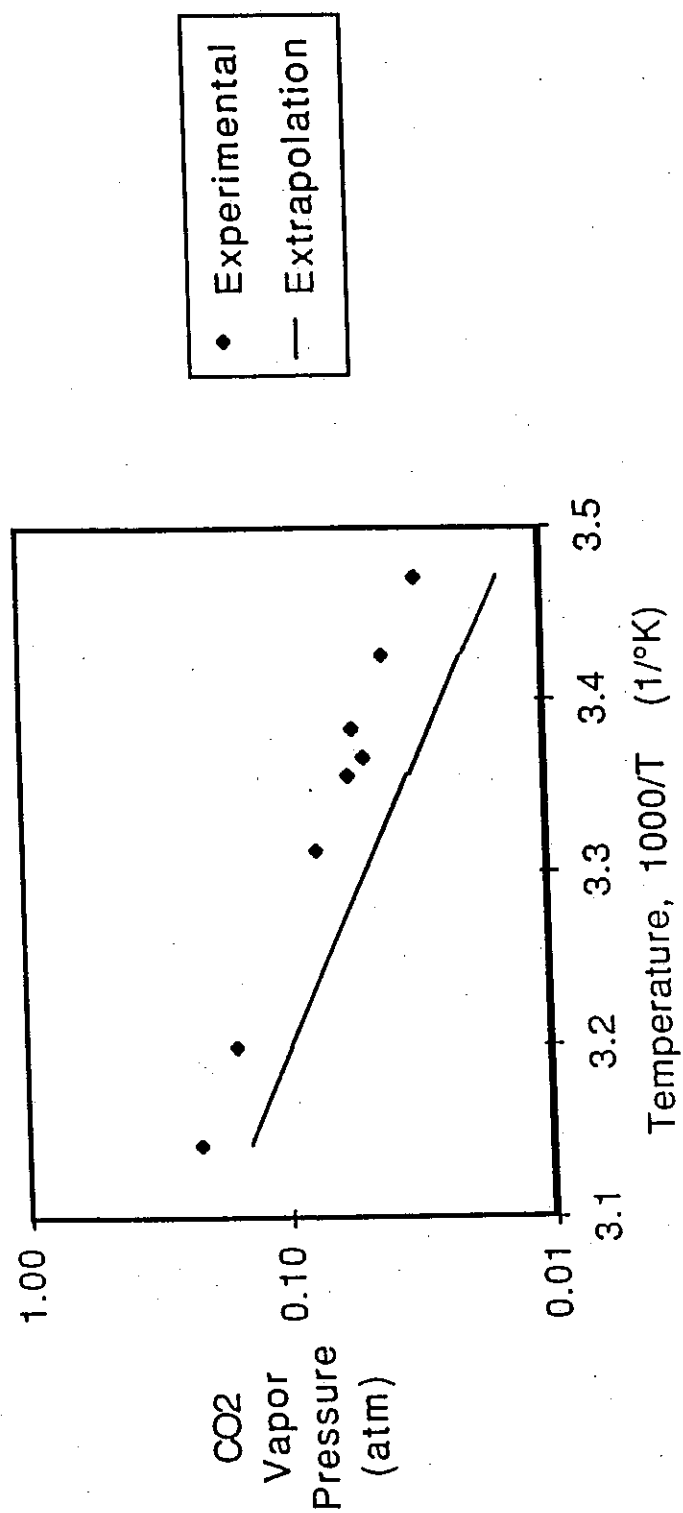


Figure 18: Comparison of measured CO₂ vapor pressure in 2 m MDEA with those predicted from the extrapolation of Jou et al's data. CO₂ content is approximately 860 mM for all data.

where Y is the loading of CO_2 in mole per mole amine
 Y_{meas} indicates the loading at the measured equilibrium values
 Y_{exp} indicates the loading at the experimental conditions

This equation contains the assumptions that 1) the equilibrium constant is a minor function of ionic strength in the range applied and 2) HCO_3^- represents the extreme majority of the total CO_2 present. From examination of Hermes' fit of Jou et al's data the maximum error (extrapolating from 0.86 to 0.97 M total CO_2) in estimated equilibrium vapor pressure is on the order of 10 to 20%. As can be seen from figure 18, this potential error is much smaller than the difference between the measured values of CO_2 vapor pressure and the extrapolation of Jou et al's data to this molarity. Therefore the estimated experimental values were used in data interpretation.

Figure 19 shows the comparison between the rate constants measured in absorption and desorption. The desorption values show error bars which indicate the importance of error introduced by the equilibrium estimation technique. The data demonstrate that a more accurate equilibrium estimation technique is required in order to study desorption with greater confidence. Consequently, all subsequent desorption experiments were conducted in a manner which yielded both rate and equilibrium estimates.

Because the desorption data are slightly higher than the absorption values, it is possible that some effect of kinetically active impurities is encountered in the desorption experiments. However, the error introduced by the equilibrium estimation procedure is sufficiently large that conclusions should not be drawn on the effect of impurities in these experiments.

It can be concluded that within the experimental error the agreement between the absorption and desorption values is fair. This result is expected since it was demonstrated in the theory section that for a single reaction with simple second order kinetics the rate expression should not change with the direction of the driving force.

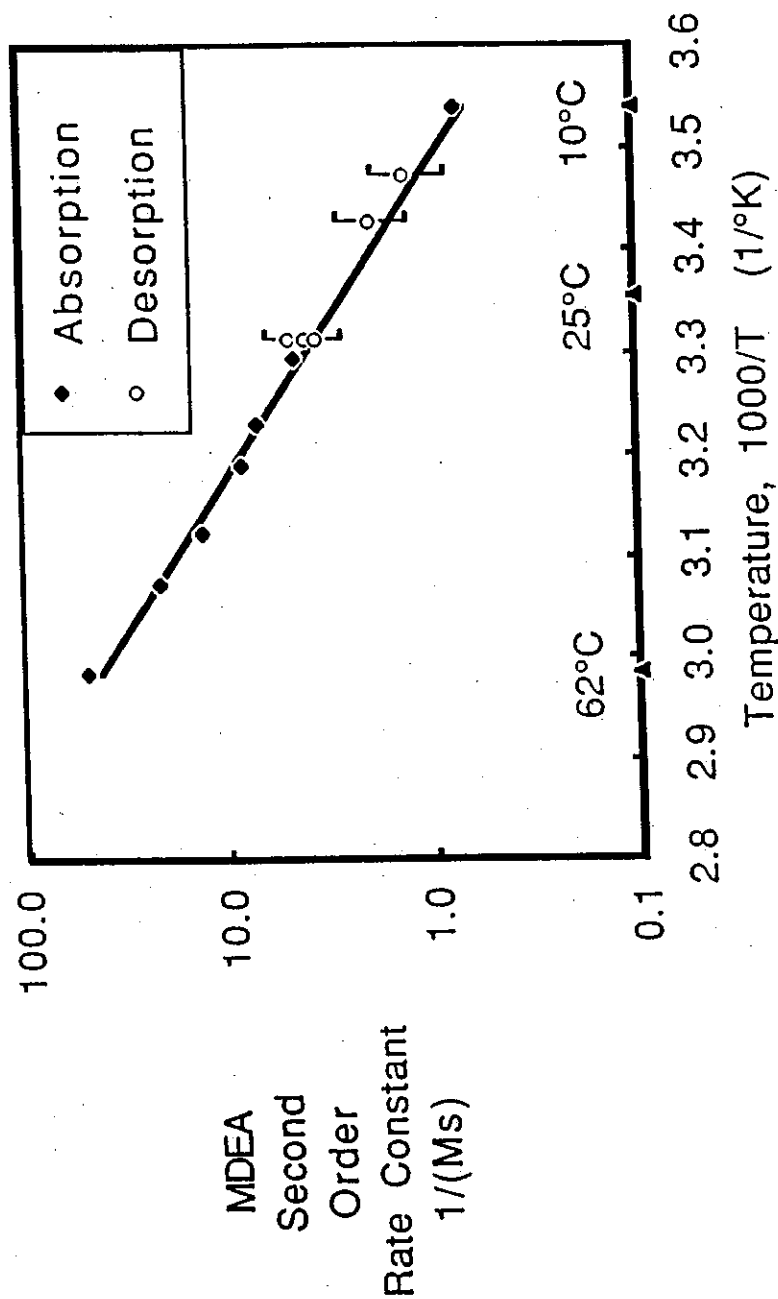


Figure 19: Comparison of MDEA rate constants measured in high driving force absorption and in desorption. Error bars represent 20% error in the estimation of the equilibrium CO_2 vapor pressure.

Section 6

VAPOR LIQUID EQUILIBRIUM

6.1 DEA

In order to interpret the desorption rates in terms of apparent rate constants, it was found that an estimate of the equilibrium solubility was required. This fact proved to be a constraint of all desorption experiments conducted.

An estimate of the equilibrium partial pressure was made by extrapolation of a series of observed desorption rates to zero rate. The desorption rate was manipulated by varying the sweep gas (N_2) flow rate through the reactor. The basis of this technique is the fact that when the rate is zero, the driving force must also be zero, and so the measured CO_2 vapor pressure must be an equilibrium value.

Figure 20 shows results of the technique at $25^\circ C$ for the 2 M DEA experiments. In figure 20 it can be seen that the extrapolation to zero rate is linear on the low end of the rate data. In most cases, extremely linear behavior was observed. When non-linear behavior was indicated, the sweep gas rate was decreased to lower the mass transfer driving force until linear behavior was encountered.

Figure 21 compares the estimated equilibrium vapor pressures with the correlation of the Kent and Eisenberg model (1976) and the data of Maddox et al (1987) and of Mason and Dodge (1936). The experimental technique is validated by the excellent agreement between the results of this work and the literature data.

The Kent and Eisenberg model contains two adjusted equilibrium constants (K_a and K_c) to allow for solution non-idealities. All other equilibrium constants are accepted as at infinite dilution. The Kent and Eisenberg constants are shown below, along with fit values of the K_a and K_c for the 2 M DEA data collected. The fit values show good agreement with the values from the Kent and Eisenberg model. The carbamate instability constant is defined by equation 1.9:

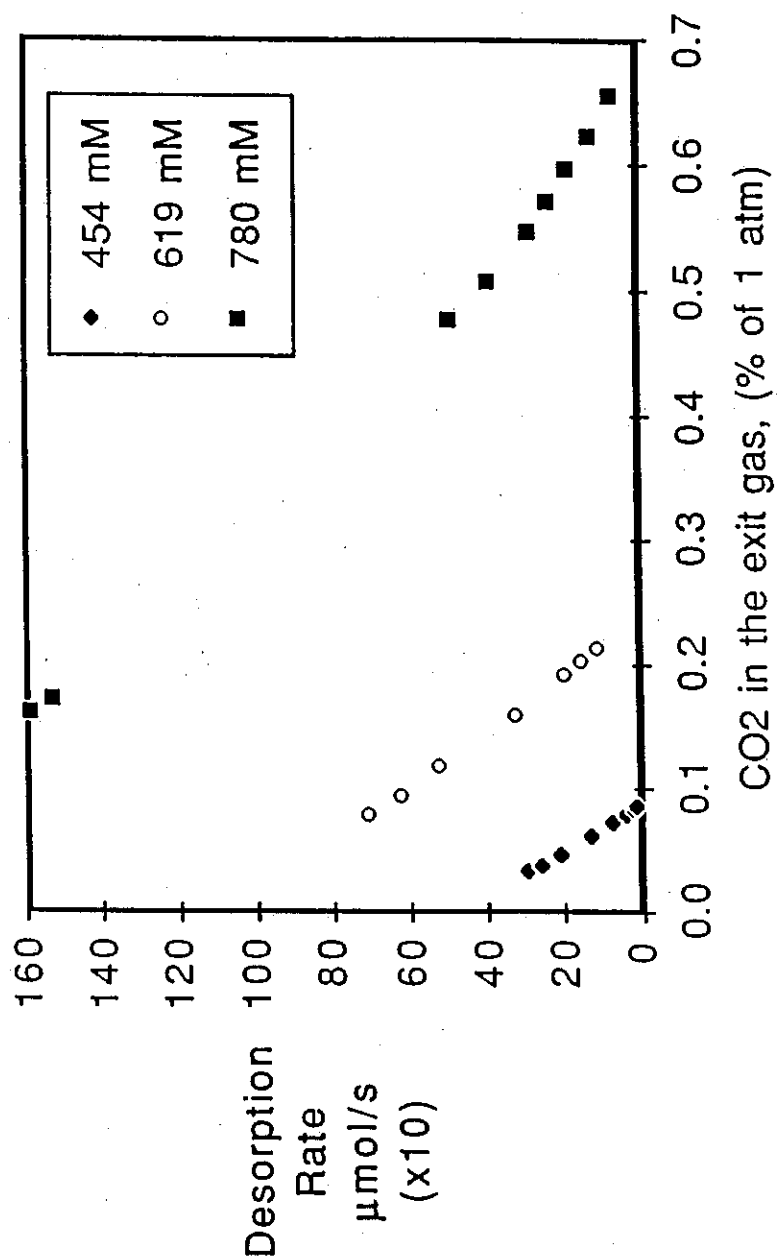


Figure 20: Desorption rates and CO₂ content in 2 M DEA at 25° C. Extrapolation gives an estimate of the equilibrium value of the vapor pressure. CO₂ contents are shown in the key.

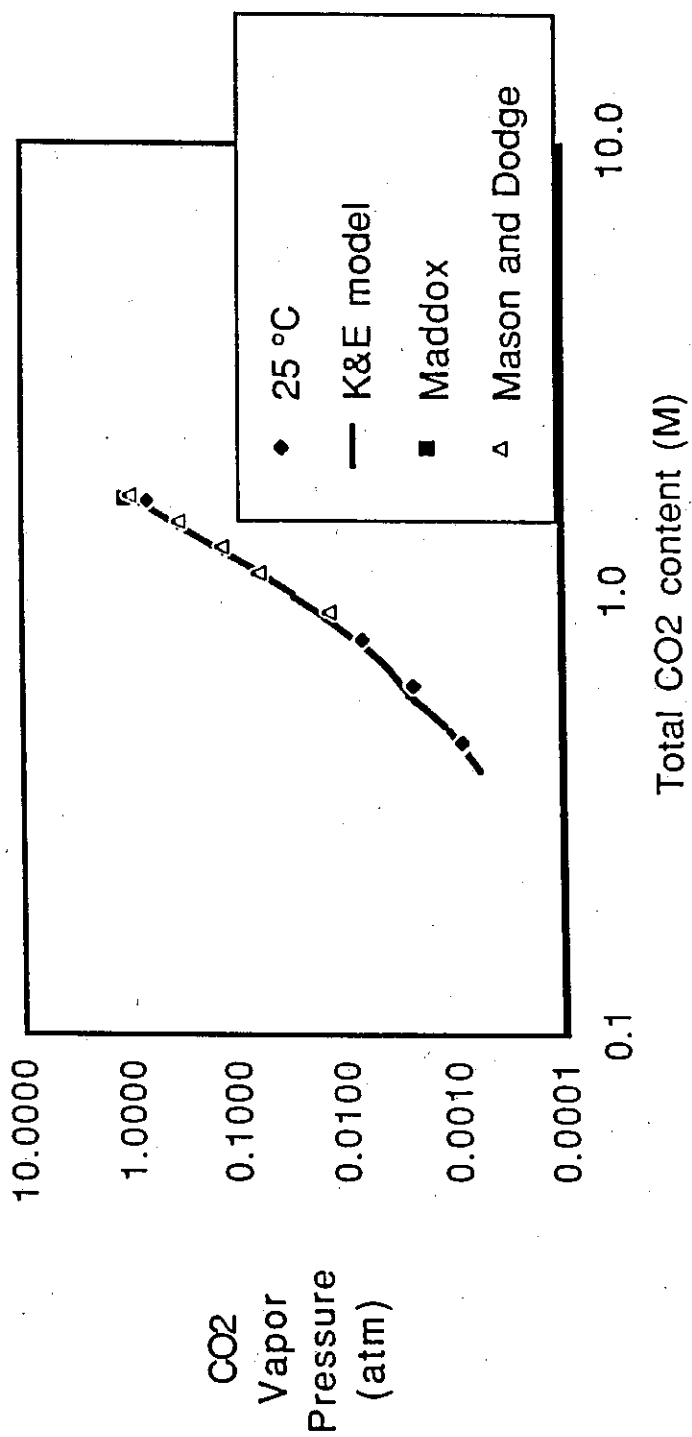


Figure 21: Comparison of measured equilibria with predictions from the Kent and Eisenberg equilibrium model and literature values. Data are for 2 M DEA at 25°C.

$$K_{c-DEA} = \frac{[HCO_3^-][DEA]}{[DEACO_2^-]} \quad (6.1)$$

$$K_c (298 \text{ }^\circ\text{K}) = 0.221 \text{ (Kent and Eisenberg, 1976)}$$

$$K_c (298 \text{ }^\circ\text{K}) = 0.266 \text{ (best fit value for 2 M DEA data)}$$

$$K_{c-MEA} = \frac{[HCO_3^-][MEA]}{[MEACO_2^-]} \quad (6.2)$$

$$K_c (298 \text{ }^\circ\text{K}) = 0.0254 \text{ (Kent and Eisenberg, 1976)}$$

The protonation constant of the alkanolamine is defined by equation 1.7:

$$K_{a-DEA} = \frac{[DEA][H^+]}{[DEAH^+]} \quad (6.3)$$

$$pK_a (298 \text{ }^\circ\text{K}) = 9.35 \text{ (Kent and Eisenberg, 1976)}$$

$$pK_a (298 \text{ }^\circ\text{K}) = 9.40 \text{ (best fit value for 2 M DEA data)}$$

$$K_{a-MEA} = \frac{[MEA][H^+]}{[MEAH^+]} \quad (6.4)$$

$$pK_a (298 \text{ }^\circ\text{K}) = 9.99 \text{ (Kent and Eisenberg, 1976)}$$

From the definitions in equations 1.3 and 1.4, the first and second dissociation constants of CO_2 are expressed as follows:

$$K_1 = \frac{[HCO_3^-][H^+]}{[CO_2]} \quad (6.5)$$

$$pK_1 (298 \text{ }^\circ\text{K}) = 6.34 \text{ (Kent and Eisenberg, 1976)}$$

$$K_2 = \frac{[CO_3^{2-}][H^+]}{[HCO_3^-]} \quad (6.6)$$

$$pK_2 (298 \text{ }^\circ\text{K}) = 10.3 \text{ (Kent and Eisenberg, 1976)}$$

$$K_w = [H^+][OH^-] \quad (6.7)$$

$$pK_w (298 \text{ }^\circ\text{K}) = 13.97 \text{ (Kent and Eisenberg, 1976)}$$

The Henry's law constant for the solubility of CO₂ in water is defined by equation 1.2:

$$H_{\text{CO}_2} (298 \text{ }^\circ\text{K}) = 30 \text{ atm M}^{-1} \quad (\text{Kent and Eisenberg, 1976})$$

6.2 MDEA

Values of the equilibrium vapor pressure of CO₂ over 2 M MDEA solution were also determined by the desorption technique. Figure 22 shows the experimental results in comparison with the data of Jou et al (1981). Figure 23 shows the normalized vapor pressures in order to contrast the data. Throughout the low and moderate loading range the experimental vapor pressures exceed those reported by Jou et al. A sufficient number of data were collected to fit the overall equilibrium constant defined by equation 1.10 as a function of ionic strength:

$$HK = 0.269 \exp(0.4412 I - 2.0654 I^{1/2}) \quad (6.8)$$

The form of the above equation was suggested by Astarita et al (1983) for the ionic strength dependence of the overall equilibrium constant in the system H₂S-amine-water. The fit of the equation was generated by adjusting the constants in equation 6.8 to minimize the percent difference between predicted and measured vapor pressures. All solution non-ideality was lumped into the overall equilibrium constant (HK), which was used to calculate the K_a of MDEA. Reference state values of the Henry's law constant for MDEA-water solutions and for the first dissociation constant of CO₂ in water were applied:

$$K_{a\text{-MDEA}} = \frac{HK K_1}{H_{\text{CO}_2}} = \frac{[\text{MDEA}][\text{H}^+]}{[\text{MDEAH}^+]} \quad (6.9)$$

In the MDEA-only system, the "salting out" effect of MDEA concentration on the Henry's law constant was demonstrated by Haimour and Sandall (1984). In

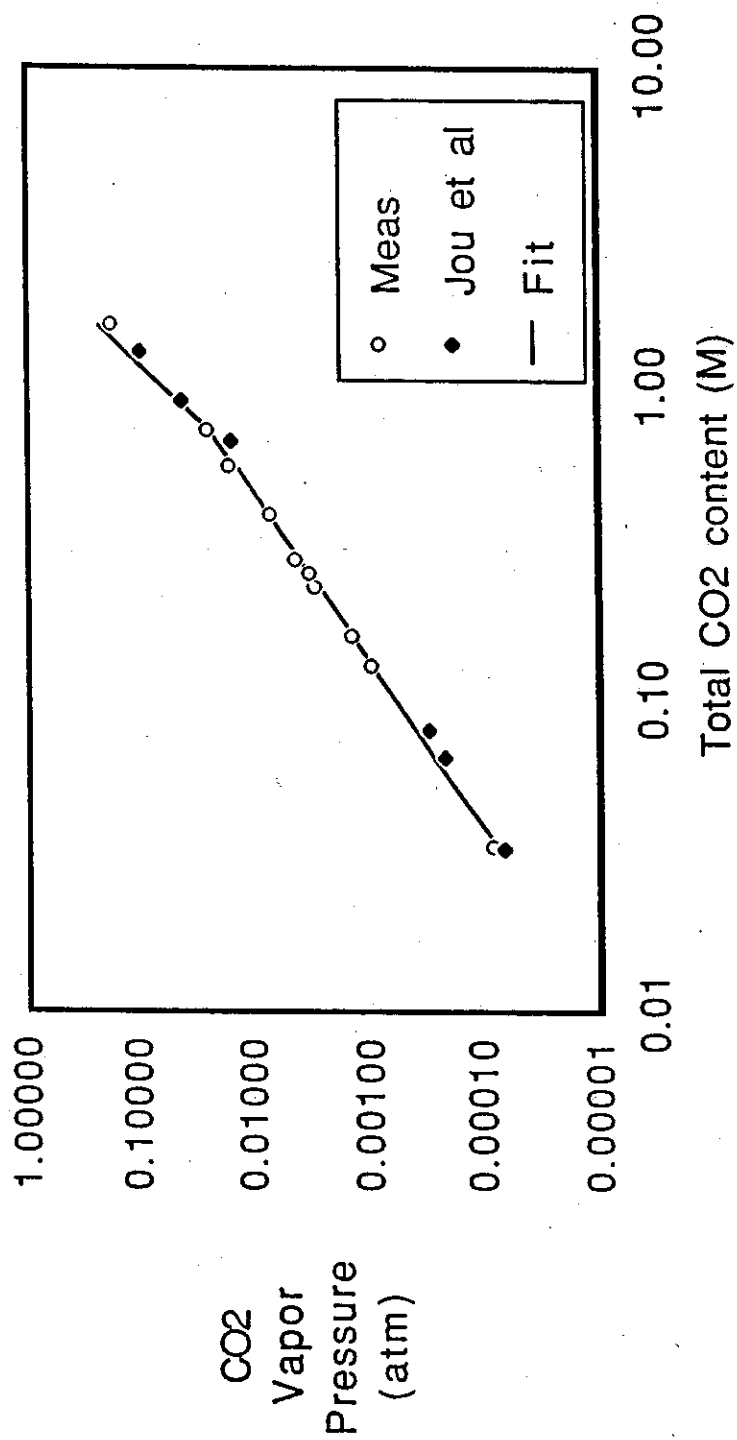


Figure 22: Comparison of measured equilibria with the results of Jou et al. Data are for 2 M MDEA at 25°C. The fit values are generated by adjusting the overall equilibrium constant as a function of ionic strength.

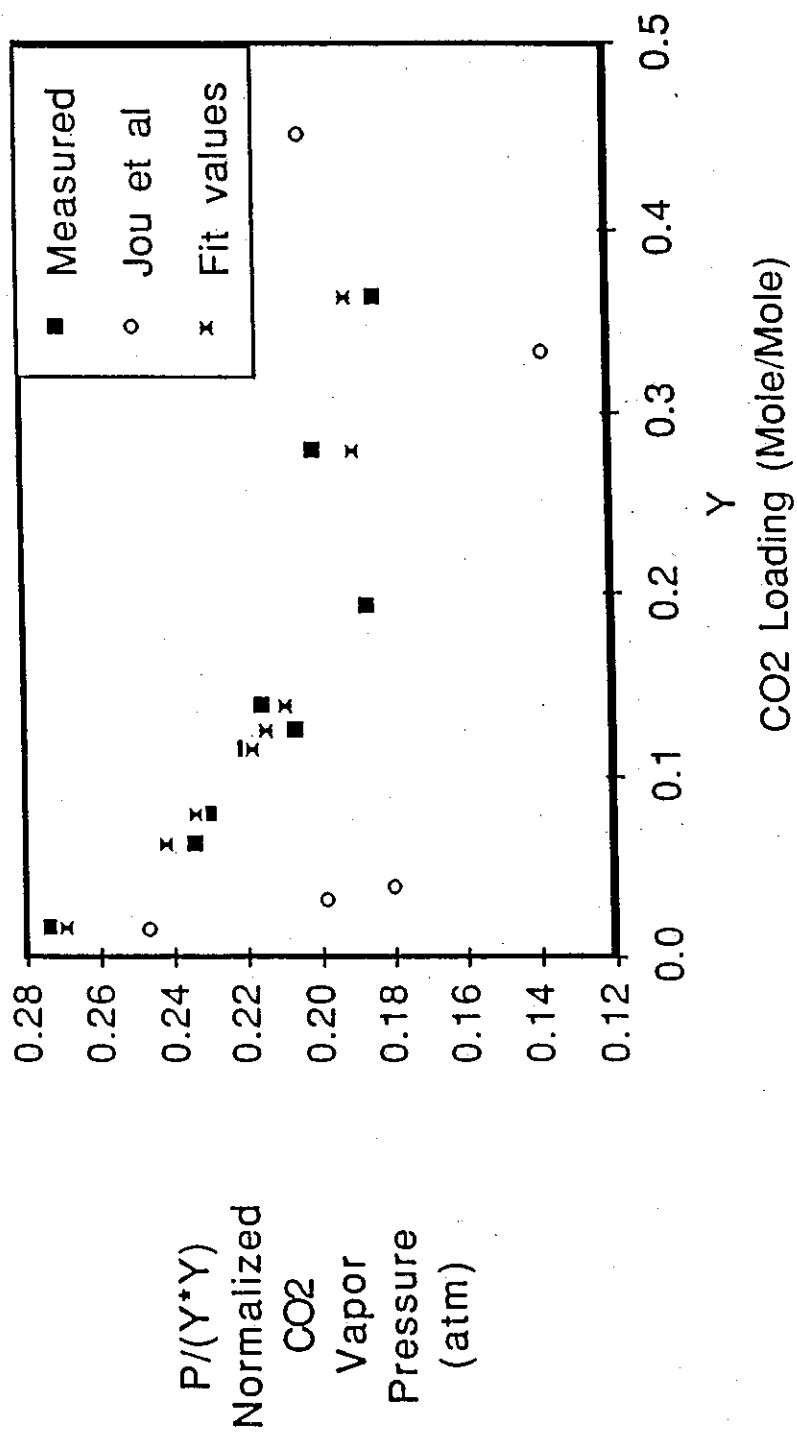


Figure 23: Comparison of normalized equilibria with the results of Jou et al. Data are for 2 M MDEA at 25°C.

the fit of the MDEA-only system the data of Haimour et al were used to adjust the reference state (zero ionic strength) Henry's law constant:

$$H_{CO_2}(298\text{ }^{\circ}\text{K}) = \exp(3.38 + 0.0724\{\text{total MDEA, M}\}) \quad (6.10)$$

Figure 23 shows that the technique is extremely successful in correlating the measured vapor liquid equilibrium data.

6.3 Mixed Systems: DEA-MDEA and MEA-MDEA

The desorption of CO_2 from 5 and 30 mole % DEA mixtures (in 2 M DEA-MDEA solution) was studied at 25° C. The experiments were conducted in the same way as the earlier CO_2 desorption experiments from DEA-water and MDEA-water solutions. The estimates of CO_2 vapor pressure generated are shown in figure 24 in comparison with predictions from a Kent and Eisenberg-type model. In order to apply the Kent and Eisenberg model to the mixed amine system, the correlated value of the MDEA overall equilibrium constant has been combined the values of the Kent and Eisenberg constants.

The approximate model is based on the adjusted equilibria from the DEA-only and MDEA-only systems. However, the Henry's law constant for the mixed solution must be estimated. The Kent and Eisenberg model uses the Henry's law constant for CO_2 in water, which is the zero-MDEA content reference state for the value used in the MDEA-only system. Therefore the MDEA-only equation also gives the correct value for the Kent and Eisenberg (MEA or DEA-only) reference state. Application of the equation to mixtures of MDEA and DEA or MEA constitutes an interpolation between reference states for the Henry's law constant.

No additional adjustable constants were used in representing the equilibrium vapor pressures in the mixtures. The agreement shown in figure 24 appears to be good, but the span of 5 decades on the log scale obscures the deviations. Figure 25 shows a more rigorous test of the fit. The normalized CO_2 vapor pressure is shown as a function of the known loading. The MDEA and the DEA data are well correlated without apparent bias as would be expected since the constants were

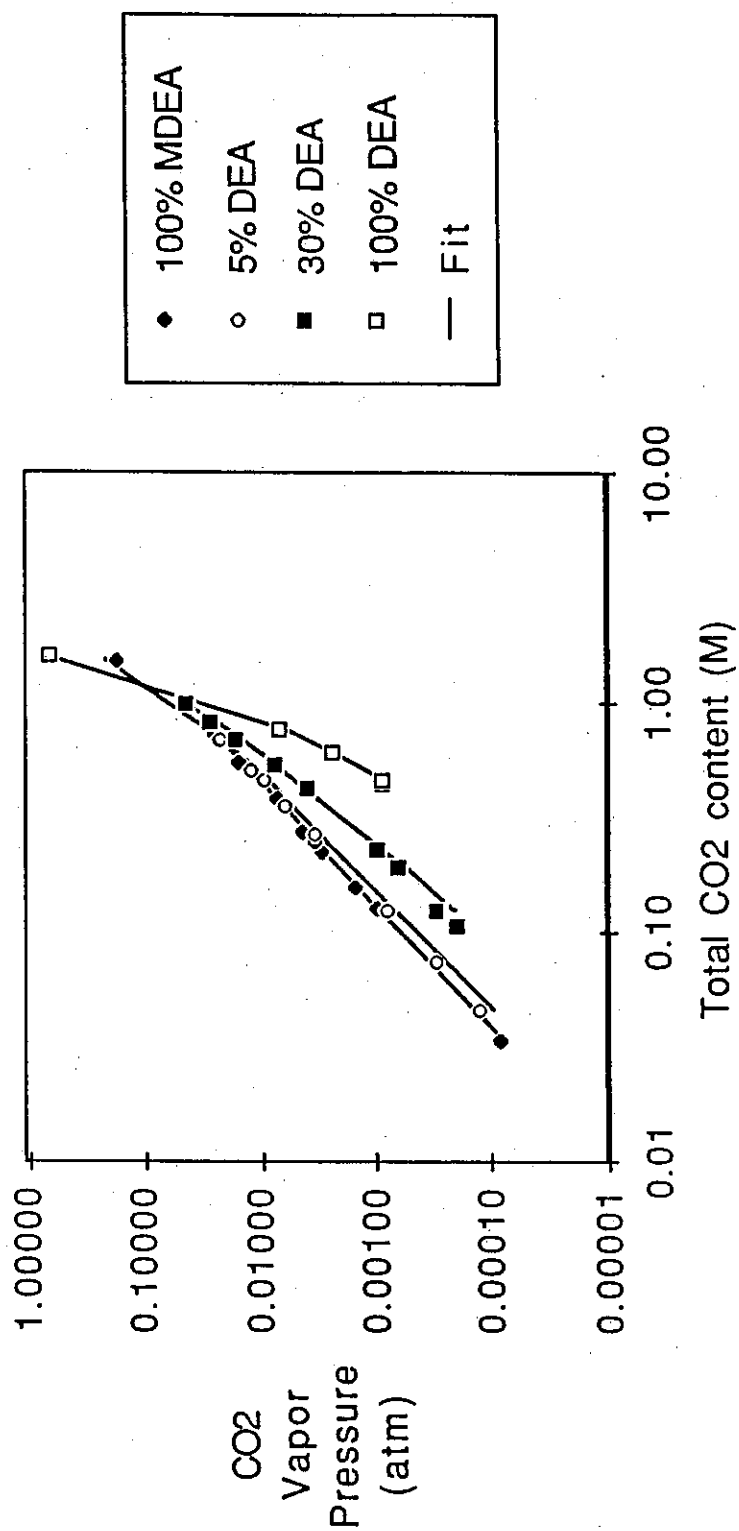


Figure 24: Attempt at fitting the system MDEA/DEA/H₂O/CO₂ with three adjusted equilibria. Data are in 2 M solutions and at 25° C.

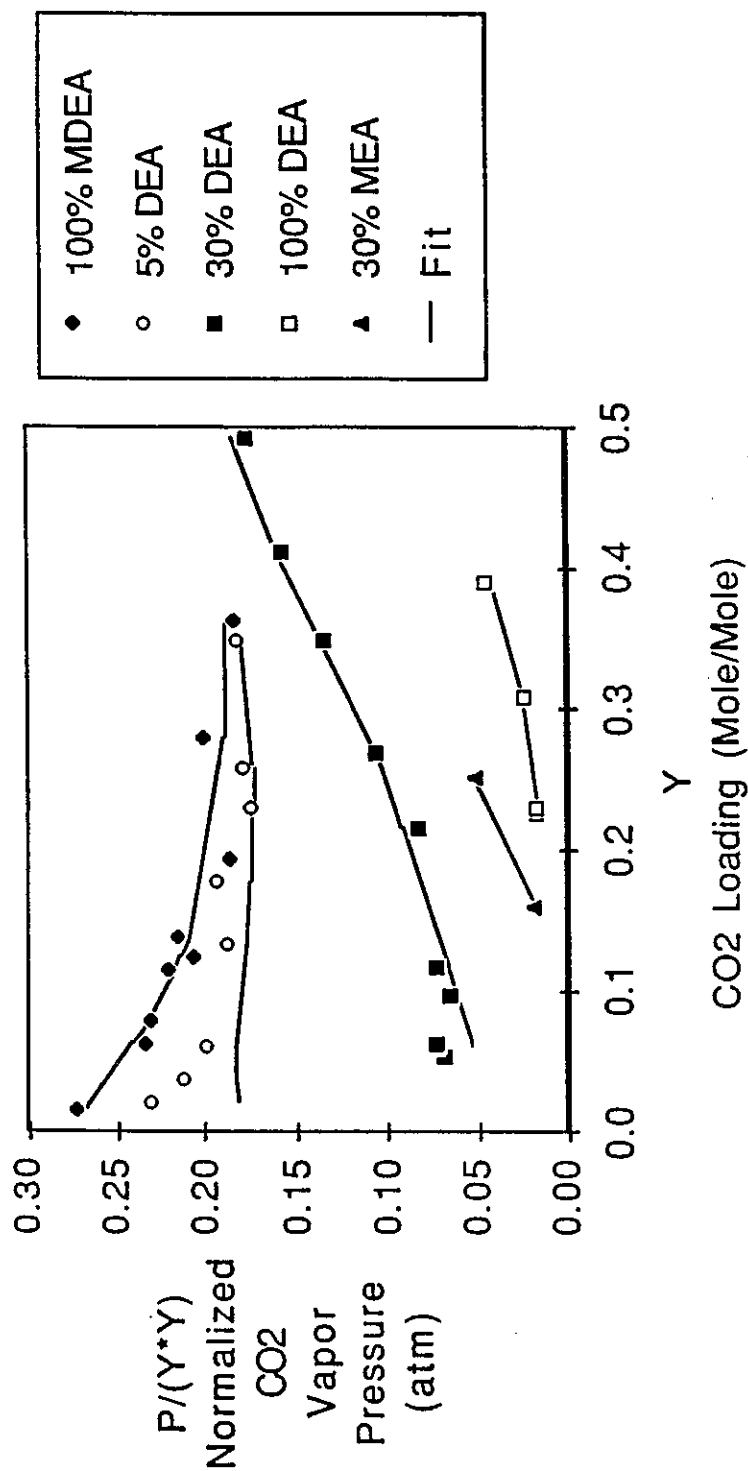


Figure 25: Fit of the MDEA/DEA(or MEA)/H₂O/CO₂ system with three adjusted equilibria. Data are for 2 M solutions at 25° C.

adjusted in these systems. The 30 % DEA in MDEA data are also fairly well correlated by the approximate model. However, the 5 % DEA in MDEA data show a bias in the fit. It can be concluded from figure 25 that the approximate modelling technique is less successful at lower CO₂ loadings and lower DEA contents in the mixture.

The system MEA-MDEA was also studied with desorption at 25° C in a 2 M solution (with 30 mole % MEA). The technique described previously for the DEA-MDEA system was used in the attempt to represent these data. Figure 26 shows the result of this fit. The MEA-MDEA data are also shown on the deviation plot (figure 25). The agreement between the predictive model and the experimental results is good.

Considering the assumptions inherent in the approximate technique, it is remarkable that the approximate technique represents the vapor pressures with a maximum error of 30% and an average error of less than 10%. Because correlation of the equilibria with the approximate technique was imperfect, a more rigorous equilibrium modelling technique, such as that of Deshmukh and Mather (1981), would be useful.

In the absence of an exact equilibrium model, apparent rate constants can still be extracted from desorption experiments provided that equilibrium vapor pressure values are estimated during each run. Unfortunately, the interpretation of the derived apparent rate constants is limited by the lack of species equilibrium since in loaded solutions the free amine concentrations cannot be calculated without a speciation model. The approximate model presented in this work is adopted only for the purpose of speciation of known total CO₂ concentrations--not for vapor pressure prediction.

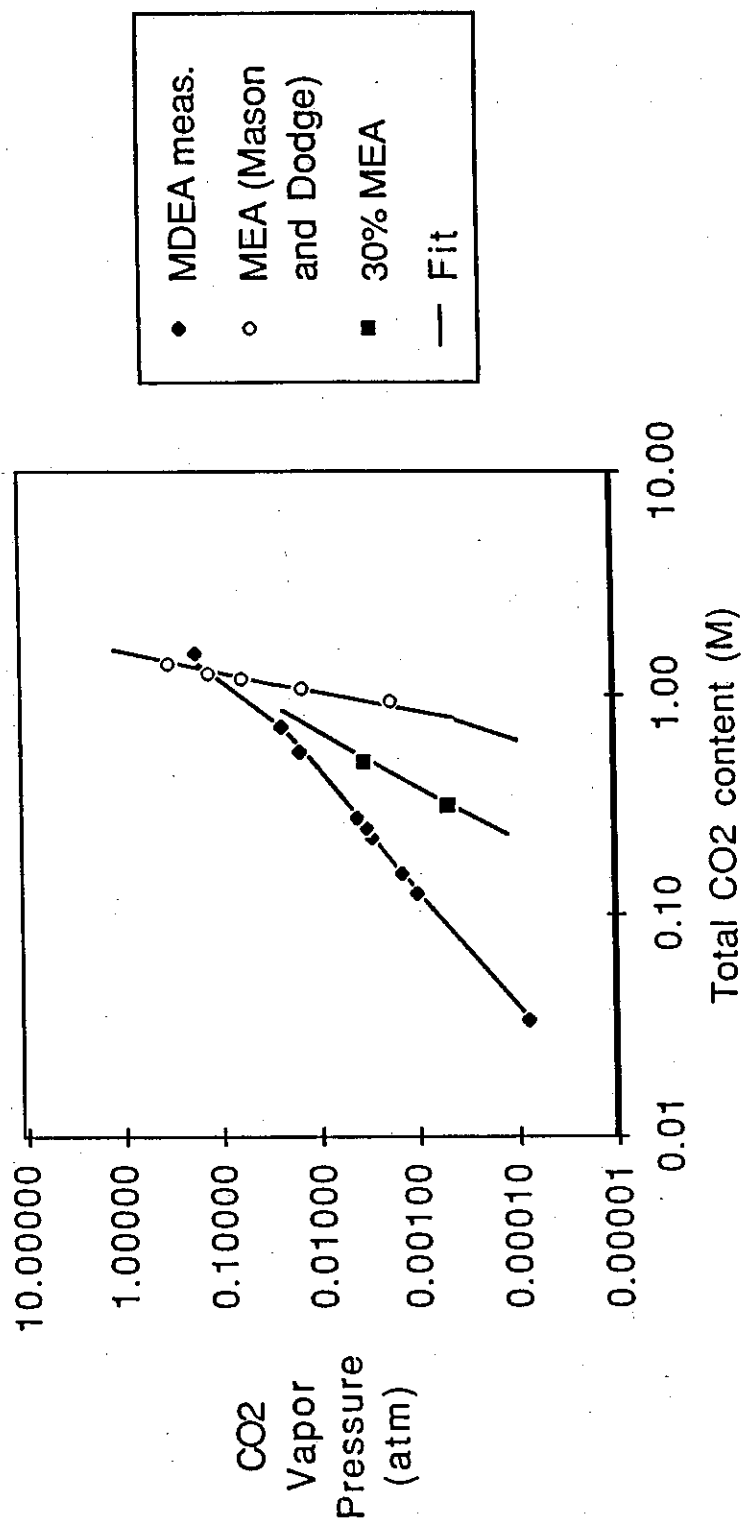


Figure 26: Attempt at fitting the system MDEA/MEA/MEA/H₂O/CO₂ with three adjusted equilibria. Data are for 2 M solutions at 25° C.

Section 7

MEA-MDEA-ABSORPTION

7.1 High Driving Force

The absorption rate of CO₂ into 1.36 m MDEA with 0.61 m MEA was determined at 31° C and 0.96 atm CO₂ in the high driving force reactor configuration (figure 27). The predicted dependence of CO₂ concentration on time is shown in addition to the experimental data. The experimental results are poorly predicted by assuming that the reaction paths are parallel and that both amines compete in a pseudo-first order reaction. Forcing the MEA reaction to completion at the gas-liquid interface, and allowing the MDEA reaction to proceed in the film (shuttle mechanism) yields the best prediction of the data. The shuttle mechanism slightly underpredicts the data, possibly because of mass transfer enhancement due to surface tension gradients generated under high driving force absorption. Surface tension effects (Marangoni effects) were observed qualitatively by Thomas and McK. Nicholl (1967) and were demonstrated as important experimentally in absorption in the CO₂-MEA system by Brian et al (1967). Versteeg (1987) also noted this effect at high flux in his rate data.

7.2 Low Driving Force

Figure 28 shows the results of CO₂ absorption into MEA-MDEA at a lower CO₂ partial pressure. The low driving force reactor configuration was employed. Under this lower driving force, it is expected that the interface would be less saturated with CO₂ and a contribution of CO₂-MEA kinetics to the observed reaction rate is expected. Also, due to the decreased flux resulting from the lower driving force, surface tension effects should be of less importance. The experimental data bear out these expectations. The shuttle mechanism provides a gross overprediction to the observed profile, and the pseudo-first order reaction

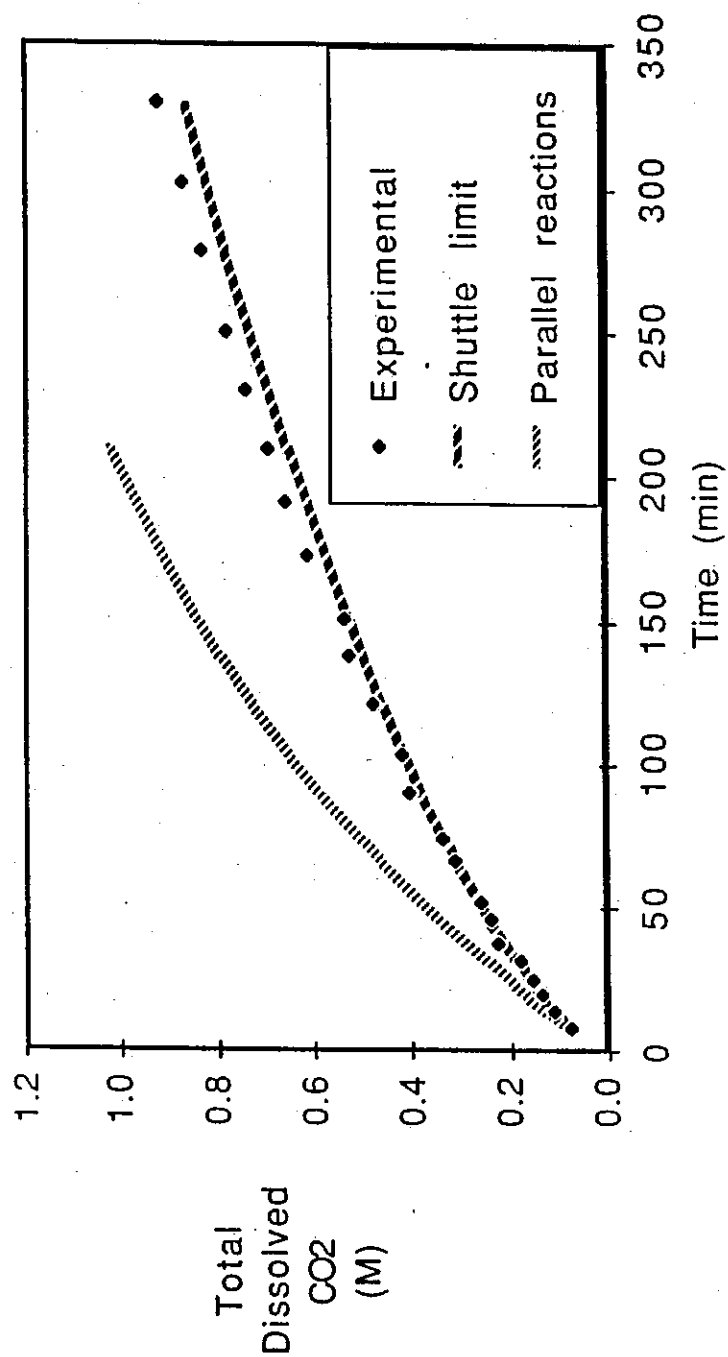


Figure 27: The shuttle model better predicts high driving force absorption. Data are for 1.36 m MDEA/0.61 m MEA at 31° C and 0.96 atm CO₂.

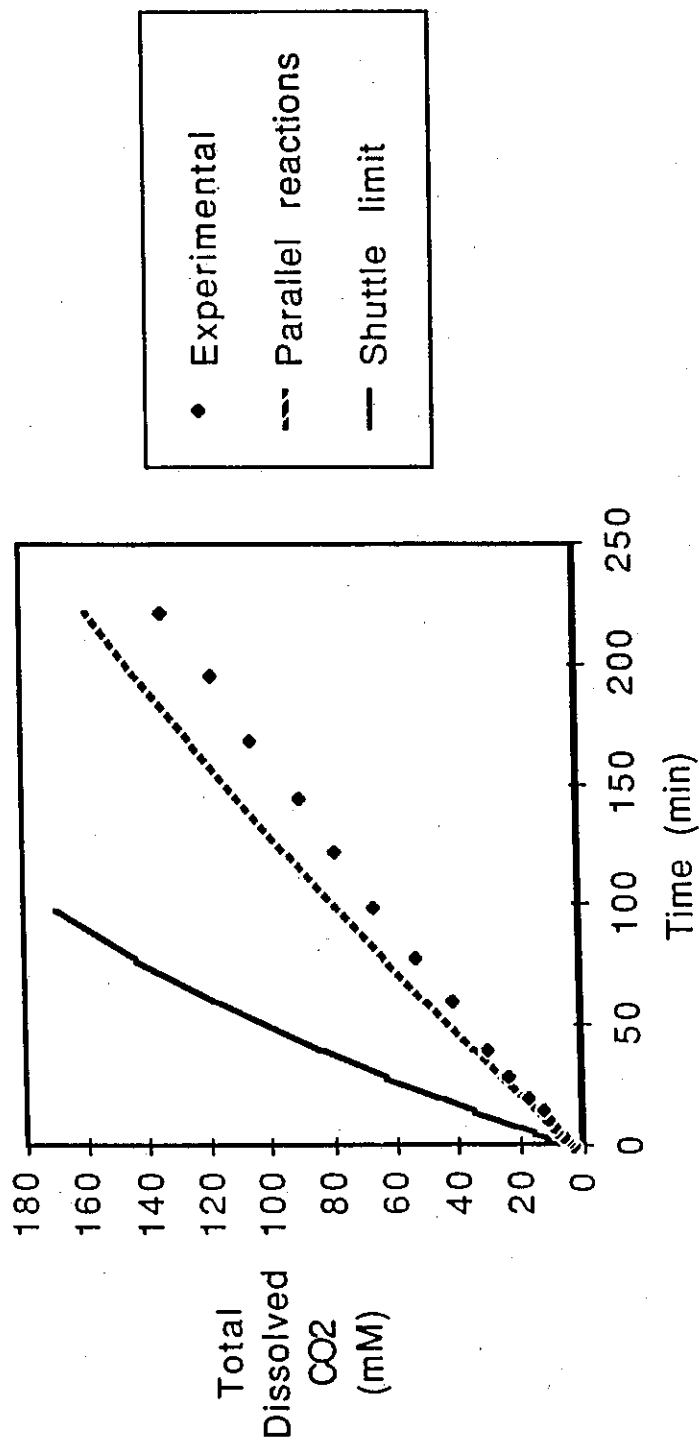


Figure 28: Absorption of CO₂ into 2 m MEA/MDEA solution. MEA content is 30 mole %, temperature is 23°C and CO₂ partial pressure is 0.033 atm.

mechanism is the best predictor of the data in this case. The deviation of the data from the pseudo-first order mechanism is probably due to the existence of liquid gradients. At still lower driving forces, the data should be completely controlled by the reaction rate and the effects of liquid phase diffusion should be completely eliminated.

Figure 29 shows the apparent rate constants obtained at very low driving forces. From figure 29 it can be seen that the data are well modelled by the pseudo-first order rate constant for MEA, and that the rate constant is independent of the absorption driving force. Consequently, it is concluded that the low driving force experiments are kinetically controlled and that the high driving force experiments are controlled by a shuttle mechanism.

It can be concluded from the kinetic data that the presence of MDEA appears to have no special effect on the reaction rate constant for CO_2 -MEA. The overall second order dependence of the CO_2 -MEA reaction is an indication that the zwitterion formation kinetics control the reaction rate. This conclusion is consistent with the kinetic model of equation 1.19. Therefore, the addition of another base in the solution would then not affect the observed kinetics of the reaction. The case for the DEA-MDEA system would be expected to be more complex due to the interaction of all bases in solution with the CO_2 -DEA reaction rate constant (Blauwhoff et al, 1984).

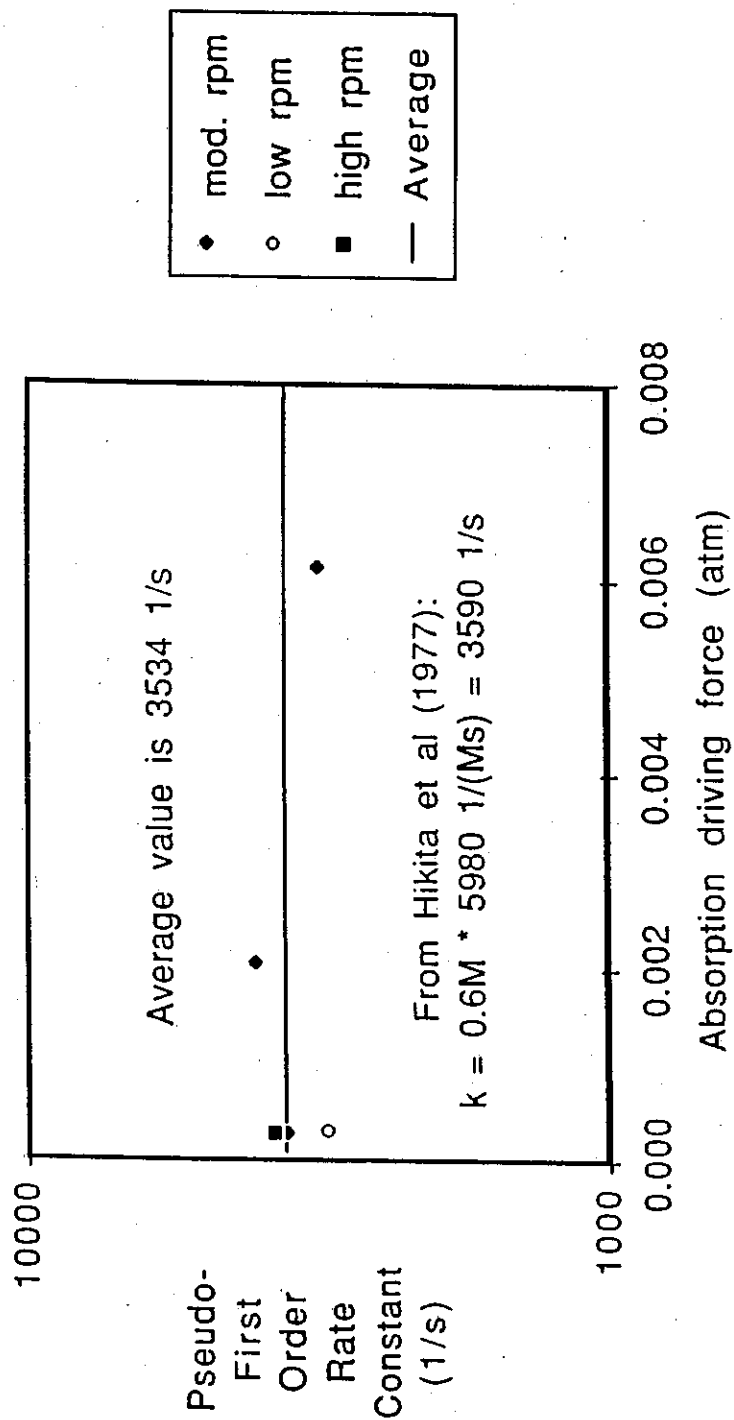


Figure 29: Pseudo-first order rate constants are independent of driving force (in 2 M total amine, 30% MEA at 25° C). The MEA rate constant accounts for the observed rate without interaction with MDEA.

Section 8

DEA-ABSORPTION AND DESORPTION

8.1 Absorption as a Function of Driving Force

The absorption rate of CO₂ into 2 M DEA was measured at 25° C in the low driving force configuration. The resulting rate apparent rate constants were not determined with the rigorous mass transfer model as in the MDEA experiments since the DeCoursey model has not been proven to apply to the complex kinetic case. However, the importance of diffusion limitations in the data is indicated experimentally by the low values of the apparent rate constants found at higher driving forces (figure 30). The driving force was therefore lowered experimentally until a constant value of the apparent rate constant was found. Table 4 contains the values of the parameters used in the interpretation of all 2 M rate data in terms of pseudo-first order rate constants.

The resulting rate constants are plotted with the results of several previous researchers in figure 31. Good agreement was found with the results of Laddha and Danckwerts (1981) and with Blauwhoff et al (1984), but the values of Sada et al (1976) and Donaldson and Nguyen (1980) are much larger than those found in the current work.

In their review article on CO₂-amine kinetics, Blauwhoff et al (1984) suggest that the higher rate constants are possibly due to the presence of primary amine impurities. The possibility of pollution of the observed absorption rate by contributions from primary amine contaminants is diminished in the current work by studying absorption in significantly loaded solutions. However, it is necessary to provide a driving force small enough that the DEA rate constant itself is unaffected by diffusion limitations. This technique was demonstrated by Versteeg (1987) to be necessary in the measurement of rate constants for tertiary alkanolamines.

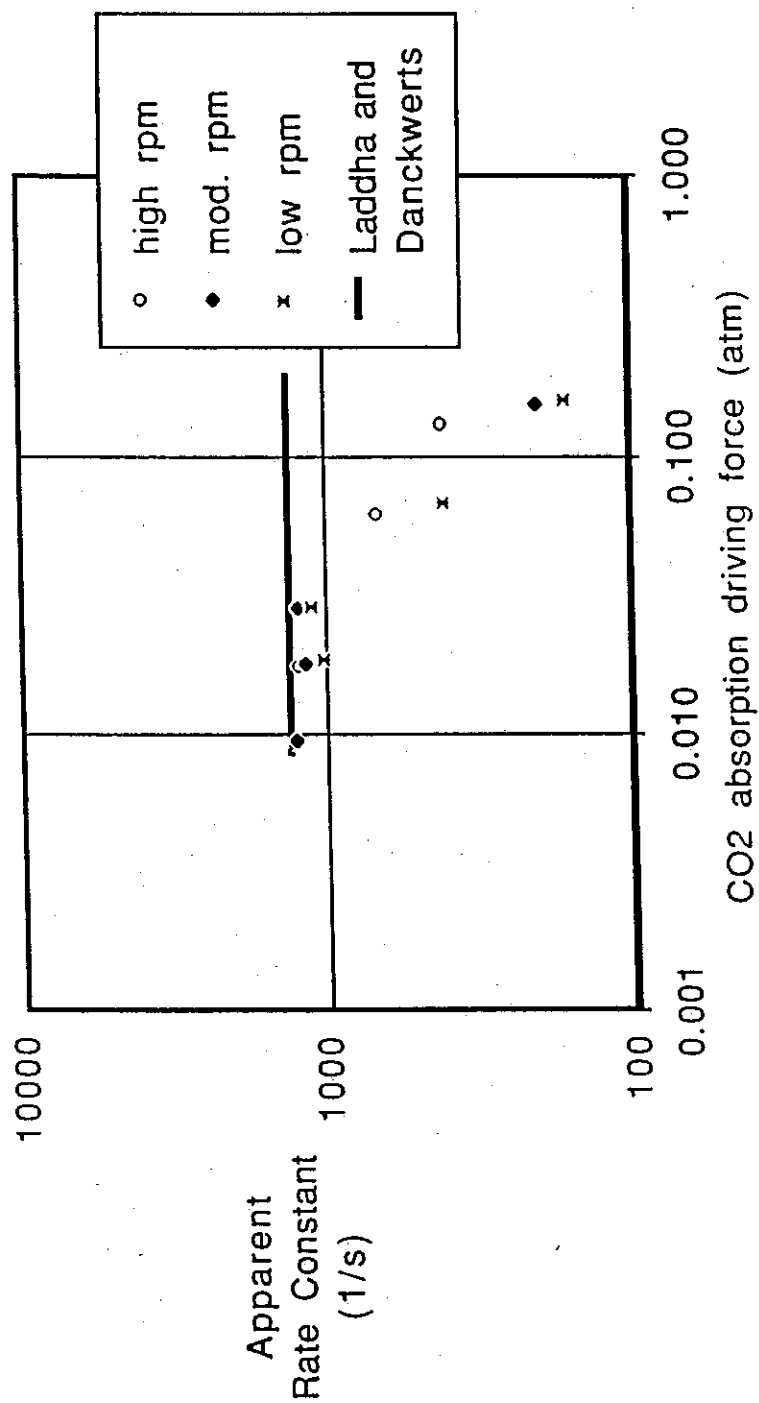


Figure 30: Apparent rate constants for CO₂ absorption in 2 M DEA measured at 25° C. Pseudo-first order conditions are encountered at low driving forces.

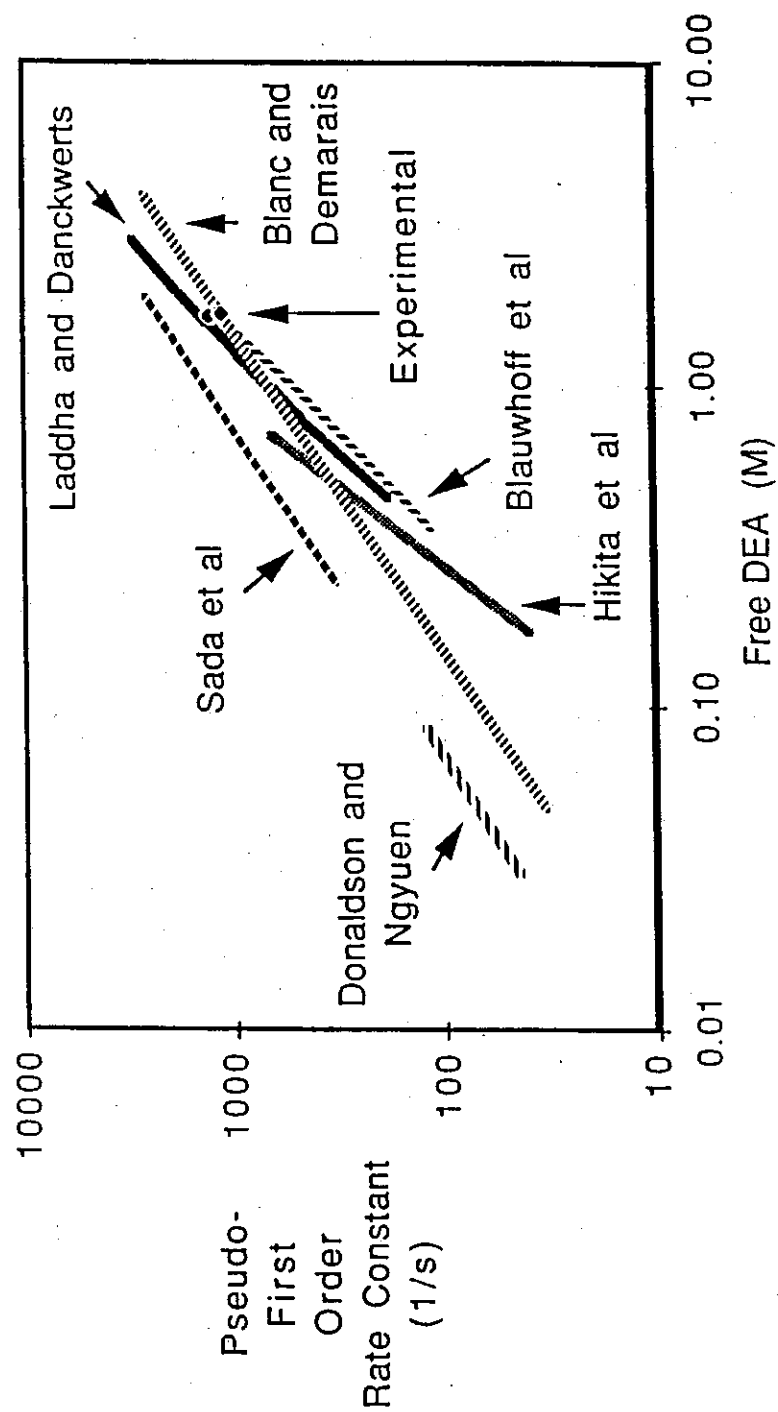


Figure 31: Comparison of rate constants measured in absorption with values from the literature at 25°C.

The experimental data shown in figure 31 do not cover enough range in concentration to allow the extraction of "partial rate constants" of OH⁻ and H₂O as did Blauwhoff et al (1984). However, we can conclude from the good agreement shown in figure 31 that Blauwhoff et al's (1984) and Laddha and Danckwerts' (1981) results are confirmed by the present work.

8.2 Desorption

In order to test the reversibility of the CO₂-DEA reaction mechanism CO₂ desorption was studied from a loaded solution of 2 M DEA. The loading was varied over a wide range, and the desorption rate was determined both as a function of loading and of sweep gas rate. The equilibrium vapor pressure of CO₂ was estimated from extrapolation of the measured rate data to zero desorption rate. The results of the equilibrium technique are discussed later in this work. Once the equilibrium vapor pressure was known, the desorption rates were used for finding rate constants only if the measured partial pressure in the outlet gas was less than 80% of the equilibrium value. By directly specifying the CO₂ vapor pressure at the experimental condition, this technique eliminated the uncertainty introduced into the estimate of the rate constant from application of an approximate vapor-liquid equilibrium model.

Figure 32 compares the apparent rate constants found in desorption with the values found in absorption. It is evident from the figure that the absorption and desorption results agree quite well. This is an important conclusion because it indicates that the complex reaction mechanism can be extended to predict reversibility in the CO₂-DEA reaction. In addition, it shows that the same limiting step in the mechanism must apply under the widely different loadings employed in the two types of experiments.

Figure 32 also compares the measured constants with the results of Blauwhoff et al (1984) and Laddha and Danckwerts (1981). In order to compare the rate constants measured at higher CO₂ loadings with values from the literature, the equilibrium model of Kent and Eisenberg (1976) was adopted for speciation calculations. The amount of free (unreacted) DEA was therefore known for each

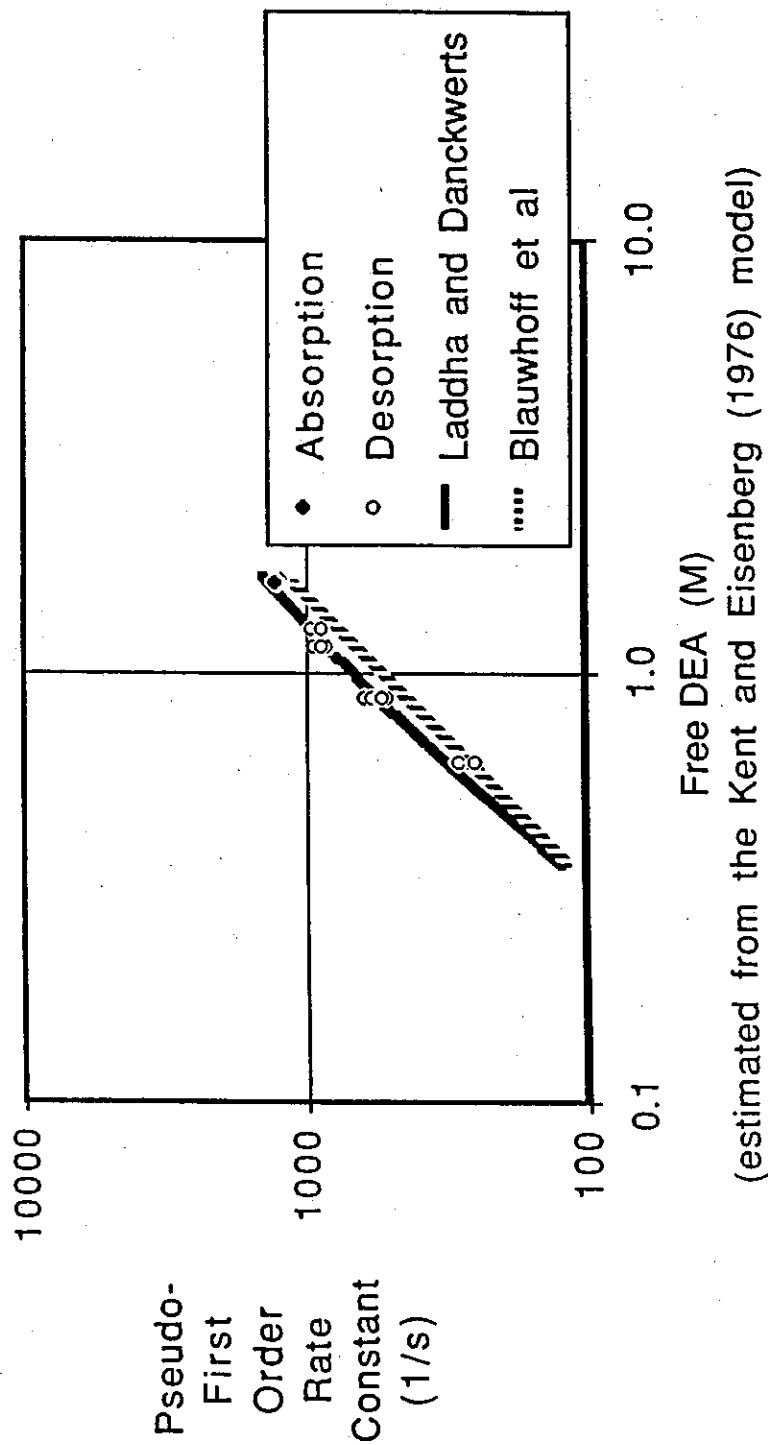


Figure 32: Rate constants for CO₂ measured under low driving forces in 2 M DEA at 25°C and at 1 atm total pressure.

loading condition. This free DEA was used to calculate the value of the apparent rate constant from the reported rate laws of Laddha and Danckwerts (1981) and Blauwhoff et al (1984). Very good agreement is demonstrated with the values of Laddha and Danckwerts (1981), a fact which indicates that the complex kinetic mechanism must be employed to represent the apparent order found with respect to DEA in the rate data.

Section 9

DEA-MDEA-ABSORPTION AND DESORPTION AND MEA-MDEA-DESORPTION

9.1 DEA-MDEA in Absorption as a Function of Driving Force

The absorption rate of CO_2 into 30% DEA in 2 M total alkanolamine was studied at 25° C. In the absorption experiments the driving force was maintained at low values in order to minimize the effects of liquid phase gradients. Figure 33 shows the effect of the driving force on the determined value of the apparent rate constant. At sufficiently low driving forces the rate constant is independent of driving force, but as the driving force increases the apparent rate constant falls. The decrease in the rate constant is evidence of the limitation of diffusion of reactants to the interface. At sufficiently high driving force, the data appear to be limited by a shuttle mechanism.

Figure 33 is important because it indicates that the data at low driving force and high agitation rate are kinetically controlled. It demonstrates that the rate constants obtained in this region can be interpreted with a pseudo-first order model since any effects of liquid phase gradients have been ruled out experimentally. Consideration of the criterion of equation 2.20 (Q values) yields values on the order of < 0.1 ; therefore interface conditions can be approximated by bulk conditions. A small effect of gas phase resistance is indicated from the lowest rpm data as would be expected from the size of the rate constants measured.

Because a significant amount of DEA is present in the blend, and because the loading of CO_2 was purposefully restricted to low values, in these data the free DEA concentration can be approximated by the total DEA concentration. This fact results in the applicability of irreversible absorption conditions; insufficient products exist in the bulk liquid to affect the DEA content appreciably.

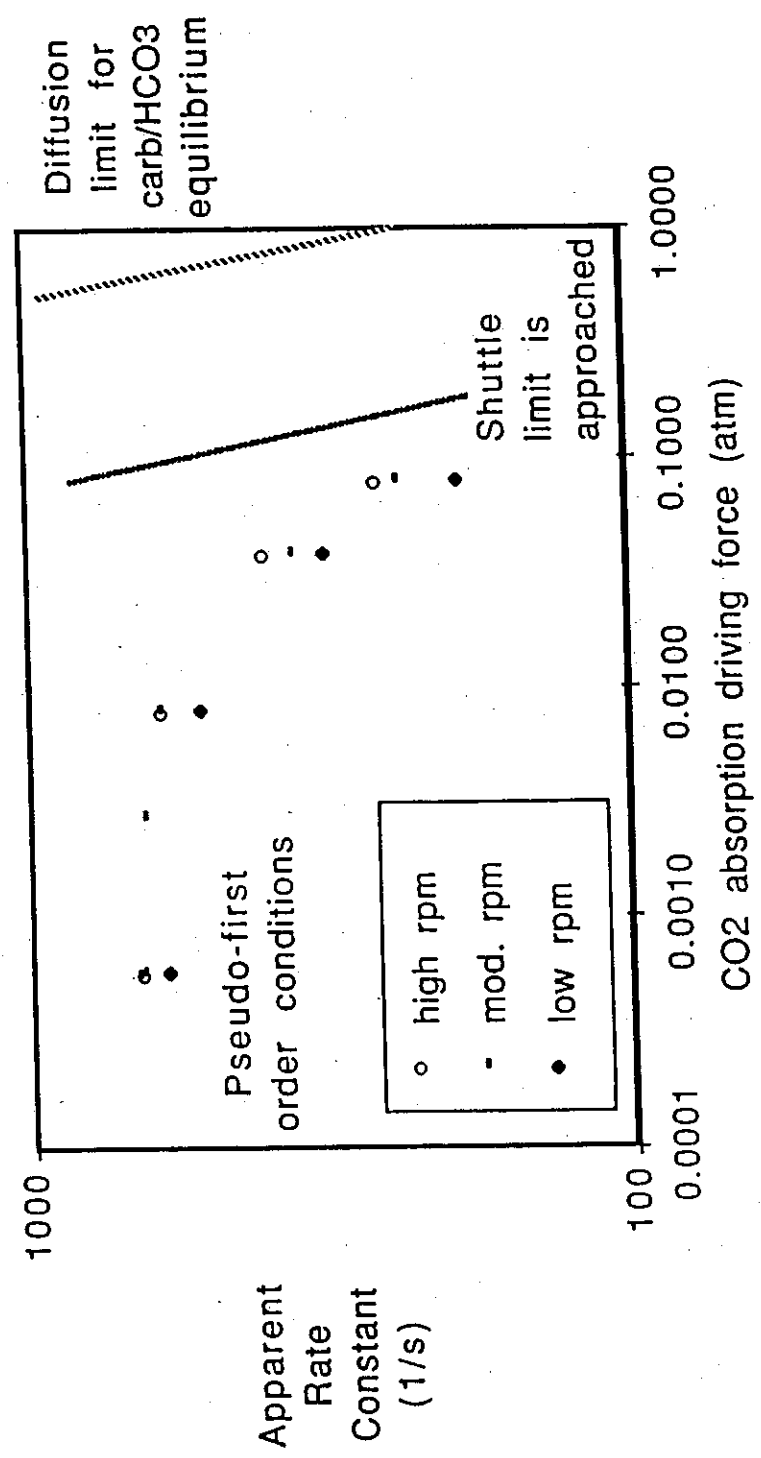


Figure 33: Apparent rate constants for CO₂ reaction measured from absorption in 2 M amine (30 % DEA, 70 % MDEA). The data are at 25° C and the CO₂ content of the bulk liquid is below 15 mM.

9.2 DEA-MDEA in Desorption

Because both DEA and MDEA have individually shown that the rate constants measured in absorption are identical to the values found in desorption, the effects of reversibility on the mixed system were studied. The apparent rate constant was measured in two blend compositions -- 5 and 30% DEA in 2 M total alkanolamine. Figure 34 shows the apparent rate constants measured as a function of CO₂ content. Each point in figure 34 is calculated from the measured rate using the experimentally estimated value of the equilibrium vapor pressure. The absorption values are plotted on figure 34 for comparison purposes: the comparison was made at the 30% composition and the agreement is quite good.

The good agreement between the absorption and desorption values in the mixed system is important. It indicates that irreversible absorption data taken (even in the more complex mixed systems) can be applied to the reverse reaction rate. However, further interpretation of the mixed system in terms of "partial" rate constants (as in Laddha and Danckwerts' model) cannot be achieved with the desorption data without the application of an equilibrium model to speciate the known solution composition. This complication is encountered because the desorption data are, by necessity, collected at much higher CO₂ loadings than the absorption data, and so the free DEA concentration cannot be directly approximated as the total DEA concentration.

Application of the approximate equilibrium speciation model results in an estimate of the free DEA, MDEA, and OH⁻ concentrations for the CO₂ loading at each datum. Figure 35 has been prepared from combination of the speciation model with the kinetic model of Laddha and Danckwerts (1981), which simply represents the contribution of the free DEA to the apparent rate constant. In figure 35 no contribution of MDEA to the DEA kinetics is considered; only the contribution of DEA as a base in the proton abstraction step is incorporated. Since this "non-interactive" model does a poor job of representing the apparent rate constants an "interactive" model must be defined which considers MDEA in the DEA kinetics.

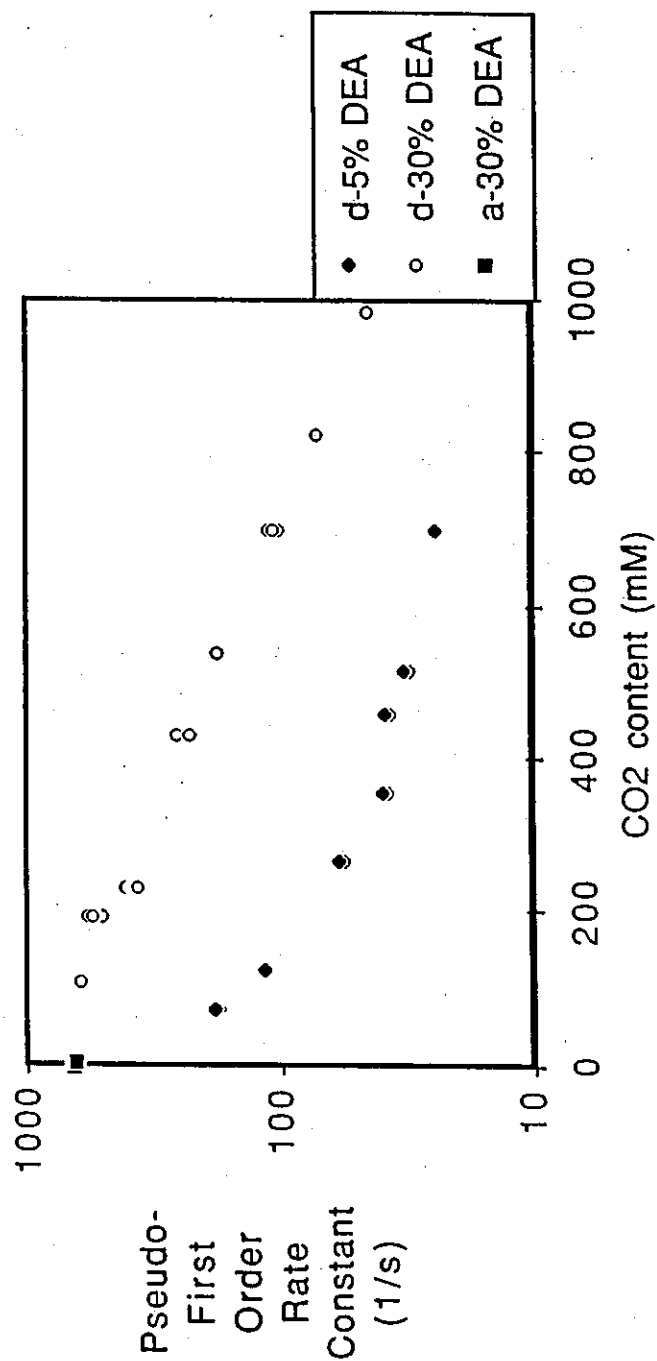


Figure 34: Rate constants for CO₂ reaction measured in 2 M DEA/MDEA at various DEA contents and at 25° C. Data are for absorption (a-) or desorption (d-) as indicated.

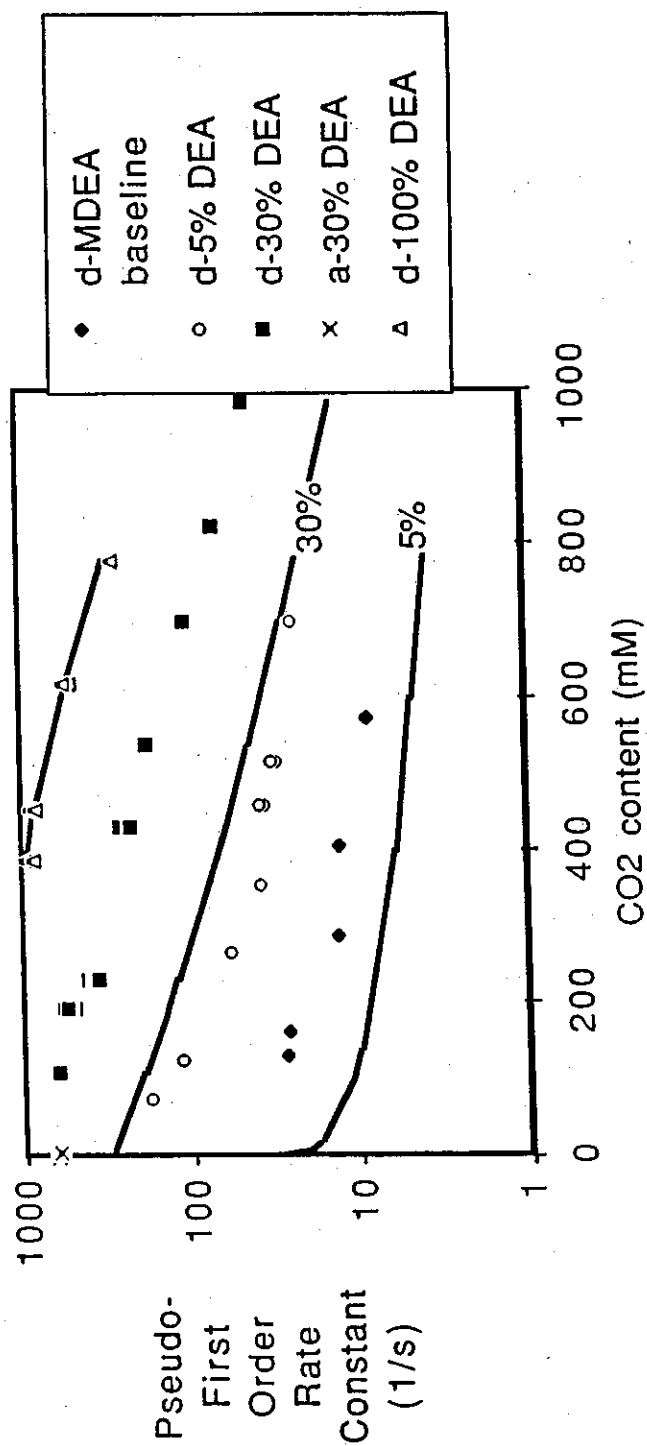


Figure 35: Test of a kinetically non-interactive model for rate constants in the DEA/MDEA mixtures. Data are for 2 M DEA/MDEA at various DEA contents and at 25° C. A kinetically non-interactive model does not fit the data.

The basis of the interactive model for the mixed system arises from Blauwhoff et al's recognition of the role all bases present in solution play in the DEA kinetics. The lumped base interaction constant for MDEA in the DEA kinetic scheme, $k_{b\text{-eff}}$, was determined by application of a non-linear optimization package to the experimental data. The improved fit of the interactive model is shown in figure 36. Only the 30% DEA data were employed in the optimization of $k_{b\text{-eff}}$ (defined by equation 2.37) this was done in order to avoid possible sensitivity problems in the 5% DEA data. The constant determined from the 30% data was successfully used in a predictive manner to represent the majority of the 5% data.

The value of $k_{b\text{-eff}}$ for MDEA determined was $2326 \text{ M}^{-2}\text{s}^{-1}$. This compares in magnitude with the value of $k_{b\text{-eff}}$ found by Laddha and Danckwerts (1981) for DEA of $1200 \text{ M}^{-2}\text{s}^{-1}$, which was demonstrated to fit the current results for DEA well. However, the fact that MDEA appears to be nearly twice as effective as DEA in the proton abstraction step lies contrary to the trend suggested by Blauwhoff et al (1984) for the effect of pK_a on the proton abstraction rate constant.

The representation of the 5% data is less successful at low CO_2 loadings: this is not surprising considering that this is the region where the equilibrium model itself fits poorly. Therefore the speciation model may not succeed in representing the solution composition at these conditions.

9.3 MEA-MDEA in Desorption

The desorption of CO_2 from an MEA-MDEA mixture was studied and compared to the results of the absorption work discussed earlier. The desorption work was of course conducted at much higher CO_2 loadings than the absorption work and consequently the application of a speciation model was required in the interpretation of the results. The same type of model that was successful in the DEA-MDEA system was adopted and speciation was calculated for the known solution loadings. The non-interactive model which represented the absorption results well was then extended to model the higher loadings of the desorption experiments.

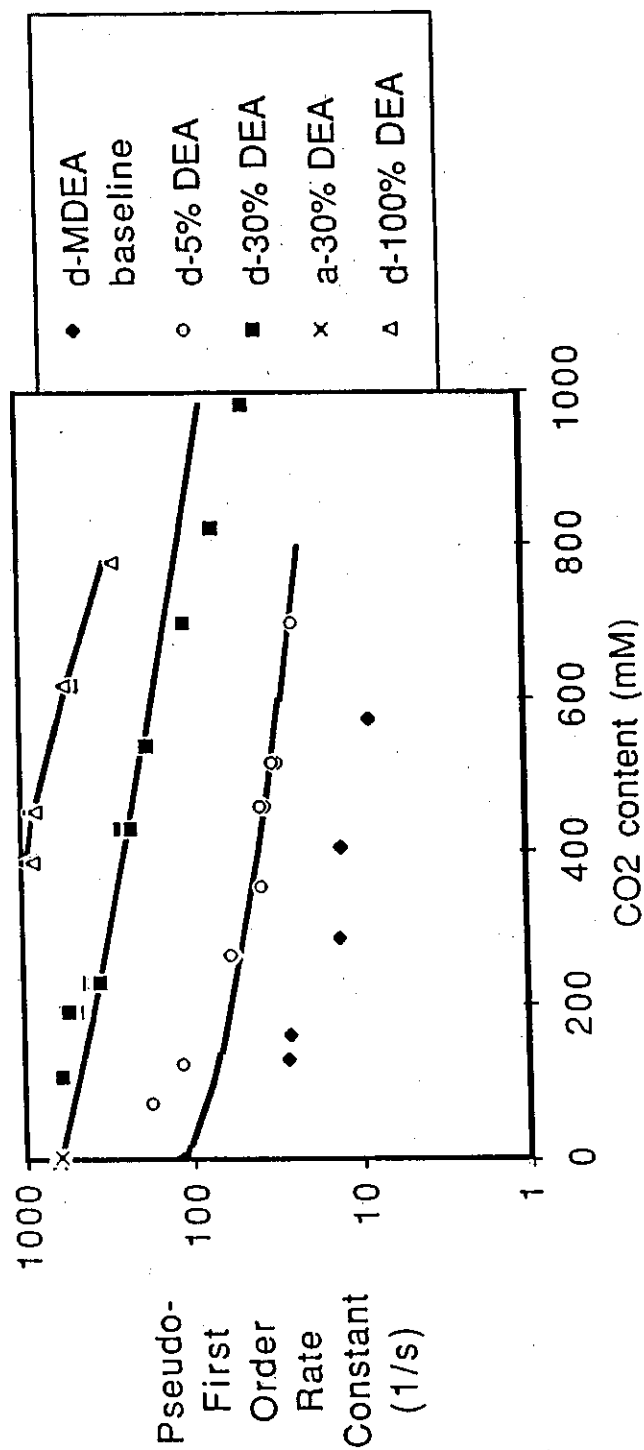


Figure 36: Test of a kinetically interactive model for rate constants in the DEA/MDEA mixtures. Data are for 2 M DEA/MDEA at various DEA contents and at 25° C. A single interaction rate constant models both DEA concentrations.

Figure 37 shows that no anomalies exist in the MEA-MDEA system. The absorption and desorption values are successfully modelled with a kinetically non-interactive rate constant model that calculates the overall pseudo-first order constant. Consequently, the representation of CO₂ desorption from MEA-MDEA solutions presents no new challenge.

9.4 Comparison between DEA and MEA as Promoters

From comparison of the apparent rate constants in 1.4 M MDEA promoted by 0.6 M DEA or MEA, it can be concluded that in unloaded solutions MEA is nearly six times as effective a promoter as DEA on a molar basis. If MDEA did not interact in the DEA kinetics, MEA would react twelve times faster than DEA. As the loading increases, MEA becomes somewhat less effective: at a loading of 0.25 mole CO₂/mole amine, MEA is only 1.5 times as effective as DEA as a promoter. The gain that DEA makes with loading is a result of its lower pK_a, smaller carbamate stability and the interaction of MDEA in the DEA kinetics.

Figure 38 shows the relative effectiveness of MEA and DEA as promoters for the MDEA system on the basis of pseudo-first order rate constants. The ratio of pseudo-first order rate constants is shown for 2 M solutions of varying promoter content at 25° C. When the solutions are 100 % MEA or DEA, the ratio is approximately 6.5 at zero loading. As the loading increases, the ratio also increases due to the slightly higher reaction order exhibited by DEA (≈ 1.5 in 2 M solution).

In the mixtures of MEA or DEA with MDEA, the trend is reversed. The enhancing effect of MDEA on the kinetics of DEA reaction, combined with the pH and carbamate instability advantages of DEA, serves to make DEA nearly as attractive a promoter on a rate basis as MEA at higher loadings.

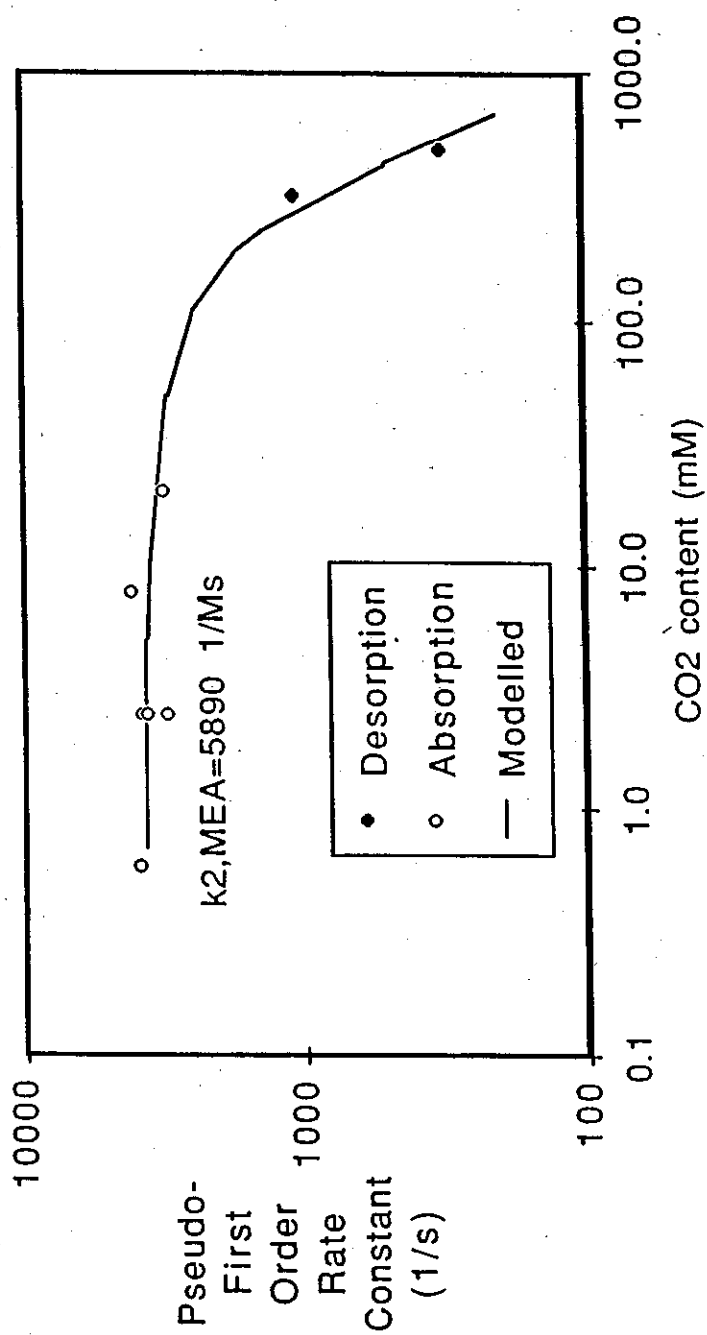


Figure 37: A kinetically non-interactive model predicts the MEA/MDEA mixture rate constant. Data are for 2 M total amine (30 % MEA) and at 25° C.

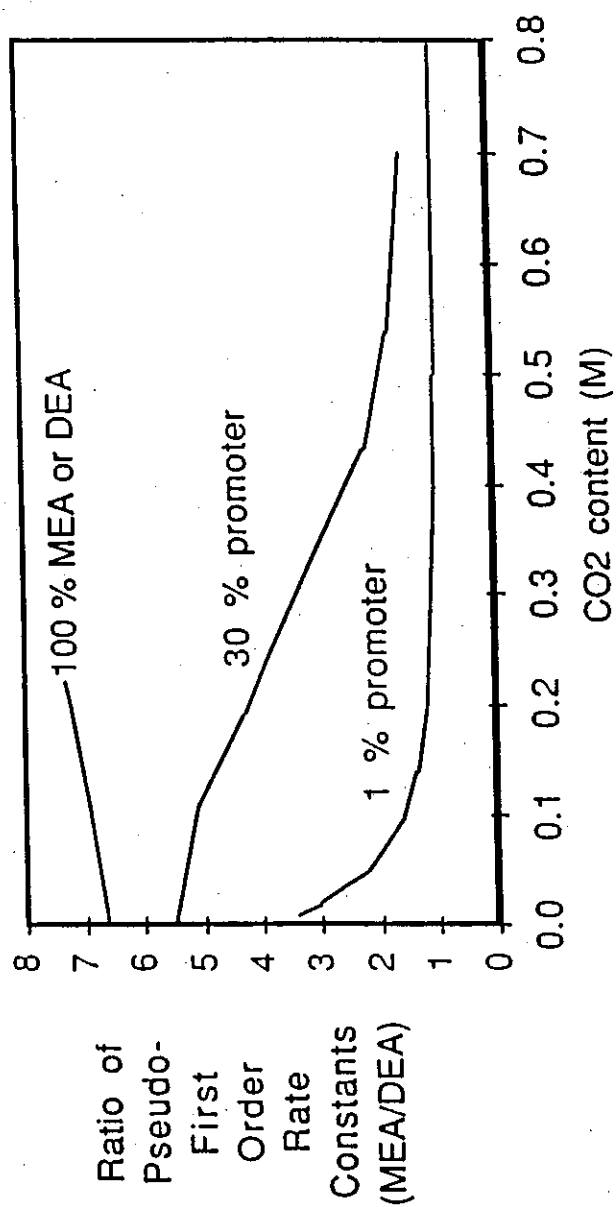


Figure 38: The effectiveness of MEA or DEA as a promoter depends strongly on the equilibrium amount of free amine. The curves shown are for 2 M total amine at 25° C. The kinetic advantage that MEA has at low loadings diminishes at higher loadings due to its greater pK_a and carbamate stability.

9.5 Effect of Impurities on the Pseudo-First Order Rate Constant for MDEA

The possible presence of 1' or 2' amine impurities in the MDEA is indicated by examination of the MDEA baseline. Because of their low driving force nature, desorption experiments are particularly sensitive to the presence of kinetically active impurities. The elimination of liquid gradients allows the small amount of impurities present to contribute to the transport rate by increasing the pseudo-first order rate constant. This effect is shown with the simulation model in figure 39.

In figure 39 the MDEA baseline is interpreted in terms of the amount of impurity required to fit the observed rate constant. The MDEA rate constant (k_{MDEA}) used in the simulation is that determined from large driving force absorption. This rate constant should be largely unaffected by the presence of small amounts of primary or secondary alkanolamine impurities since, as evidenced experimentally, the 1' or 2' amine impurities act in a shuttle mechanism under large driving force absorption and so do not contribute significantly to the absorption rate.

The amount of impurity necessary to explain the rate is less than 1% if the impurity is considered to be MEA, and slightly more than 1% if the impurity is considered to be DEA. The fact that MDEA from a different source yielded different (and higher) rate constants under the low driving force conditions lends credence to the kinetic importance of impurities in these experiments.

Because the experimental data for the amine mixtures were collected at sufficiently large 1' and 2' amine compositions, the impurity effects demonstrated in the MDEA baseline are not significant with respect to the overall magnitude of the observed mixture rate constants at the 30% promoter composition. The determined value of $k_{b\text{-eff}}$ is therefore not affected by the possible presence of impurities.

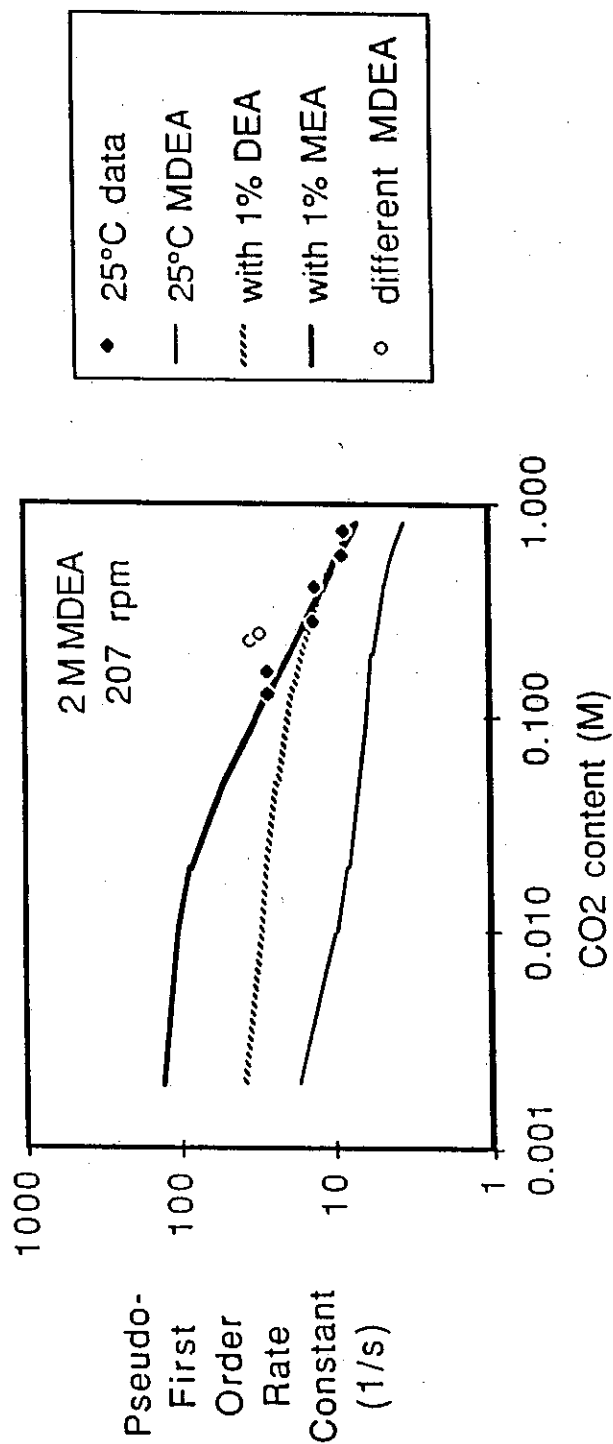


Figure 39: The pseudo-first order rate constant is a strong function of the impurity content. The lines are rate constants calculated for given compositions with the equilibrium speciation model. The data are for low driving force desorption.

Section 10

CONCLUSIONS

The transport of CO_2 was studied in MDEA, MDEA promoted with DEA and with MEA, and in DEA solutions at 25°C . The measured rates were normalized with the known driving forces and reported as apparent rate constants. The potential contribution of gas phase resistance was quantified and demonstrated to be unimportant for the systems of interest. The absorption rates were kinetically controlled at low driving forces. At high driving force, a shuttle limit existed in both the MEA-MDEA and DEA-MDEA systems.

A reversible reaction model was confirmed by studying the reverse reaction rate. Desorption rates of CO_2 from loaded solutions of DEA, MDEA, DEA-promoted MDEA and MEA-promoted MDEA were measured. The low mass transfer driving force experiments yielded pseudo-first order rate constants.

The Kent and Eisenberg (1976) equilibrium model for the system CO_2 -DEA- H_2O was used to speciate liquid concentrations in order to interpret the pseudo-first order rate constants in terms of the kinetic models of Laddha and Danckwerts (1981) and Blauwhoff et al (1983). Very good agreement was found with the results of Laddha and Danckwerts. Therefore under the experimental conditions H_2O and OH^- in solution are not important contributors to the decomposition of the postulated intermediate.

No difference existed between the rate constants measured for CO_2 reaction with DEA in absorption and in desorption experiments. This fact confirms the application of the reversible model for the DEA system.

The rate of absorption into DEA-promoted MDEA solution was independent of liquid diffusion effects at low driving force. The rate constants measured at low driving force absorption compared well with the rate constants measured in desorption experiments. This result validates the application of a reversible kinetic model for the conditions studied in the DEA-MDEA system.

The pseudo-first order rate constants measured in DEA-promoted MDEA as a function of loading at 25° C were interpreted with an approximate speciation model. The apparent rate constants were correlated with the free DEA and MDEA calculated at each measured loading, and a kinetically-interactive model represented the data fairly well:

$$\text{rate} = \frac{[\text{DEA}]([\text{CO}_2] - [\text{CO}_2]_e)}{\frac{1}{1410} + \frac{1}{1200[\text{DEA}] + 2326[\text{MDEA}]}}$$

A kinetically non-interactive model ($k_{b\text{-eff}}$ for MDEA = 0) did not represent the data.

The results of CO₂ absorption and desorption into MEA-MDEA at low driving forces show that MDEA has no special effect on the MEA kinetics. A kinetically non-interactive model represented both the absorption and desorption data well.

Although MEA reacts much faster than DEA with CO₂, in MDEA solution this difference is diminished by the interaction of MDEA in the DEA kinetics. This fact, combined with the effects of the lower carbamate stability and pK_a of DEA, make DEA nearly as attractive a promoter as MEA at higher loadings.

Each desorption experiment performed yielded an estimate of the equilibrium vapor pressure of CO₂ over the solution. The vapor pressures over 2 M DEA compared very well with literature values. The vapor pressures found over 2 M MDEA were somewhat higher than the single set of data available in the literature.

The equilibrium data in the single amine systems were very well fitted with approximate models. The approximate model proposed for the mixed system did a fair job of representing the equilibrium vapor pressures with no additional adjustable constants. No experimental data on the mixed systems were available in the literature for comparison.

Notation

The numbers in () designate the equation in which the quantity is defined.

Symbols

A	dissolved gas involved in a bimolecular reaction	M
Δ	driving force for a bimolecular reaction	{2.11} M
a	effective mass transfer area	dm ²
B	base involved in a bimolecular reaction with A	M
base	species capable of abstracting a proton	{2.33} M
C	product of a bimolecular reaction	M
C ₉	constant in the DeCoursey model	{2.38} 1.1
D	product of a bimolecular reaction	M
d _{imp}	diameter of impellor in the liquid	cm
D	diffusion coefficient	dm ² s ⁻¹
E	enhancement factor	{2.8}
E _a	activation energy	kcal gmol ⁻¹
Ha	Hatta number	{2.7}
H	Henry's law constant	atm M ⁻¹
HK	overall equilibrium constant	{1.10} atm M ⁻¹
I	ionic strength of the solution	equiv per liter
k _{app}	apparent rate constant	{2.15} s ⁻¹
k _b	proton abstraction rate constant	{2.33} M ⁻¹ s ⁻¹
k _{-b}	first order reverse rate constant	{2.33} M ⁻¹ s ⁻¹
k _{b-eff}	effective rate constant	{2.37} M ⁻² s ⁻¹
k _{ga}	gas phase mass transfer coefficient	{4.4} gmol atm ⁻¹ s ⁻¹
k _{lo}	liquid phase mass transfer coefficient	dm s ⁻¹
k _{MEA}	second order rate constant for CO ₂ -MEA reaction	{1.15} M ⁻¹ s ⁻¹
k _o	pseudo-first order rate constant	{2.10} s ⁻¹
k _{OH-}	second order rate constant	{1.12} M ⁻¹ s ⁻¹

k_1	first order rate constant {2.32} s^{-1}
k_2	second order rate constant, $M^{-1}s^{-1}$
k_{-2}	second order rate constant {2.28} $M^{-1}s^{-1}$
K_a	acid dissociation constant of MDEA {1.6} M
K_{a1}	acid dissociation constant of the promoter {1.7} M
K_c	carbamate instability constant {1.9}
K_f	equilibrium constant for carbamate formation {1.8} M^{-1}
K_w	water dissociation constant {1.1} M^2
K_1	first dissociation constant of CO_2 {1.3} M
K_2	second dissociation constant of CO_2 {1.4} M
L	film thickness in the film theory {2.1} dm
m	molality, gmol per kg- H_2O
M	molarity, gmol per liter
M_R	dimensionless rate parameter {2.39} $k_o D k_l^{-1} - 2$
n	reaction order with respect to the liquid phase reactant
P	partial pressure atm
prom	the primary or secondary amine promoter
Q	enhancement factor ratio {2.20}
R	absorption or desorption rate, gmol s^{-1}
rate	reaction rate $M s^{-1}$
Re	Reynolds number $d_{imp}^2 V \rho \mu^{-1}$
s	fractional surface renewal rate {2.4} s^{-1}
Sc	Schmidt number for the liquid $\mu \rho^{-1} D^{-1}$
Sh	Sherwood number for mass transfer $k_l^0 d_{imp} D^{-1}$
t	contact time {2.2} s
T	temperature $^{\circ}K$
v	stoichiometric coefficient of the promoter
V	rotation speed of impeller rev s^{-1}
Y	fractional loading of amine {1.5}
[]	denoting a molar concentration M

Greek Symbols

β	ratio of interface to bulk concentration {2.40}
θ	dimensionless driving force {2.41}
Δ	denoting a concentration-based driving force
Σ	denoting the summation of species
ρ	the liquid density g cm ⁻³
μ	the liquid viscosity cPoise
μ_k	the liquid kinematic viscosity cStokes

Subscripts

AMINE	in an aqueous solution of alkanolamine
b	a value in the bulk liquid phase
e	a value in chemical equilibrium
f	in the forward direction
F	for pseudo-first order conditions
g	a value in the bulk gas phase
H ₂ O	in water only; no alkanolamine
i	a value at the gas-liquid interface
IONS	denoting all ionic species involved in reactions with CO ₂
irrev	for an irreversible reaction: A + B ---> products
r	in the reverse direction
shuttle	referring to the shuttle mechanism
total	summation of all chemical forms
∞	under conditions where chemical reaction is so fast that it may be considered to be instantaneous with respect to mass transfer
∞ -prom	representing the contribution of the promoter to the shuttle mechanism

References

- Alper, E., W.-D. Deckwer and P. V. Danckwerts, "Comparison of Effective Interfacial Areas with the Actual Contact Area for Gas Absorption in a Stirred Cell," Chem. Eng. Sci., **35**, 1263, 1980.
- Alper, E. and P. V. Danckwerts, "Laboratory Scale-Model of a Complete Packed Column Absorber," Chem. Eng. Sci., **31**, 599, 1976.
- Alvarez-Fuster, C., N. Midoux, A. Laurent and J. C. Charpentier, "Chemical Kinetics of the Reaction of CO₂ with Amines in Pseudo m-nth Order Conditions in Polar and Viscous Organic Solutions," Chem. Eng. Sci., **36**, 1513, 1981.
- Astarita, G. and D. W. Savage, "Theory of Chemical Desorption," Chem. Eng. Sci., **35**, 649, 1980a.
- Astarita, G. and D. W. Savage, "Gas Absorption and Desorption with Reversible Instantaneous Chemical Reaction," Chem. Eng. Sci., **35**, 1755, 1980b.
- Astarita, G., D. W. Savage and A. Bisio, Gas Treating with Chemical Solvents, John Wiley and Sons, New York, 1983.
- Astarita, G., D. W. Savage and J. M. Longo, "Promotion of CO₂ Mass Transfer in Carbonate Solutions," Chem. Eng. Sci., **36**, 581, 1981.
- Barth, D., C. Tondre, G. Lappai and J. J. Delpuech, "Kinetic Study of Carbon Dioxide Reaction with Tertiary Amines in Aqueous Solutions," J. Phys. Chem., **85**, 3659, 1981.

Barth, D., C. Tondre and J. J. Delpuech, "Kinetics and Mechanisms of the Reactions of Carbon Dioxide with Alkanolamines: A Discussion Concerning the Cases of MDEA and DEA," Chem. Eng. Sci., **39**, 1753, 1984.

Bin, A. K., "Mass Transfer to the Free Interface in Stirred Vessels," Chem. Eng. Commun., **31**, 155, 1984.

Bird, R. B., W. E. Stewart and E. N. Lightfoot, Transport Phenomena, John Wiley and Sons, New York, 1960.

Blanc, C. and D. Denfrais, "The Reaction Rate of CO₂ with Diethanolamine," Int. Chem. Eng., **24**, 43, 1984.

Blanc, C. and J. Elgue, "MDEA Process Selects H₂S," Hydr. Proc., **60**, 111, 1981.

Blauwhoff, P. M. M. and W. P. M. Van Swaaij, "Simultaneous Mass Transfer of Hydrogen Sulfide and Carbon Dioxide with Complex Chemical Reaction in an Aqueous Diisopropanolamine Solution," Chemical Reaction Engineering, ACS Symp. Series. **196**, 377, 1982.

Blauwhoff, P. M. M., G. F. Versteeg and W. P. M. Van Swaaij, "A Study on the Reaction between CO₂ and Alkanolamines in Aqueous Solutions," Chem. Eng. Sci., **40**, 207, 1984.

Brian, P. L. T. and M. C. Beaverstock, "Gas Absorption Accompanied by a Two-step Chemical Reaction," Chem. Eng. Sci., **20**, 47, 1965.

Brian, P. L. T., J. E. Vivian and D. C. Matiatos, "Interfacial Turbulence During the Absorption of Carbon Dioxide into Monoethanolamine," AIChE J., **13**, 28, 1967.

Caplow, M., "Kinetics of Carbamate Formation and Breakdown," J. Am. Chem. Soc., **90**, 6795, 1968.

Chakravarty, T., U. K. Phukan and R. H. Weiland, "Reaction of Acid Gases With Mixtures Of Amines," Chem. Eng. Progr., **81**, 32, Apr. 1985.

Chakma, A. and A. Meisen, "Solubility of CO₂ in Aqueous Methyldiethanolamine and N,N-Bis(hydroxyethyl)piperazine Solutions," Ind. Eng. Chem. Res., **26**, 2461, 1987.

Chang, C. S. and G. T. Rochelle, "Surface Renewal Theory for Simultaneous Mass Transfer and Equilibrium Chemical Reaction," presented at AIChE 88th National Meeting, Philadelphia, 1980.

Cornelisse, R., A. A. C. Beenackers, F. P. H. Van Beckum and W. P. M. Van Swaaij, "Numerical Calculation of Simultaneous Mass Transfer of Two Gases Accompanied by Complex Reversible Reactions," Chem. Eng. Sci., **35**, 1245, 1980.

Danckwerts, P. V., "Gas Absorption with Instantaneous Reaction," Chem. Eng. Sci., **23**, 1045, 1968.

Danckwerts, P. V., Gas-Liquid Reactions, McGraw-Hill, New York, 1970.

Danckwerts, P. V., "The Reaction of CO₂ with Ethanolamines," Chem. Eng. Sci., **34**, 443, 1979.

Danckwerts, P. V. and K. M. McNeil, "The Effects of Catalysis on Rates of Absorption of CO₂ into Aqueous Amine-Potash Solutions," Chem. Eng. Sci., **22**, 925, 1967.

- DeCoursey, W. J., "Enhancement Factors for Gas Absorption with Reversible Reaction," *Chem. Eng. Sci.*, **37**, 1483, 1982.
- Deshmukh, R. D. and A. E. Mather, "A Mathematical Model for Equilibrium Solubility of Hydrogen Sulfide and Carbon Dioxide in Aqueous Alkanolamine Solutions," *Chem. Eng. Sci.*, **36**, 355, 1981.
- Donaldson, T. L. and Y. N. Nguyen, "Carbon Dioxide Reaction Kinetics and Transport in Aqueous Amine Membranes," *Ind. Eng. Chem. Fundam.*, **19**, 260, 1980.
- Frazier, H. D. and A. L. Kohl, "Selective Absorption of Hydrogen Sulfide from Gas Streams," *Ind. Eng. and Chem.*, **42**, 2288, 1950.
- Glasscock, D., "Modelling of CO₂ Reaction in Alkanolamines," Presentation to the Separations Research Program at the University of Texas at Austin, Oct. 14, 1987.
- Haimour, N., A. Bidarin and O. C. Sandall, "Absorption of CO₂ into Aqueous Solutions of Methyldiethanolamine," presented at AIChE Spring National Meeting, Houston, 1985.
- Haimour, N. and O. C. Sandall, "Absorption of Carbon Dioxide into Aqueous Methyldiethanolamine," *Chem. Eng. Sci.*, **39**, 1791, 1984.
- Hall, N. F. and M. R. Sprinkle, "Relations Between the Structure and Strength of Certain Organic Bases in Aqueous Solution," *J. Am. Chem. Soc.*, **54**, 3469, 1932.
- Hermes, J., "A Mass Transfer-based Process Model of Acid Gas Absorption/Stripping using Methyldiethanolamine," MS Thesis at the University of Texas at Austin, 1987.

Higbie, R., "The Rate of Absorption of a Pure Gas into a Still Liquid during Short Periods of Exposure," *Trans. Am. Inst. Chem. Engrs.*, **31**, 365, 1935.

Hikita, H. H., and S. Asai, "Gas Absorption with (m,n)-th Order Irreversible Chemical Reaction," *Kagaku Kogaku*, **2**, 77, 1964.

Hikita, H., S. Asai, H. Ishikawa, "Simultaneous Absorption of Two Gases in a Reactive Liquid, One Gas Reacting Instantaneously," *Chem. Eng. J.*, **18**, 169, 1979.

Hikita, H., S. Asai, N. Ishikawa and Y. Saito, "Kinetics of Absorption of Chlorine in Aqueous Acidic Solutions of Ferrous Chloride," *Chem. Eng. Sci.*, **30**, 607, 1975.

Hikita, H., H. Ishikawa, K. Uku and T. Murakami, "Diffusivities of Mono-, Di-, and Triethanolamines in Aqueous Solutions," *J. Chem. Eng. Data*, **25**, 324, 1980.

Hikita, H., S. Asai, H. Ishikawa and M. Honda, "The Kinetics of Reactions of Carbon Dioxide with Monoethanolamine, Diethanolamine and Triethanolamine by a Rapid Mixing Method," *Chem. Eng. J.*, **13**, 7, 1977.

Holmes, J. W., M. L. Spears and J. A. Bullin, "Sweetening LPG's with Amines," *Chem. Eng Prog*, May, 47, 1984.

Jensen, M. B., E. Jorgensen and C. Faurholt, "Reactions between Carbon Dioxide and Amino Alcohols," *Acta Chem. Scand.*, **8**, 1137, 1954.

Jhaveri, A. S., "Absorption of a Gas into a Solution Containing Two Reactants," *Chem. Eng. Sci.*, **24**, 1738, 1969.

Jou, F. Y., D. Lal, A. E. Mather and F. D. Otto, "The Solubility of H₂S and CO₂ in Aqueous Methyldiethanolamine Solutions," presented at the AIChE Spring National Meeting, Houston, 1981.

Katti, S. S., and R. A. Wolcott, "Fundamental Aspects of Gas Treating with Formulated Amine Mixtures," presented at the AIChE National Meeting, Minneapolis, August 1987.

Kent, R. L., and B. Eisenberg, "Better Data for Amine Treating," *Hydrocarbon Proc.*, **55**, 87, 1976.

Kohl, A. L. and F. C. Riesenfeld, Gas Purification, 4th ed., Gulf Publishing Company, Houston, 1985.

Laddha, S. S. and P. V. Danckwerts, "Reaction of CO₂ with Ethanolamines: Kinetics from Gas-Absorption", *Chem. Eng. Sci.*, **36**, 479, 1981.

Laddha, S. S. and P. V. Danckwerts, "The Absorption of CO₂ by Amine-Potash Solutions," *Chem. Eng. Sci.*, **37**, 665, 1982.

Mason, J. W. and B. F. Dodge, "Equilibrium of Carbon Dioxide by Solutions of the Ethanolamines," *Trans. Am. Inst. Chem. Engrs.*, **32**, 27, 1936.

Maddox, R. N., A. H. Bhairi, J. R. Diers and P. A. Thomas, "Equilibrium Solubility of Carbon Dioxide or Hydrogen Sulfide in Aqueous Solutions of Monoethanolamine, Diglycolamine, Diethanolamine and Methyldiethanolamine," Gas Processors Association Research Report RR-104, Tulsa, 1987.

Meissner, R. E. and U. Wagner, "Low Energy Process Recovers CO₂," *Oil and Gas J.*, Feb., **55**, 1983.

Meldon, J. H., A. S. Smith and C. K. Colton, "The Effect of Weak Acids upon the Transport of Carbon Dioxide in Alkaline Solutions," Chem. Eng. Sci., **32**, 939, 1977.

Nernst, W., "Theorie der Reaktionsgeschwindigkeit in Heterogenen Systemen," Z. Phys. Chem., **47**, 52, 1904.

Olander, D. R., "Simultaneous Mass Transfer and Equilibrium Chemical Reaction," AIChE J., **6**, 233, 1960.

Onda, K., E. Sada, T. Kobayashi, M. Fujine, "Gas Absorption Accompanied with Complex Chemical Reactions - I Reversible Chemical Reactions," Chem. Eng. Sci., **25**, 753, 1970a.

Onda, K., E. Sada, T. Kobayashi, M. Fujine, "Gas Absorption Accompanied with Complex Chemical Reactions - II Consecutive Chemical Reactions," Chem. Eng. Sci., **25**, 761, 1970b.

Onda, K., E. Sada, T. Kobayashi, M. Fujine, "Gas Absorption Accompanied with Complex Chemical Reactions - III Parallel Chemical Reactions," Chem. Eng. Sci., **25**, 1023, 1970c.

Ouwerkerk, C., "Design for Selective H₂S Absorption," Hydrocarbon Proc., **57**, 89, 1978

Pinsent, B. R., L. Pearson and F. J. W. Roughton, "The Kinetics of Combination Of Carbon Dioxide with Hydroxide Ions," Trans. Faraday Soc., **47**, 263, 1951.

Pinsent, B. R., L. Pearson and F. J. W. Roughton, " Trans. Faraday Soc., **52**, 1512, 1956.

Roper, G. H., T. F. Hatch Jr. and R. L. Pigford, "Theory of Absorption and Reaction of Two Gases in a Liquid," *Ind. Eng. Chem. Fundam.*, **1**, 144, 1962.

Sada, E., H. Kumazawa and M. A. Butt, "Solubility and Diffusivity of Gases in Aqueous Solutions of Amines," *J. of Chem. Eng. Data*, **23**, 161, 1978.

Sada, E., H. Kumazawa and M. A. Butt, "Chemical Absorption Kinetics over a Wide Range of Contact Time: Absorption of Carbon Dioxide into Aqueous Solutions of Monoethanolamine," *AIChE J.*, **22**, 196, 1976.

Sada, E., H. Kumazawa, M. A. Butt and D. Hayashi, "Simultaneous Absorption of Carbon Dioxide and Hydrogen Sulfide into Aqueous Monoethanolamine Solutions," *Chem. Eng. Sci.*, **31**, 839, 1976.

Sada, E., H. Kumazawa, M. A. Butt, "Gas Absorption with Consecutive Chemical Reaction: Absorption of Carbon Dioxide into Aqueous Amine Solutions," *Can. J. Chem. Eng.*, **54**, 421, 1976.

Sada, E., H. Kumazawa, Z. Q. Han and H. Matsuyama, "Chemical Kinetics of the Reactions of Carbon Dioxide with Ethanolamines in Nonaqueous Solvents," *AIChE J.*, **31**, 1297, 1985.

Sardar, H., "Development of a Non-equilibrium Stage Model for the Design and Simulation of Gas Processing Units and Verification with Plant Data," PhD Dissertation at Clarkson University, Pottsdam, N.Y., 1985.

Savage, D. W., G. Astarita and S. Joshi, "Chemical Absorption and Desorption of Carbon Dioxide from Hot Carbonate Solutions," *Chem. Eng. Sci.*, **35**, 1513, 1980.

Schwabe, K., W. Graichen and D. Spiethoff, "Physikalisch-chemische Untersuchungen an Alkanolaminen," *Z. Phys. Chem.*, **20**, 68, 1959.

Sharma, M. M. and P. V. Danckwerts, "Fast Reactions of CO₂ in Alkaline Solutions--(a) Carbonate Buffers with Arsenite, Formaldehyde and Hypochlorite as Catalysts (b) Aqueous Monoisopropanolamine solutions," Chem. Eng. Sci., **18**, 729, 1963.

Sherwood, T. K., R. L. Pigford and C. R. Wilke, Mass Transfer, McGraw-Hill, Inc., New York, 1975.

Schwabe, K., W. Graichen and D. Spiethoff, "Physikalisch-Chemische Untersuchungen an Alkanolaminen," Physik. Chem., **20**, 68, 1959.

Thomas, W. J. and E. McK. Nicholl, "An Optical Study of Interfacial Turbulence Occuring During the Absorption of CO₂ into Monoethanolamine," Chem. Eng. Sci., **22**, 1877, 1967.

Toman, J. J. and R. H. Weiland, "CO₂ Absorption by DEA-MDEA Blends-Theory and Experiment," Presentation at the Spring National Meeting of AIChE, Houston, Texas, Session 43, April 30, 1987.

Tomjcek, R. A., D. Lal, H. A. Rangwala and F. D. Otto, "Absorption of Carbon Dioxide into Aqueous Solutions of Methyldiethanolamine," presented at the AIChE Annual Meeting, Miami Beach, 1986.

Ulanowicz, R. E. and G. C. Frazier, "Interphase Transfer with Non-Equilibrium Chemical Reaction," Chem. Eng. Sci., **23**, 1335, 1968.

Ulrich, R. K., "Sulfite Oxidation under Flue Gas Desulfurization Conditions: Enhanced Oxygen Absorption Catalyzed by Transition Metals," PhD Dissertation at the University of Texas at Austin, 1983.

Vidaurri, F. C. and L. C. Kahre, "Recover H₂S Selectively from Sour Gas Streams," Hydrocarbon Proc., **56**, 333, 1977.

Versteeg, G. F., "Mass Transfer and Chemical Reaction Kinetics in Acid Gas Treating Processes," PhD Dissertation at Twente University of Technology, The Netherlands, Jan. 1987.

Versteeg, G. F. and W. P. M. van Swaaij, "On the Kinetics between CO₂ and Alkanolamines both in Aqueous and Non-Aqueous Solutions. Part 2: -Tertiary Amines," Chem. Eng. Sci., **43**, 587, 1988a.

Versteeg, G. F. and W. P. M. van Swaaij, "Absorption of CO₂ in Aqueous Solutions of Mixtures of Alkanolamines," Presented at the Spring National AIChE Meeting, New Orleans, Louisiana, March 8, 1988b.

Weast, R. C. and M. J. Astle, (editors), CRC Handbook of Chemistry and Physics, 60th edition, CRC Press, Inc. Boca Raton, Florida, 1979.

Weiland, R. H., "Simulating Gas Treating with Blended Amines," Presentation at the Spring National AIChE Meeting, Houston, Texas, April 31, 1987.

Wolcott, R. A., Dow Chemical Company, Freeport, Texas, personal communication, Aug. 1987.

Yu, W.C., G. Astarita and D.W. Savage, "Kinetics of Carbon Dioxide Absorption in Solutions of Methyldiethanolamine," Chem. Eng. Sci., **40**, 1585, 1985.

Yu, W. C. and G. Astarita, "Selective Absorption of Hydrogen Sulfide in Tertiary Amine Solutions," Chem. Eng. Sci., **42**, 419, 1987a.

Yu, W. C. and G. Astarita, "Design of Packed Towers for Selective Chemical Absorption," Chem. Eng. Sci., **42**, 425, 1987b.

Appendix A: Analytical Techniques.

Total CO₂ in the liquid phase

Liquid phase total CO₂ concentrations were measured with an Oceanography International Model 525 Total Carbon Analyzer. Samples of the liquid phase of the reactor were taken and injected into 30 wt% phosphoric acid contained in a sparging tube. Because total CO₂ solubility is directly related to pH, the acidic environment reversed all forms of dissolved CO₂ back to free CO₂. The free CO₂ was stripped from the solution with a CO₂-free N₂ carrier gas. The carrier gas was sent first through two consecutive magnesium perchlorate drying tubes to remove water traces from the gas, and then through a Horiba Model PIR-2000 infrared CO₂ analyzer. The signal from the analyzer was integrated and recorded as Area Response (AR).

Calibration of the Total Carbon Analyzer was achieved by injecting varying volumes of a known sodium carbonate solution. Injection volumes of 20 to 100 μ liters (\pm 0.5 μ liters) of approximately 5 to 7 mM sodium carbonate standard were employed. Only freshly prepared standards were used to prevent error introduced from atmospheric CO₂ contamination.

The use of a 5 to 7 mM standard meant that the technique was calibrated to read 0.14 to 0.7 millimoles of total CO₂ upon injection. For the standard sample injection volume of 50 μ liters, this range is equivalent to concentrations of 2 to 14 mM. The constant carrier gas flowrate (a rotameter reading of 13 (\pm 0.25)) was adjusted before each injection. The injections were repeated in order to minimize random error in the calibration procedure. The AR values were recorded and an interpolating polynomial was fit to the AR-vs-total CO₂ data. Table 4 shows the results of a typical calibration. A 5.05 mM standard was used for this calibration.

The manufacturer claims that the analytical technique is accurate to \pm 2% at 1 ppm and \pm 1% at 100 ppm of inorganic carbon. The calibration procedure indicates that repeatability is less than 2% difference. The calibration was found to be quite stable and was repeated at approximately monthly intervals.

Table 4; Calibration of the liquid phase analytical technique. A calibration solution of 5.05 mM Na_2CO_3 was prepared from distilled water and 1.07 g of the anhydrous salt.

Injected volume μliter	millimoles of total CO_2 in 50 μliters	Area Response, AR
100	10.10	10300/10420/10378
75	7.575	8036/8179/8167/8131/8176/8208
50	5.05	5710/5713/5602/5700/5687/5665
40	4.04	4632/4662/4623/4640
30	3.03	3589/3591/3614/3548
20	2.02	2500/2465/2448/2445

Zero on analyzer is set at 7.115, span at 5.945. Range 1 (0 to 0.05 vol% CO_2) is always used for liquid analysis.

The calibration equation is:

$$\text{CO}_2 \text{ total in a 50 } \mu\text{liter sample (mM)} = 1.823 \times 10^{-8}(\text{AR})^2 + 7.839 \times 10^{-4}(\text{AR}) - 0.0033$$

Samples which were loaded with more than 14 mM total CO₂ had to be diluted before they could be analyzed. Standard dilution volumes of 1, 2, 3, and 4 mls of fresh distilled water were used to dilute sample volumes of 50, 100 or 200 μ liters. The dilution volumes were prepared with an Eppendorf variable volume digital pipeter. The dilution of reactor samples introduced more error into the results and increased the overall maximum possible error to approximately +/- 4%.

Cross checks with other analytical techniques confirm these good results. Figure 40 shows the titration of a CO₂-loaded 1.68 M MDEA solution with HCl. A highly loaded solution was used in the check, and so an excess of sodium hydroxide was added to the sample to prevent CO₂ loss to the atmosphere before titration occurred. The important buffer reactions are shown in each range on the figure. The buffer region accounts for the conversion of MDEAH⁺ into MDEA and CO₃⁼ into CO₂. In this region, the moles of acid titrated is equal to the moles of amine plus twice the moles of total CO₂:

$$\text{acid} = \text{MDEA} + 2(\text{CO}_2\text{T})$$

The total amine molarity is known from the solution preparation as 1.68 M. The acid titrated is indicated from the milliliters between breakpoints as 32.6 ml of 1 N HCl = 0.0326 moles of H⁺. Since a 10 ml sample of loaded MDEA solution was used, the total CO₂ molarity is determined to be 0.790 M (+/- 2%).

50 μ liters of loaded solution was diluted into 4 ml of distilled water. The diluted solution was injected and an AR of 10177 resulted. From the calibration equation in table 4, the total CO₂ molarity was found to be 0.8007 M. Therefore excellent agreement existed between the techniques and the total inorganic carbon method was confirmed.

A similar pH-titration technique was attempted with a 2 M DEA solution. However, because of the slow conversion of carbamate to bicarbonate a clear breakpoint into the buffer region was not detected and therefore pH titration could not be employed. A weight capture technique was attempted in which pure CO₂ was bubbled slowly through 113.83 +/- 0.01 g of 2 M DEA solution. The difference in weight (before and after loading) was measured to be 7.28 +/- 0.01

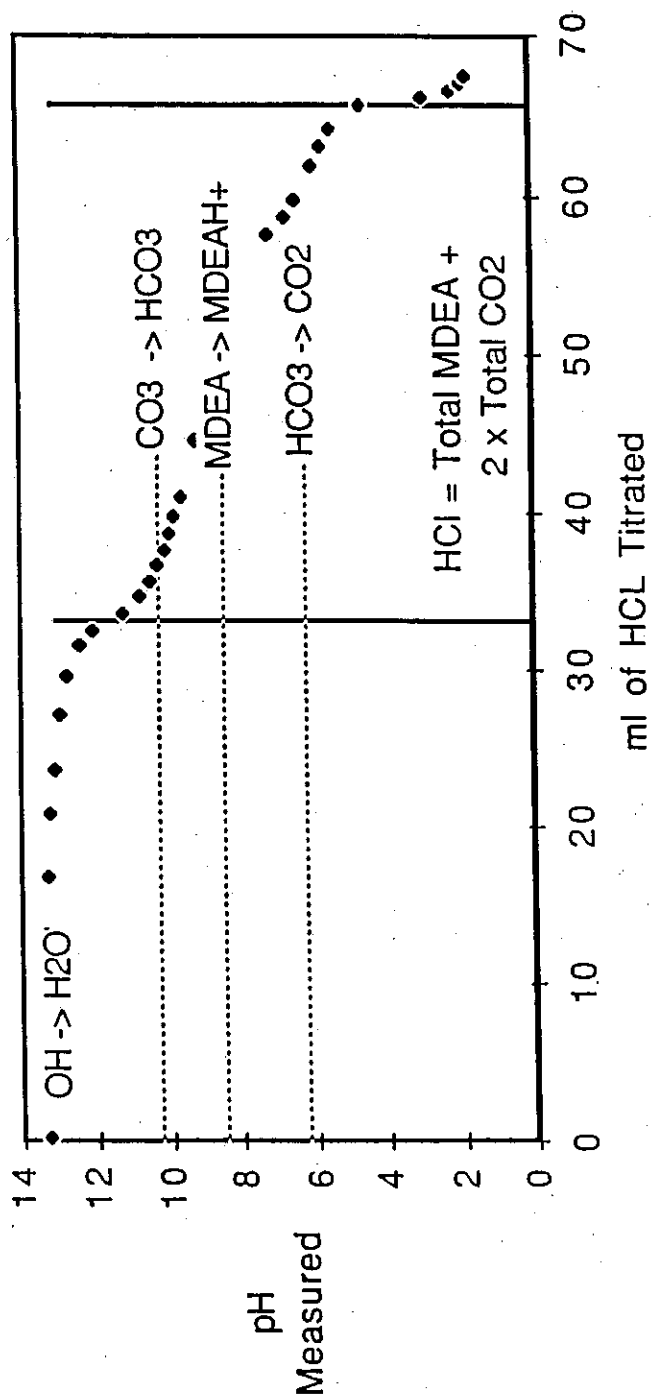


Figure 40: Results of pH titration for total carbon dioxide in 2 M MDEA.

grams. This difference is equal to a solution loading if 1.504 M (+/- .7%) total CO₂. A 30 μ liter sample was diluted in 4 ml of distilled water and 50 μ liters were injected. The area response was 11120, which by the equation in table 4 becomes 1.481 M total CO₂ (after multiplication by the dilution factor). The difference of 1.6% is well within the repeatability of the technique and confirms the total carbon analyzer technique for carbamated solutions.

Certain cautions must be heeded in order to maintain good results with this technique. First, the condition of the magnesium perchlorate drying tubes is very important. The analyzer is not very sensitive to the presence of water (1 part CO₂ is the equivalent of 5000 parts of water). However, the very low ppm range of the analysis does require the elimination of water from the analyzer input in order to prevent false CO₂ readings. For this reason the drying tubes must be maintained in good condition.

Even more important is the pressure drop through the drying tubes. Operation of the equipment at high pressure will amplify any error due to leaks in the system. If enough pressure builds in the system due to poor flow through the tubes, then the pressure relief system will blow. In some cases, the pressure relief system only partially, and not noticeably, blows. In this condition, erroneous results will be encountered since the gas entering the analyzer will not be at a lower flow rate than in the calibration. Lower flowrates than that used for calibration can result in false high readings for CO₂. However, less total gas will be sent through the analyzer since some will escape through the pressure relief system. The sum of these two effects can result in large errors in the technique.

In order to avoid these problems, do not ever operate with packed tubes which are visibly wet over more than a centimeter of their length. The wet salt swells, thereby decreasing the porosity and increasing the pressure drop. Also, when preparing the drying tube do not crush the salt particles any more than necessary to fill the tube. Smaller particles yield lower porosities and higher pressure drops. Consistency in the tube preparation technique is therefore important to avoid this difficulty.

The Horiba analyzer actually reads partial pressure, not volume percent. It should always be operated at ambient pressure in order to avoid inconsistency in the CO₂ measurement. Therefore avoid flow restrictions in the analyzer outlet.

Pressure surges in the room can affect the flow rate through the equipment if the feed gas rotameter does not operate at high pressures. When the air conditioning and heating switch on and off changes in the flowrate can be encountered. Set the N₂ source pressure at 60 psig and avoid this complication.

CO₂ pickup in strongly basic solutions or loss to the atmosphere from highly carbonated solutions can be important. Be sure to use fresh dilution solutions and to seal samples from the atmosphere.

Maintain the injection septum in good condition. A perforated septum can allow sample loss.

Finally, the condition of the Ascarite on the N₂ inlet should be checked periodically to prevent CO₂ from entering as an impurity in the carrier.

Gas phase CO₂ content

The composition of the gas leaving the reactor was determined with one of two IR CO₂ analyzers. The first is the Horiba PIR-2000 that was also used in the liquid CO₂ analysis procedure. It is equipped with two additional sensing ranges other than the 0-0.05 vol% used for that technique. Range 2 is for 0-0.15 vol%, and Range 3 is for 0-0.25 vol%. The analyzer output is only linear on the first range and the second and third ranges are increasingly nonlinear. Range 2 was the primary range used for gas phase CO₂ detection since it provided a higher and more useful detection range than Range 1 and also better linearity than Range 3.

Range 2 on the analyzer was calibrated by correlating the % full scale with known composition gases. A source gas of known composition (1420 ppm) was mixed with various amounts of essentially free N₂ and sent through the analyzer. The flowrates were controlled with Brooks Mass Flow Controller which had been calibrated previously. Table 5 contains the results of a sample analyzer calibration. The calibration was found to be fairly stable with time and was repeated at least monthly.

Table 5; Calibration of the Horiba PIR-2000 analyzer. Flows are controlled with the Brooks Mass Flow controllers and source gases are CO₂-free N₂ and 1420 ppm CO₂ in N₂. Dec 8, 1987.

1420 ppm, cc/min	N ₂ , cc/min	known ppm CO ₂	% full scale, range 2.
367.2	1278.7	316.8	30.7
367.2	892.3	414.0	37.5
0	1278.7	2.6	0
367.2	0	1420	79.4
367.2	633.6	521	43.9
294.1	633.6	450.2	39.8
111.4	633.6	212.3	23.3
111.4	1278.7	113.8	14.1

Interpolating polynomial:

$$\text{ppm CO}_2 = -23.6103 + 8.999 (\% \text{ f.s.}) + 0.0312 (\% \text{ f.s.})^2 + 0.001064 (\% \text{ f.s.})^3$$

The analyzer does take a very long time to warm up after a shut down. If the analyzer is shut off, at least 24 hours should pass before recalibration.

The second analyzer which was used was manufactured by Infrared Industries and was equipped with two ranges, 0-10 vol% and 0-30 vol%. This analyzer was also calibrated by detecting known gases. However, the calibration was found to float with time and had to be performed each day it was used.

Where possible, a flow dilution system was employed to dilute reactor gases into the range that could be used with the Horiba analyzer in order to avoid errors introduced by using the Infrared Industries analyzer.

Appendix B: Tabular Raw Data and Parameters used in Data Interpretation

Table 6; Values of $\sqrt{D/H}$ used in the interpretation of rate data at 25°C in 2 M solutions.

Source: Blauwhoff et al, 1984.

Mixture values are determined from a mole average of the values for 2 M solutions.

Solution composition	$\sqrt{D/H}$ dm/(s ^{1/2})
2 M MEA	1.32×10^{-5}
2 M MDEA	0.95×10^{-5}
2 M DEA	1.22×10^{-5}
2 M total (30 % DEA in MDEA)	1.03×10^{-5}
2 M total (5 % DEA in MDEA)	0.96×10^{-5}
2 M total (30 % MEA in MDEA)	1.06×10^{-5}

Table 7: Steady-state experiment summary (absorption experiments). All experiments were conducted with the low driving force configuration. (turbine agitator, Liquid volume=1800 ml, $a=1.46 \text{ dm}^2$) Chemicals courtesy of Dow Chemical Corp.

2 M DEA, T=25°C							
Date	RPM	Gas (N ₂) Rate cc/min	PCO ₂ inlet ppm	PCO ₂ outlet ppm	Total CO ₂ mM	Absorption Rate $\times 10^7 \text{ gmol/s}$	kapp s^{-1}
Jul 25, 1987	171	1028	18200	9700	170.5	61.7	1253
Jul 25, 1987	224	1028	18200	9600	170.5	61.7	1280
Jul 25, 1987	106	1028	18200	10300	170.5	57.3	1094
Jul 25, 1987	148	1028	53200	29200	160	184	1233
Jul 25, 1987	161	1028	33500	18400	167	112	1154
Jul 25, 1987	217	1028	33500	18150	167	114	1225
Jul 25, 1987	109	1028	33500	19000	167	108	999
Jul 25, 1987	114	1028	100000	69900	196.5	254	408
Jul 25, 1987	229	1028	100000	64100	196.5	301	682
Jul 25, 1987	199	347	265000	133000	200	483	409
Jul 25, 1987	126	347	265000	157000	214	403	204
Jul 25, 1987	104	347	265000	164000	227	379	165
30% DEA in 2M mixture of DEA/MDEA, T=25°C							
Aug 1, 1987	183	1019	100000	78200	-	182	241
Aug 1, 1987	119.5	1019	100000	80400	4.55	165	188
Aug 1, 1987	222	1019	100000	77700	6.00	188	259
Aug 1, 1987	223	633.5	52200	37500	8.84	112	399
Aug 1, 1987	138	633.5	52200	38700	9.82	104	317
Aug 1, 1987	179	633.5	52200	38050	10.68	108	359
Nov 6, 1987	208	367.2	1420	562.2	0.82	2.16	653
Nov 7, 1987	208	367.2	1420	566.3	5.23	2.15	638
Nov 7, 1987	118	367.2	1420	582.2	5.23	2.11	581
Nov 7, 1987	225	367.2	1420	564.4	5.23	2.16	645
Nov 7, 1987	117	367.2	18700	8075	5.08	2.75	513
Nov 7, 1987	225	367.2	18700	7733	5.08	2.84	596
Nov 7, 1987	208	367.2	18700	7739	3.07	2.84	594
Nov 7, 1987	208	367.2	6734	2717	1.80	1.03	632
30% MEA in 2M mixture of MEA/MDEA, T=25°C							
Nov 10, 1987	208	367.2	1420	297.4	0.6	0.75	3760
Nov 11, 1987	220	367.2	1420	298.8	2.45	2.82	3720
Nov 11, 1987	118	367.2	1420	324.1	2.45	2.76	3021
Nov 11, 1987	207	367.2	1420	304.3	2.45	2.81	3551
Nov 12, 1987	209	1279	4375	2070	7.86	2.04	4033
Nov 12, 1987	209	367.2	26500	6141.5	20.7	5.31	3116

Table 7 continued; Steady-state experiment summary (absorption experiments).

30% DEA in 2M mixture of DEA/MDEA, T=15°C							
Date	RPM	Gas (N ₂) Rate cc/min	P _{CO2} inlet ppm	P _{CO2} outlet ppm	Total CO ₂ mM	Absorption Rate x10 ⁷ gmol/s	kapp s ⁻¹
Dec 2, 1987	117	367.2	13430	6542	5.36	17.71	324*
Dec 2, 1987	207	367.2	13430	6311	5.36	18.38	375*
Dec 2, 1987	219	367.2	13430	6296	5.36	18.31	374*
Dec 2, 1987	118	367.2	9442	2082	7.01	5.76	339*
Dec 2, 1987	208	367.2	9442	2053	7.01	5.97	373*
Dec 2, 1987	220	367.2	9442	2049	7.01	6.04	384*
30% MEA in 2M mixture of MEA/MDEA, T=15°C							
Nov 11, 1987	207	367.2	1420	326.4	8.23	2.75	2964*
Nov 11, 1987	119	367.2	1420	349.9	8.23	2.70	2472*

* Using the $\sqrt{D/H}$ for 25°C

Table 8: Steady-state experiment summary (desorption experiments). The low driving force configuration was used to generate the data (liquid volume=1800 ml, turbine impellor, $a=1.46 \text{ dm}^2$). Chemicals courtesy of Dow Chemical Corp., except as noted.

30% DEA in 2M mixture of DEA/MDEA, $T=25^\circ\text{C}$

Date	RPM	Sweep Range cc/min	PCO ₂ Range ppm	PCO ₂ ^e ppm	Total CO ₂ mM	Rate Range $\times 10^7 \text{ gmol/s}$	kapp Range s^{-1}	kapp Ave. s^{-1}
Aug 3, 1987	207	503.3-183.3	161-227.6	294.6	126.9	0.556-0.286	634-547	580
Aug 4, 1987	205	51.5-6.9	259-288	290	125	0.921-0.1364	*	*
Aug 4, 1987	205	1021-120.8	215.4-518.1	634.5	196	1.509-0.4295	580-501	540
Aug 5, 1987	207	1021-21.9	299.6-951.2	994.6	234	2.10-0.1427	404-362	380
Aug 5, 1987	206	1021-36.8	956-3530	3884	433	6.70-0.891	252-224	244
Aug 6, 1987	206	1279.4-74.2	1420-6151	7710	539	12.5-6.151	177-175	176
Aug 6, 1987	206	149.2-29.3	10020-14740	16510	700.5	10.26-2.96	111-102	107
Aug 7, 1987	206	149.2-29.2	15200-23350	26850	823	15.56-4.68	74.2-70.4	72
Aug 7, 1987	206	134.2-29.4	22400-35770	42920	985	20.63-7.23	44.6-44	44.3
Nov 12, 1987	208	367.2-111.4	121.5-168.7	202.4	108.7	0.306-0.129	633-612.5	620

5% DEA in 2M mixture of DEA/MDEA, $T=25^\circ\text{C}$

Aug 11, 1987	207	149.2-36.85	197.5-268.6	304	75.6	0.2022-0.0679	182-175	177
Aug 11, 1987	206	149.2-44.34	470.4-655.8	785.7	125.4	0.4816-0.1995	119-113.4	115
Aug 12, 1987	206	753.5-51.76	585.1-2569	3415	269.3	3.025-0.9125	58.5-56.1	57
Aug 13, 1987	208	149.2-44.34	2798-4530	6114	356	2.865-1.378	38.5-36.7	37.5
Aug 14, 1987	207	149.1-44.34	4208-6843	9258	460.5	4.306-2.082	37-36	36.5
Aug 14, 1987	208	149.2-44.34	5183-8658	11976	517.4	5.3067-2.635	32.1-30	31
Aug 15, 1987	207	149.2-44.27	8874-15450	22280	699.3	9.086-4.693	24-22.5	23.3
Sep 28, 1987	206	149.2-44.42	84.4-109	123.7	46.46	0.086-.033	*	*

2M DEA, $T=25^\circ\text{C}$

Jul 27, 1987	150	1279-36.8	334-844	880	454	2.93-0.213	925-813	870
Jul 27, 1987	204	1279-36.8	332.7-855.5	888	463	2.92-0.216	940-867	900
Jul 29, 1987	202	1279-117.5	808.9-1941	2283	619	7.09-1.56	602-499	550
Jul 31, 1987	165	1428-75	1620-5488	6800	780	15.87-1.26	282-250	266
Aug 1, 1987	208	149.2-36.8	81300-227100	670000	1600	90.5-74.1	**	**

30% MEA in 2M MEA/MDEA, $T=25^\circ\text{C}$

Nov 15, 1987	210	367.2-111.4	313.6-408.9	470.7	323	0.789-0.312	1298-1240	1051
Nov 15, 1987	220	367.2-111.4	1775-2666	3400	505	3.06-2.03	390-370	314

* Experiments in which the interface pressure was within 80% of the equilibrium pressure were not used to generate rate constants, but did allow estimation of the equilibrium vapor pressure.

** The enhancement factor was smaller than 2; a value of the rate constant could not be estimated with confidence.

Table 8 continued

2M MDEA, T=25°C

Oct 22, 1987	208	367.2-112.1	872.3-1496	2914	230	1.65-1.15	34	34 ⁽¹⁾
Oct 23, 1987	211	367.2-111.4	754.9-1627	3259.1	251	1.90-1.24	30	30 ⁽¹⁾
Oct 26, 1987	209	367.2-166.2	43.1-58.6	80.8	34.4	0.109-.067	*	*
Oct 27, 1987	208	367.2-112.1	215.7-469.4	967.2	128.6	0.543-0.0361	27.3-27.1	27.2
Oct 29, 1987	222	294.1-112.1	318.9-699.9	1451	158.8	0.755-0.538	26.6-25.5	26
Nov 1, 1987	201	294.3-112.1	833.7-1656	4205	279.4	1.68-1.27	13.2-12.9	13
Nov 2, 1987	222	367.2-112.1	1177-2805	7104	390	2.96-2.15	13-12.8	12.9
Nov 3, 1987	210	367.2-112.1	2143-5368	15750	560.5	5.39-4.11	8.1	8.1
Nov 4, 1987	209	367.2-111.6	3334-8374	24341	728	8.37-6.36	8.3-8.15	8.2
Nov 5, 1987	200	14	172000	(172000)	1555	*	*	

(1) MDEA provided by Union Carbide Corp.

Table 9; Experiment summary for unsteady-state high driving force CO₂ absorption into 2 m MDEA. The large driving force configuration was used to generate these data. (magnetic stirrer, $a=1.26 \text{ dm}^2$).

Date: Sep 26, 1986 MDEA: 2 molal Agitator speed: 380 rpm Volume: 600 ml
 PCO₂: 0.900 atm

Time, min	Total CO ₂ , M	Temperature, °C
0	—	52.5
2	0.03032	52.0
4	0.03881	51.5
6	0.04657	51
9	0.05886	52.5
14	0.07447	52.5
21.5	0.1058	52.5
26.5	0.1306	52.3
33.25	0.1494	51.8
42	0.1833	52.3
52	0.2210	52.5
70.5	0.2832	52.6
85	0.3325	52.8
105	0.3988	52.7
120	0.4377	52.7
140	0.4894	52.7
157.25	0.5422	52.7

Date: Sep 28, 1986 MDEA: 2 molal Agitator speed: 380 rpm Volume: 600 ml
 PCO₂: 0.817 atm

Time, min	Total CO ₂ , M	Temperature, °C
1.5	0.0148	62
4	0.0252	61
6	0.03467	61
8	0.0450	61
11	0.0534	61.5
15	0.0691	62
21	0.1167	62.5
26.5	0.1215	62.2
34	0.1526	62.2
47.5	0.2036	62.5
52.5	0.2264	62.5
61	0.2555	62.5

Date: Sep 30, 1986 MDEA: 2 molal Agitator speed: 380 rpm Volume: 600 ml
 PCO₂: 0.920 atm

Time, min	Total CO ₂ , M	Temperature, °C
.5	0.2503	40.2
7	0.2663	41.0
13	0.2891	40.0
19	0.3017	41.0
26	0.3252	40.0
39.25	0.3592	40.5
57.5	0.4025	40.7
64	0.4213	40.8
86.25	0.4827	40.8

Date: Oct 1, 1986
PCO₂: 0.900 atm

MDEA: 2 molal

Agitator speed: 380 rpm

Volume: 600 ml

Time, min	Total CO ₂ , M	Temperature, °C
1	0.0201	46.8
2.5	0.0253	46.5
3.5	0.0288	46.8
5	0.0345	47.0
9	0.0478	46.5
15	0.0689	46.5
20	0.0875	47.5
27.5	0.1145	47.0
38.25	0.1531	46.5
45	0.1711	47.5

Date: Oct 4, 1986
PCO₂: 0.960 atm

MDEA: 2 molal

Agitator speed: 380 rpm

Volume: 600 ml

Time, min	Total CO ₂ , M	Temperature, °C
0	0.1854	30.0
5	0.1974	30.3
12	0.2143	30.5
19	0.2373	30.8
31.25	0.2655	30.1
41.5	0.2928	30.5
47	0.3078	30.5
53.5	0.3184	30.5
61.75	0.3416	30.5

Date: Oct 4, 1986
PCO₂: 0.587 atm

MDEA: 2 molal

Agitator speed: 380 rpm

Volume: 600 ml

Time, min	Total CO ₂ , M	Temperature, °C
4	0.0304	76.5
6	0.0486	77.0
8	0.0580	76.0
11	0.0690	77.0
15	0.0857	78.0
19.25	0.1092	76.5
24.25	0.1230	78.0
30	0.1456	77.0
39.5	0.1801	77.0
45	0.1994	76.0
50	0.2170	77.0

Date: Oct 5, 1986
PCO₂: 0.99 atm

MDEA: 2 molal

Agitator speed: 380 rpm

Volume: 600 ml

Time, min	Total CO ₂ , M	Temperature, °C
4	0.2346	10.0
16.5	0.2569	10.0
32.75	0.2848	9.5
42.25	0.2980	9.5
51.25	0.3142	9.3
62.75	0.3367	9.5
72.17	0.3504	9.7
82	0.3623	10.0

Table 10; tabular smoothed data for CO₂ absorption into MDEA at high driving force. The high driving force configuration was used to generate the experimental data (magnetic stirrer, liquid volume = 600 ml, $a=1.26 \text{ dm}^2$)

Temp is 9.5°C.

Total dissolved CO ₂	Rate, micromole/sec
0.2504	18.54
0.2804	18.319
0.2977	18.193
0.314	18.073
0.3347	17.92
0.3515	17.79
0.36897	17.662

Temp is 30.5°C.

Total dissolved CO ₂	Rate, micromole/sec
0.1977	26.39
0.2161	26.16
0.23433	25.94
0.26586	25.535
0.29186	25.197
0.30567	25.01
0.32136	24.801
0.3422	24.516

Temp is 40.5°C.

Total dissolved CO ₂	Rate, micromole/sec
0.26999	28.674
0.287094	28.335
0.303992	27.99
0.323442	27.58
0.359459	26.786
0.407308	25.654
0.42385	25.242
0.47839	23.8

Temp is 46.5°C.

Total dissolved CO ₂	Rate, micromole/sec
0.025224	36
0.028821	35.948
0.034207	35.866
0.048509	35.643
0.069793	35.302
0.087373	35.015
0.113466	34.563
0.150259	33.888
0.172987	33.448

Temp is 52.5°C.

Total dissolved CO ₂	Rate, micromole/sec
0.038432	39.795
0.046377	39.653
0.05824	39.432
0.077861	39.047
0.106927	38.46
0.126055	38.047
0.15146	37.472
0.183987	36.678
0.220189	35.725
0.284501	33.817
0.332372	32.22
0.394437	29.879
0.437905	28.077
0.491544	25.594
0.5338	23.426

Temp is 62°C.

Total dissolved CO ₂	Rate, micromole/sec
0.025449	44.286
0.034288	44.098
0.043089	43.911
0.056219	43.615
0.073579	43.185
0.09928	42.484
0.12484	41.857
0.153502	40.868
0.207353	38.91
0.226616	38.136
0.258439	36.734

Temp is 77°C.

Total dissolved CO ₂	Rate, micromole/sec
0.048567	43.405
0.057215	43.066
0.070051	42.501
0.086886	41.67
0.104387	40.688
0.124425	39.437
0.146642	37.833
0.181184	34.914
0.199892	33.119
0.216026	31.426

Table 11; Experiment summary for unsteady-state high driving force CO₂ absorption into a 2 m MDEA/MEA mixture (30 mole % MEA). The high driving force configuration was used to generate the data (magnetic stirrer, $a=1.26 \text{ dm}^2$)

Date: Oct 10, 1986 MDEA: 1.36 molal Agitator speed: 380 rpm Volume: 600 ml
 PCO₂: 0.96 atm MEA: 0.61 molal

Time, min	Total CO ₂ , M	Temperature, °C
8.75	0.0747	31.0
15	0.1088	31.0
20.75	0.1360	
25.33	0.1518	31.0
32.33	0.1803	
38.75	0.2234	31.0
47	0.2397	31.0
53	0.2619	
67	0.3083	
75	0.3376	
91	0.4008	31.0
104	0.4171	31.0
121.5	0.4754	31.0
139	0.5263	
151	0.5363	31.0
173	0.6143	31.0
191.5	0.6554	31.0
210.75	0.6945	31.0
230.25	0.7398	31.0
251	0.7765	31.0
279	0.8264	31.0
302	0.8704	31.0
330	0.9200	31.0

Table 12; Experiment summary for unsteady-state moderate driving force CO₂ absorption into a 2 m MDEA/MEA mixture (30 mole % MEA). The low driving force configuration was used to generate the data (turbine impellor, $a=1.46 \text{ dm}^2$).

Date: Mar 4, 1987	MDEA: 1.36 molal	Agitator speed: 204 rpm	Volume: 1800 ml
PCO ₂ : 0.0332 atm	MEA: 0.61 molal		
Time, min	Total CO ₂ , M	Temperature, °C	
.45	0.00297	24.5	
2.08	0.00406	23	
3.37	0.00497		
4.62	0.00582		
6.03	0.00815		
8.33	0.00970	23	
11.37	0.01112		
14.73	0.01258	23	
20.08	0.01691	22.8	
28.83	0.02307	22.7	
39.92	0.02976	22.7	
60.72	0.04111	22.8	
78.58	0.05295	22.7	
99.25	0.06630	22.7	
122.75	0.07803	23	
145.08	0.08955		
168.88	0.1050		
195.42	0.1179		
222.33	0.1334		

Table 13; Calibration of the 100 Canon-Fenske viscometer.

Calibration data.

Date	Solution composition	Temperature °C	Time min:sec	Viscosity cS	Cell constant cS/s
Feb 10	26.88 wt% Ethylene Glycol	21	2:22.3	1.83	0.01288
Feb 10	100 wt% Ethylene Glycol	21.3	22:02.1	17.40	0.01316
Feb 12	39.92 wt% Ethylene Glycol	20	3:35.1	2.69	0.0125
		20	3:36.8		0.01241
Feb 12	50.63 wt% Ethylene Glycol	20	4:48.2	3.596	0.01248
		20	4:48.0		0.01245
Feb 13	58.83 wt% Ethylene Glycol	20	5:58.5	4.524	0.01262
		20	5:57.0		0.01267
		20	5:54.0		0.01278
		20	5:55.4		0.01273
Feb 13	49.97 wt% Ethylene Glycol	20	4:36.2	3.534	0.01280
		20	4:36.1		0.01280
average:					0.01267

Table 14a; Viscosity data for 3.53 m amine mixtures.

Date	Solution composition	CO2 content mM	Temperature °C	Time min:sec	Viscosity cS
Feb 16	29.6 wt% MDEA (3.53 m)	<1	21.25	4:33.9	3.47
				4:34.9	3.48
Feb 17	(same)	0.6	21.3	4:34.1	3.47
		0.6	50.0	1:58.4	1.50
		0.6	41.5	2:28.1	1.88
		520	30.0	3:29.0	2.65
		520	40.8	2:33.8	1.95
		520	40.8	2:33.8	1.95
		520	56.0	1:47.6	1.36
Feb 17	(same)	1700	22.1	4:23.2	3.33
Feb 18	(same)	1640	21.0	4:30.6	3.43
Feb 18	3.53 m total amine, MEA+MDEA (30 mol % of which is MEA)	2.45	22	3:47.6	2.88
		2.45	33.5	2:36.9	1.99
		2.45	44.5	1:57.3	1.49
		2.45	51.8	1:40.1	1.27
		208	23.8	3:22.8	2.57
		208	23.8	3:21.4	2.55
		208	23.8	3:21.9	2.56
		208	34.5	2:25.3	1.84
		208	45.0	1:52.1	1.42
		1310	23	3:40.5	2.79

Table 16; Density data for the 2 m amine mixtures.

Date	Solution Composition	CO ₂ content mM	Temperature °C	Density g/cc
Mar 2 1987	2 m mixture, MEA only	0.56	20	1.0025
		0.56	15	1.0038
		0.56	15	1.0039
		0.56	25	1.0011
		0.56	35	0.9978
Mar 2 1987	2 m mixture, MEA+MDEA (90 mol % of which is MEA)	0.17	20	1.0038
Mar 2 1987	2 m mixture, MEA+MDEA (80 mol % of which is MEA)	0.31	20	1.0053
		0.31	35	1.0003
Mar 2 1987	2 m mixture, MEA+MDEA (50 mol % of which is MEA)	0.50	20	1.0093
		0.50	15	1.0107
		0.50	25	1.0076
		0.50	25	1.0075
		0.50	35	1.0040
Mar 2 1987	2 m mixture, MEA+MDEA (30 mol % of which is MEA)	0.46	20	1.0120
		0.46	15	1.0134
		0.46	15	1.0135
		0.46	25	1.0103
		0.46	25	1.0104
Mar 2 1987	2 m mixture, MEA+MDEA (15 mol % of which is MEA)	0.46	35	1.0065
		0.96	20	1.0139
		0.96	20	1.0140
		0.96	15	1.0154
		0.96	25	1.0120
Mar 2 1987	2 m mixture, MEA+MDEA (5 mol % of which is MEA)	0.96	25	1.0119
		0.96	35	1.0083
		0.51	20	1.0147
		0.51	15	1.0161
		0.51	25	1.0129
Mar 2 1987	2 m MDEA	0.51	25	1.0130
		0.51	35	1.0090
		0.51	35	1.0089
		0.95	20	1.0153
		0.95	15	1.0168
Mar 2 1987	2 m MDEA	0.95	25	1.0135
		0.95	25	1.0136
		0.95	25	1.0096

Table 15; Viscosity data for DEA, DEA+MDEA, MEA+MDEA, all at 2 M solutions. The calibration constant of the viscometer is 0.01267 cS/s.

Date	Solution composition	Temperature °C	Time s	Viscosity cS
Dec 10	2 M DEA	25	158.42	
		25	158.42	
		25	159.15	
		25	159.70	
			ave=159.17	2.017
		35	123.25	
		35	123.52	
		35	123.10	
		35	123.26	
			ave=123.28	1.562
		45	97.02	
		45	96.91	
		45	98.18	
		45	98.31	
			ave=97.605	1.237
Dec 10	2 M total amine, DEA+MDEA (30 mol % of which is DEA)	25	177.28	
		25	178.21	
		25	178.00	
		25	177.89	
			ave=177.845	2.253
		35	132.56	
		35	132.86	
		35	132.76	
		35	132.67	
			ave=132.713	1.681
		45	104.3	
		45	104.3	
		45	104.5	
		45	104.4	
			ave=104.38	1.322
Dec 10	2 M total amine, MEA+MDEA (30 mol % of which is MEA)	25	158.2	
		25	158.0	
		25	158.0	
		25	158.0	
			ave=158.05	2.002
		35	122.6	
		35	122.0	
		35	122.0	
		35	122.0	
			ave=122.15	1.548
		45	96.8	
		45	96.9	
		45	97.0	
		45	96.8	
			ave=96.88	1.22

Table 14b; Viscosity data for 2 m amine mixtures (MEA/MDEA)

Feb 25	2.00 m total amine, MEA+MDEA (15 mol % of which is MEA)	—	20	2:47.8	2.13
			25.8	2:23.0	1.81
			36.5	1:48.2	1.37
Feb 25	2.05 m total amine, MEA only	—	20.25	1:56.0	1.47
			16.5	2:09.5	1.64
			31.0	1:29.6	1.14
Feb 25	2.03 m total amine, MEA+MDEA (80 mol % of which is MEA)	—	27.5	1:46.9	1.35
			20.5	2:07.7	1.62
			32	1:35.9	1.22
Feb 25	2.006 m total amine, MEA+MDEA (50 mol % of which is MEA)	—	26	2:00.0	1.52
			20.25	2:19.8	1.77
			20.25	2:21.6	1.79
			16.5	2:36.8	1.99
			32	1:42.9	1.30
Feb 25	2.01 m total amine, MEA+MDEA (30 mol % of which is MEA)	—	26.9	2:11.5	1.67
			20.25	2:38.0	2.00
			20.25	2:36.3	1.98
			16	3:02.1	2.31
			32	1:54.1	1.45
Feb 25	2.00 m total amine, MEA+MDEA (5 mol % of which is MEA)	—	32.5	1:55.3	1.46
			16	3:16.0	1.96
			20	2:51.0	2.17
			20.3	2:49.6	2.15
			27.5	2:19.0	1.76
Feb 25	2.00 m total amine, MDEA only	—	27.5	2:23.1	1.81
			20	2:57.6	2.25
			16	3:24.4	2.59
			32.5	2:04.8	1.58
			38.5	1:47.8	1.37
			44	1:34.7	1.20

Vita

James Edward Critchfield was born in South Charleston, West Virginia on October 1, 1961, the son of Carolyn and Frank Critchfield. After graduation from South Charleston High School in 1979 he entered West Virginia University where he majored in Chemical Engineering. During the summers he worked at Union Carbide's Research Center in South Charleston before graduating with a B.S. degree in May of 1983. That fall he entered graduate school at the University of Texas at Austin, where he worked with Dr. Gary Rochelle on mass transfer with simultaneous reaction in CO₂/alkanolamine systems. After graduating with his Ph.D. in May of 1988, he accepted a position with Shell Development Company in the Environmental Engineering Department at their Westhollow Research Laboratories.

Permanent Address: 2102 Stratford Road
South Charleston, WV 25303
(304) 343-0249

This dissertation was typed by the author.